

THERMAL, PHYSICO-MECHANICAL AND DEGRADATION CHARACTERISTICS OF
COMPATIBILIZED BIODEGRADABLE BIOPOLYMERS AND COMPOSITES

A Thesis
Submitted to the Graduate Faculty
of the
North Dakota State University
of Agriculture and Applied Science

By

Nikushi Shakyadevi Yatigala

In Partial Fulfillment of the Requirements
for the Degree of
MASTER OF SCIENCE

Major Department:
Agricultural and Biosystems Engineering

October 2017

Fargo, North Dakota

North Dakota State University
Graduate School

Title

THERMAL, PHYSICO-MECHANICAL AND DEGRADATION
CHARACTERISTICS OF COMPATIBILIZED BIODEGRADABLE
BIOPOLYMERS AND COMPOSITES

By

Nikushi Shakyadevi Yatigala

The Supervisory Committee certifies that this *disquisition* complies with North Dakota
State University's regulations and meets the accepted standards for the degree of

MASTER OF SCIENCE

SUPERVISORY COMMITTEE:

Sreekala G. Bajwa

Chair

Dilpreet S. Bajwa

Dennis P. Wiesenborn

Om P. Yadav

Approved:

11/14/2017

Date

Dr. Sreekala Bajwa

Department Chair

ABSTRACT

Due to negative effects of petroleum-based plastic waste on environment, a significant consideration is given to biopolymers as sustainable alternatives. However, incompetence in technology and cost prevent the applications of biopolymers. This study evaluated the effect of compatibilizer and wood fiber filler on five types of biopolymers. To assess weathering characteristics, biocomposites were subjected to 2000 h of accelerated weathering. Biocomposites were soil buried at temperatures of 30°C and 60°C for quantifying biodegradation. Compatibilization improved thermal and physico-mechanical properties. All properties deteriorated upon weathering, but no considerable differences were observed between compatibilized and uncompatibilized composites. After soil biodegradation, weight loss and increased water absorption were observed. Biodegradation was significant after soil burial at 60°C. Compatibilized composites after 30°C soil burial showed lower biodegradation than uncompatibilized composites, but at 60°C, it was reversed. Results confirm improved properties with compatibilization without affecting UV weathering characteristics, and achieving higher biodegradation at elevated temperatures.

ACKNOWLEDGEMENTS

I would like to thank my advisors, Dr. Sreekala Bajwa and Dr. Dilpreet Bajwa for invaluable guidance and wisdom they gave me throughout my research. They have shown me the true satisfaction of research, and I enjoyed many discussions we had on the subjects of biopolymers and degradation. I want to gratefully acknowledge Dr. Dennis Wiesenborn and Dr. Om Yadav for serving in my graduate committee. I appreciate your comments and constructive feedback throughout my research. I thank you all for your encouragement for me to become a better researcher.

I am very grateful for North Dakota Agricultural Experiment Station and North Dakota NSF EPSCoR for funding this project. I sincerely thank James Moos and Chad Rehovsky for their assistance throughout the project. I thank Melanie Ziegler, Sara Ogundolani, Julie Bietz, and Deb Baer for their continuous help on administrative procedures.

Finally, I like to thank my family for their relentless support in every way, and my husband for giving me strength thorough out this work.

DEDICATION

To my Husband:

Vidura

To my Parents:

Krishni and Lal

To my siblings:

Shann and Minushi

Thank you for your unconditional love and encouragement.

TABLE OF CONTENTS

ABSTRACT.....	iii
ACKNOWLEDGEMENTS.....	iv
DEDICATION.....	v
LIST OF TABLES.....	x
LIST OF FIGURES.....	xii
LIST OF ABBREVIATIONS.....	xv
LIST OF SYMBOLS.....	xvii
LIST OF APPENDIX FIGURES.....	xix
DISSERTATION ORGANIZATION.....	1
GENERAL INTRODUCTION.....	2
Research Objectives.....	4
References.....	4
CHAPTER 1. LITERATURE REVIEW.....	6
Biobased Biodegradable Polymers.....	6
Degradation.....	9
Biodegradation.....	10
Biodegradation Characteristics of Biopolymer Composites.....	12
Effect of Compatibilization on Biodegradation.....	15
Degradation of Biopolymer Composites due to Weathering.....	17
Accelerated Weathering.....	17
Applications.....	19
PLA.....	19
PHA.....	20
Starch.....	21

Other	21
Conclusion.....	22
References	23
CHAPTER 2. COMPATIBILIZATION IMPROVES PHYSICO-MECHANICAL PROPERTIES OF BIODEGRADABLE BIOBASED POLYMER COMPOSITES	29
Abstract	29
Introduction	29
Experimental Procedure	32
Materials	32
Polymer Composite Manufacturing	32
Characterization of Composites	35
Results and Discussion.....	39
Thermal Properties	39
Melt Flow Index (MFI)	41
Water Absorption	42
Mechanical Properties	44
Effect of MA Grafting on Biopolymer- Discussion.....	50
Conclusion.....	54
References	54
CHAPTER 3. COMPATIBILIZATION IMPROVES PERFORMANCE OF BIODEGRADABLE BIOPOLYMER COMPOSITES WITHOUT AFFECTING UV WEATHERING CHARACTERISTICS	60
Abstract	60
Introduction	61
Experimental Procedure	62
Materials	63

Polymer Composite Manufacturing	63
Accelerated Weathering	64
Characterization of Composites	65
Results and Discussion.....	68
Optical Microscopy	68
Surface Color of Composite Material.....	72
Water Absorption	75
Differential scanning calorimetry (DSC)	77
Thermo-Gravimetric Analysis (TGA).....	79
Mechanical Properties	82
Conclusion.....	89
References	90
CHAPTER 4. BIODEGRADATION PROPERTIES OF COMPATIBILIZED BIOPOLYMER COMPOSITES.....	95
Abstract	95
Introduction	96
Experimental	98
Materials	98
Polymer Composite Manufacturing	99
Soil Biodegradation.....	100
Characterization of Composites	101
Results and Discussion.....	102
Water Absorption	102
Soil Biodegradation.....	104
Optical Microscopy	105
Surface Color.....	108

Mechanical Properties	111
Discussion	114
Conclusion.....	116
References	117
CHAPTER 5. GENERAL CONCLUSIONS.....	121
References	123
CHAPTER 6. RECOMMENDATIONS FOR FUTURE WORK	124
References	125
APPENDIX A. ADDITIONAL INFORMATION OF BIOFLEX BIOPOLYMER	127
References	128

LIST OF TABLES

<u>Table</u>	<u>Page</u>
2.1. Compositions of maleic anhydride (MA) grafted Polymers.....	33
2.2. Temperature profile used for extrusion for grafting with maleic anhydride (MA) and compounding of polymer with wood fiber (WF).....	33
2.3. Compositions of biocomposites made with five different biopolymers with wood fiber (WF), and with and without maleic anhydride (MA).....	34
2.4. Temperature profile used for compression molding.....	35
2.5. Temperatures at which MFI was calculated for each polymer.....	36
2.6. Evaluated mechanical properties.....	37
2.7. Thermal properties of the composites with and without compatibilizer, in relation to that of neat polymer used in the study. Here, T_g is glass transition temperature, T_{cc} is cold crystallization temperature, T_m is melting temperature, ΔH_c is crystallization enthalpy, ΔH_m is melting enthalpy and X (%) is crystallinity of the specimens.....	39
2.8. Equilibrium water content (M_m) and diffusivity (D) of the neat biopolymer and composite specimens.....	44
2.9. Weight-average molecular weight (M_w) of SL, SL/WF, and MA-g-SL/WF.....	50
3.1. Comparison of surface morphology of the specimens before and after weathering at 1000h and 2000h for five biopolymers, and their composites with and without compatibilizer: PLA, PLA/WF, MA-g-PLA/WF, BF, BF/WF, MA-g-BF/WF.....	69
3.2. Comparison of surface morphology of the specimens before and after weathering at 1000h and 2000h: PHB, PHB/WF, MA-g-PHB/WF, PHBV, PHBV/WF, MA-g-PHBV/WF.....	70
3.3. Comparison of surface morphology of the specimens before and after weathering at 1000h and 2000h: SL, SL/WF, MA-g-SL/WF.....	71
3.4. Maximum moisture content (M_m) and standard deviation of the composite and neat biopolymer specimens before weathering, and 1000h and 2000h after weathering.....	76
3.5. Thermal properties of the unweathered composite specimens with and without compatibilizer, in relation to neat polymer, for the five biopolymers used in the study. Here, T_g is glass transition temperature, T_m is melting temperature, and X (%) is crystallinity of the specimens.....	78

3.6.	Starting thermal degradation temperature (T_{onset}), the temperature corresponding to the maximum mass loss (T_{peak}), the temperature corresponding to the end of the thermal degradation stage (T_{endset}), and the total weight loss (W%) for the five biopolymers and their composites, derived from thermo-gravimetric analysis.....	80
3.7.	Flexural strength and modulus all the specimens at 0, 1000 and 2000 h of UV weathering. Different letters indicate statistically significant differences at $P < 0.05$ between the specimens in each polymer type.....	83
3.8.	Impact fracture energy and hardness of all the specimens before weathering and after weathering (1000h and 2000h). Different letters indicate statistically significant differences type at $P < 0.05$ between the specimens in each polymer type.....	84
4.1.	Comparison of surface morphology of the specimens before, and after soil burial at 30°C and 60°C: PLA, PLA/WF, MA-g-PLA/WF, BF, BF/WF, MA-g-BF/WF.....	106
4.2.	Comparison of surface morphology of the specimens before, and after soil burial at 30°C and 60°C: PHB, PHB/WF, MA-g-PHB/WF, PHBV, PHBV/WF, MA-g-PHBV/WF.....	107
4.3.	Comparison of surface morphology of the specimens before, and after soil burial at 30°C and 60°C: SL, SL/WF, MA-g-SL/WF.....	108
4.4.	Digital camera photos of the specimens before, and after soil burial at 30°C and 60°C: PLA, PLA/WE, BF/WF, SL, MA-g-PHBV/WF.....	110

LIST OF FIGURES

<u>Figure</u>	<u>Page</u>
1.1. Types of Biopolymers (adapted from Madbouly et al., 2012).....	7
1.2. Origin of Biobased Biodegradable Polymers (adapted from Madbouly et al., 2012)	8
1.3. General mechanism of plastic biodegradation under aerobic and anaerobic conditions.....	12
2.1. Melt flow index of the neat, uncompatibilized, and MA compatibilized polymer specimens (PLA, BF, SL, PHB and PHBV).....	42
2.2. Impact fracture energy of the neat biopolymer and composite specimens. The error bars indicate standard deviation. Different letters above the bars indicate statistically significant differences at $P < 0.05$	45
2.3. Flexural strength of all the 15 biopolymer compositions. The error bars indicate standard deviation. Different letters above the bars indicate statistically significant differences at $P < 0.05$	46
2.4. Flexural modulus of all the 15 biopolymer compositions. The error bars indicate standard deviation. Different letters above the bars indicate statistically significant differences at $P < 0.05$	47
2.5. Surface hardness of the composite and neat biopolymer specimens. The error bars indicate standard deviation. Different letters above the bars indicate statistically significant differences at $P < 0.05$	48
2.6. Compressive strength of the biopolymer compositions. The error bars indicate standard deviation. Letters above the bars indicate statistically significant differences at $P < 0.05$	49
2.7. Cost of all the neat polymers and their composites with and without compatibilizer.	49
2.8. FTIR spectra of (a) SL and (b) Yam starch (Copyright Wiley-VCH Verlag GmbH & Co. KGaA. Reproduced with permission (Ogunmolasuyi et al., 2016)).....	52
2.9. FTIR spectra of PHB composites. (a): MA-g-PHB, MA-g-PHB/WF, PHB/WF from Magna spectrometer; (b) PHB from photoacoustic detector.....	53
3.1. The lightness (ΔL^*) and total color changes (ΔE^*) of the specimens after 2000h of accelerated weathering. Different letters above the bars indicate statistically significant differences type at $P < 0.05$ between the specimens in each polymer type. The error bars show standard deviation.	73

3.2.	The total color change (ΔE^*) of the 15 biopolymer compositions during 2000 h of weathering: (a) PLA, PLA/WF, MA-g-PLA/WF, BF, BF/WF, MA-g-BF/WF; (b) PHB, PHB/WF, MA-g-PHB/WF, PHBV, PHBV/WF, MA-g-PHBV/WF; (c) SL, SL/WF, MA-g-SL/WF.....	74
3.3.	Maximum moisture (M_m) content of the 15 biopolymer compositions before weathering, and after 1000 h and 2000 h weathering (884 h instead of 1000 h for SL/WF, and 1479 h instead of 2000 h for MA-g-SL/WF).	75
3.4.	First derivative thermo-gravimetric (DTG) curves of (a) PLA and BF specimens (b) SL, PHB, and PHBV specimens.	81
3.5.	Impact fracture energy of the neat biopolymer and composite specimens before weathering, and after 1000 h and 2000 h of weathering (884 h instead of 1000 h for SL/WF, and 1479 h instead of 2000 h for MA-g-SL/WF).....	85
3.6.	Flexural strength of the neat biopolymer and composite specimens before weathering, and after 1000 h and 2000 h of weathering (884 h instead of 1000 h for SL/WF, and 1479 h instead of 2000 h for MA-g-SL/WF).....	86
3.7.	Flexural modulus of the neat biopolymer and composite specimens before weathering, and after 1000 h and 2000 h of weathering (884 h instead of 1000 h for SL/WF, and 1479 h instead of 2000 h for MA-g-SL/WF). Different letters indicate statistically significant difference of the specimen on the property at each weathering exposure.	87
3.8.	Hardness of the neat biopolymer and composite specimens before weathering, and after 1000 h and 2000 h of weathering (884 h instead of 1000 h for SL/WF, and 1479 h instead of 2000 h for MA-g-SL/WF). Different letters indicate statistically significant difference of the specimen on the property at each weathering exposure.	88
4.1.	Maximum moisture content of all the neat polymers and composites before soil burial (SB), and after soil burial at 30°C and 60°C. Different letters indicate statistically significant difference of the specimens after SB at 60°C with respect to specimens after SB at 30°C.	103
4.2.	% Weight loss of all the neat polymers and composites after soil burial (SB) at 30°C and 60°C. Different letters indicate statistically significant difference of the specimens after SB at 60°C with respect to specimens after SB at 30°C.	104
4.3.	The lightness (ΔL^*) and total color changes (ΔE^*) of the specimens after soil burial at 30°C and 60°C.	109
4.4.	Surface hardness of all the neat biopolymers and composites before and after soil burial at 30°C. Different letters indicate statistically significant difference of the specimen on the property after soil burial at 30°C with respect to specimens before soil burial.	112

- 4.5. Compressive strength of the biopolymer compositions before and after soil burial (SB) at 30°C and at 60°C. Different letters indicate statistically significant difference of the specimen on the property after SB at 30°C and at 60°C with respect to specimens before SB. 113
- 4.6. Compressive modulus of all the neat biopolymers and composites before and after soil burial (SB) at 30°C and at 60°C. Different letters indicate statistically significant difference of the specimens after SB at 30°C and 60°C with respect to specimens before SB..... 113

LIST OF ABBREVIATIONS

AA-g	Acrylic acid grafted
ASTM	American Society for Testing and Materials
BC	Bacterial cellulose
BF	Bioflex (PLA blend)
BP	Benzoyl Peroxide
DMA	Dynamic mechanical analyzer
DSC	Differential scanning calorimetry
DTG	Differential thermo-gravimetric
FTIR	Fourier transform infrared spectroscopy
GCF	Green coconut fiber
GPC	Gel permeation chromatography
KBF	Kenaf bast fiber
LB	Softwood lignin
LO	Hardwood lignin
L101	Luperox 101: 2,5-bis(tert-butylperoxy)-2,5-dimethylhexane
MA-g	Maleic anhydride grafted
MFI	Melt flow index
MW	Molecular weight
NDSU	North Dakota State University
NY11	Nylon 11
PBS	Polybutylene succinate
PBs	Phosphate buffered saline
PCL	Polycaprolactone

PE.....	Polyethylene
PES.....	Poly(ether sulfones)
PF	Phenol formaldehyde
PHA.....	Polyhydroxyalkanoate
PHB.....	Polyhydroxybutyrate
PHBV	Poly(3-hydroxybutyrate-co-3-hydroxyvalerate)
PLA.....	Poly(lactic acid)
PLLA.....	Poly-L-lactic acid
PPp	Peach palm particles
PPW-FR	Potato peel waste fermentation residue
RH.....	Relative Humidity
SB.....	Soil Burial
SF	Sisal fibers
SL.....	Solanyl (starch-based)
SPF.....	Sugar palm fiber
SPS.....	Sugar palm starch
TBPB.....	Luperox® P: tert-Butyl peroxybenzoate
TGA	Thermogravimetric analysis
TPS.....	Thermoplastic starch
USDA.....	United States Department of Agriculture
UV.....	Ultra Violet
WF.....	Wood fiber
Wf	Wood flour

LIST OF SYMBOLS

atm.....	atmospheric pressure
a^*	red (+ a^*) to green (- a^*) coordinate
b^*	yellow (+ b^*) to blue (- b^*) coordinate
$^{\circ}\text{C}$	Celsius
cm^{-1}	1/ centimeter
D.....	Diffusivity
Eq.	Equation
ΔE^*	Total color difference
h.....	hour
ΔH_c	Crystallization enthalpy
ΔH_m	Melting enthalpy
ΔH_m^0	Estimated melting enthalpy
J.....	Joule
J/g.....	Joule/gram
kg.....	kilogram
kJ/m^2	kilojoule/square meter
kN.....	kilo Newton
L^*	Lightness
min.....	Minute
mL/min.....	milliliter/ minute
mm.....	millimeter
mm/min.....	millimeter/minute
M_m	Maximum water absorption capacity
MPa.....	Mega Pascal

M_w	Weight average molecular weight
M_w/M_n	Polydispersity Index
μL	micro liter
N.....	Newton
pH.....	potential Hydrogen
phr	parts per hundred parts of resin
T_{cc}	Cold crystallization temperature
T_{endset}	Temperature at the end of the thermal degradation
T_g	Glass transition temperature
T_m	Melting temperature
T_{onset}	Degradation temperature
T_{peak}	Temperature at maximum mass loss
W%	Total weight loss
wt%	Weight percent
X%	Crystallinity

LIST OF APPENDIX FIGURES

<u>Figure</u>	<u>Page</u>
A1. FTIR spectra of PLA and Bioflex (BF).	127

DISSERTATION ORGANIZATION

This dissertation consists of a general introduction and six chapters. Chapter 1 is a literature review of current state of art in the field of biopolymers and degradation. Chapter 2, titled “Compatibilization improves physico-mechanical properties of biodegradable biobased polymer composites”, discusses the effects of compatibilizer on five types of biopolymer composites with wood fiber filler on physical, mechanical and thermal properties. Chapter 3, titled “Compatibilization improves performance of biodegradable biopolymer composites without affecting UV weathering characteristics”, describes the effects of accelerated weathering on five types of neat biopolymers and their compatibilized and uncompatibilized composites. In addition to physical, mechanical and thermal properties, surface color change and optical microscopy images were taken to assess the degradation rate. Chapter 4, titled “Biodegradation properties of compatibilized biopolymer composites” summarizes the effects of compatibilization of five types of biobased polymer composites on soil biodegradation properties. Biodegradation rate was determined by the weight loss. Chapter 5 discusses the general conclusions based on chapter 2, 3 and 4 research work. Important aspects of processing of the polymers have been addressed in chapter 6, titled “Recommendations for future work.” The appendix at the end of the dissertation contain supplementary material.

Two manuscripts are currently under review for journal publications. The research results are presented at two conferences including Association for the Advancement of Industrial Crops, and Advancements in Fiber-Polymer Composites Symposium.

GENERAL INTRODUCTION

Petroleum based polymer products have become indispensable in our society due to their wide variety of applications in packaging, agriculture, food, medical appliances and construction materials. However, widespread use of petroleum in production of plastics has a negative impact on environment because of the CO₂ released and long degradation life of plastics. Due to the finite supply of petroleum and the increasing concern of environmental pollution, a special emphasis has been placed on biodegradable polymers from renewable resources. Use of renewable resources decreases the dependence of petroleum and waste accumulation. Biodegradability, biocompatibility, air permeability and low temperature sealability are beneficial properties of biopolymers that are invaluable in agricultural, packaging and medical applications. Nonetheless, replacing petroleum based polymers with biodegradable biobased alternatives is a challenge due to technical and economic complications (Halley & Dorgan, 2011).

Biopolymers are expensive compared to petroleum-based polymers. They are brittle, sensitive to thermal degradation, and have other inferior physical properties. Natural fibers are added to biopolymers to counter some of these undesirable properties creating biocomposites. Natural fibers are inexpensive and abundantly available in nature. Properties such as low density, high specific strength, biodegradability, and non-abrasiveness of natural fibers are vital in polymer composites (Saheb & Jog, 1999). In order to use biocomposites in commercial applications, it is important to study their degradation characteristics under different environmental conditions. Degradation is usually evaluated by weight loss and deterioration of physico-mechanical properties when subjected to degrading environments.

Even though creating biocomposites with natural fibers are a solution in terms of strength and dimensional stability, these biocomposites exhibit poor physico-mechanical properties due to poor adhesion between the hydrophobic polymer matrix and hydrophilic fiber (Luckachan & Pillai, 2011). The fiber-matrix interaction can be improved by incorporating reactive functional groups such as compatibilizers to composites. Compatibilizers bond with fiber by covalent and/or hydrogen bonding, and molecular entanglement with the polymer matrix (Gunning, Geever, Killion, Lyons, & Higginbotham, 2014). Compatibilization is shown to improve strength properties of some polymer composites (Gunning, Geever, Killion, Lyons, & Higginbotham, 2013). Effect of compatibilization of biodegradable biobased polymers with wood fiber is not well known yet. Also, long-term performance of biocomposites with compatibilizers in outdoor conditions need further investigations. Low soil biodegradation rate due to increased water resistance of compatibilized biocomposites is a potential drawback of compatibilization (C.-S. Wu, 2009; C. S. Wu, 2006, 2012). However, studies showed increased water absorption of biobased biodegradable polymers at higher temperatures indicating an opportunity to achieve higher biodegradation, as the activity of microorganisms is closely connected to the presence of water (Grundmann, Bilitewski, Zentner, Wonschik, & Focke, 2013).

Despite the positive impact of biodegradable biopolymers on the environment, these polymers need to be engineered to have comparably good performance. Further investigations should be done regarding the degradation characteristics of these composites in order to understand their durability in degrading environment, and gain technological usefulness of the biopolymers in commercial applications.

Research Objectives

The overall goal of this research project was to evaluate thermal, physical, mechanical and degradation properties of biodegradable biobased polymer composites. The specific objectives of this research were to:

- I. Evaluate the effect of wood fiber filler and compatibilizer on five different biobased biodegradable polymers in terms of mechanical, thermal and water absorption properties.
- II. Asses the wood fiber filler and compatibilizer on biobased biodegradable polymers under accelerated UV weathering.
- III. Asses the effect of wood fiber filler and compatibilizer on soil biodegradation properties of biopolymers under different temperatures.

References

- Grundmann, V., Bilitewski, B., Zentner, A., Wonschik, C.-R., & Focke, M. (2013). Hydrolysis and anaerobic co-fermentation of different kinds of biodegradable polymers. *Waste and Biomass Valorization*, 4(2), 371-376.
- Gunning, M. A., Geever, L. M., Killion, J. A., Lyons, J. G., & Higginbotham, C. L. (2013). Mechanical and biodegradation performance of short natural fibre polyhydroxybutyrate composites. *Polymer Testing*, 32(8), 1603-1611.
- Gunning, M. A., Geever, L. M., Killion, J. A., Lyons, J. G., & Higginbotham, C. L. (2014). Effect of Compatibilizer Content on the Mechanical Properties of Bioplastic Composites via Hot Melt Extrusion. *Polymer-Plastics Technology and Engineering*, 53(12), 1223-1235.

- Halley, P., & Dorgan, J. (2011). Next-generation biopolymers: Advanced functionality and improved sustainability. *Materials Research Society*, 36, 687-691.
doi:10.1557/mrs.2011.180
- Luckachan, G. E., & Pillai, C. (2011). Biodegradable polymers-a review on recent trends and emerging perspectives. *Journal of Polymers and the Environment*, 19(3), 637-676.
- Saheb, D. N., & Jog, J. P. (1999). Natural fiber polymer composites: a review. *Advances in polymer technology*, 18(4), 351-363.
- Wu, C.-S. (2009). Renewable resource-based composites of recycled natural fibers and maleated polylactide bioplastic: Characterization and biodegradability. *Polymer Degradation and Stability*, 94(7), 1076-1084.
- Wu, C. S. (2006). Assessing biodegradability and mechanical, thermal, and morphological properties of an acrylic acid-modified poly (3-hydroxybutyric acid)/wood flours biocomposite. *Journal of applied polymer science*, 102(4), 3565-3574.
- Wu, C. S. (2012). Preparation, characterization, and biodegradability of renewable resource-based composites from recycled polylactide bioplastic and sisal fibers. *Journal of Applied Polymer Science*, 123(1), 347-355.

CHAPTER 1. LITERATURE REVIEW

Petroleum based polymers cause substantial environmental problems at disposal because of their slow degradation and harmful degradation products. Most of the plastic wastes end up in landfills, causing water and soil pollution. Biobased biodegradable polymers and natural fibers have the advantage of low environmental impact and high sustainability. They reduce waste accumulation, control carbon dioxide emission and minimize the dependency on petroleum-based products. Incorporation of natural fibers to biobased polymers can increase in specific strength and degradation rate, while reducing its cost. During biodegradation, polymers experience deterioration in physical and chemical properties, and reduced molecular mass as a result of microbial activity. This chapter discusses the current state of knowledge on the behavior of biobased biodegradable polymers and their composites when subjected to soil, aerobic, anaerobic, UV accelerated weathering and thermal degradation. Effects of chemical additives such as compatibilizers to biobased polymers and composites are also discussed. A range of biobased biodegradable polymer composites are presented in this chapter, focusing on their degradation characteristics and mechanisms, and applications.

Biobased Biodegradable Polymers

Polymers can be produced from various renewable and nonrenewable resources. Biobased polymers are the polymers produced by or from living systems. There are some biobased plastics that are not biodegradable. For example, biobased polyethylene is not biodegradable. Biodegradable plastics are polymers that degrade from the action of microorganisms. Not all biodegradable plastics are biobased (Figure 1.1). There are synthetic polymers produced from nonrenewable petroleum resources that are biodegradable (Vroman & Tighzert, 2009). This chapter discusses the degradation characteristics of biobased biodegradable

polymers and composites. As Figure 1.2 illustrates, these biobased biodegradable polymers can be divided into three categories: (i) those synthesized from bio-derived monomers (PLA), (ii) those produced by microorganisms (PHAs, bacterial cellulose), and (iii) those directly extracted from biomass with partial modification to meet the requirements (Bessadok, Belgacem, Dufresne, & Bras, 2010; Madbouly et al., 2012).

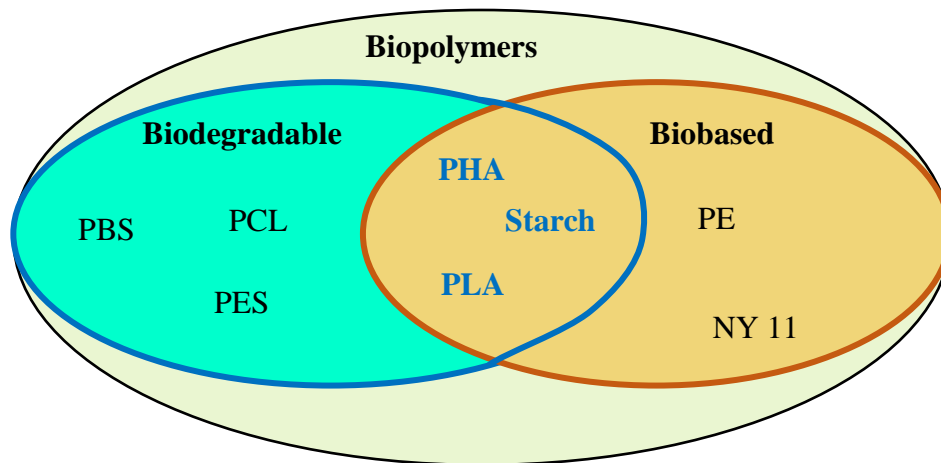


Figure 1.1. Types of Biopolymers (adapted from Madbouly et al., 2012)

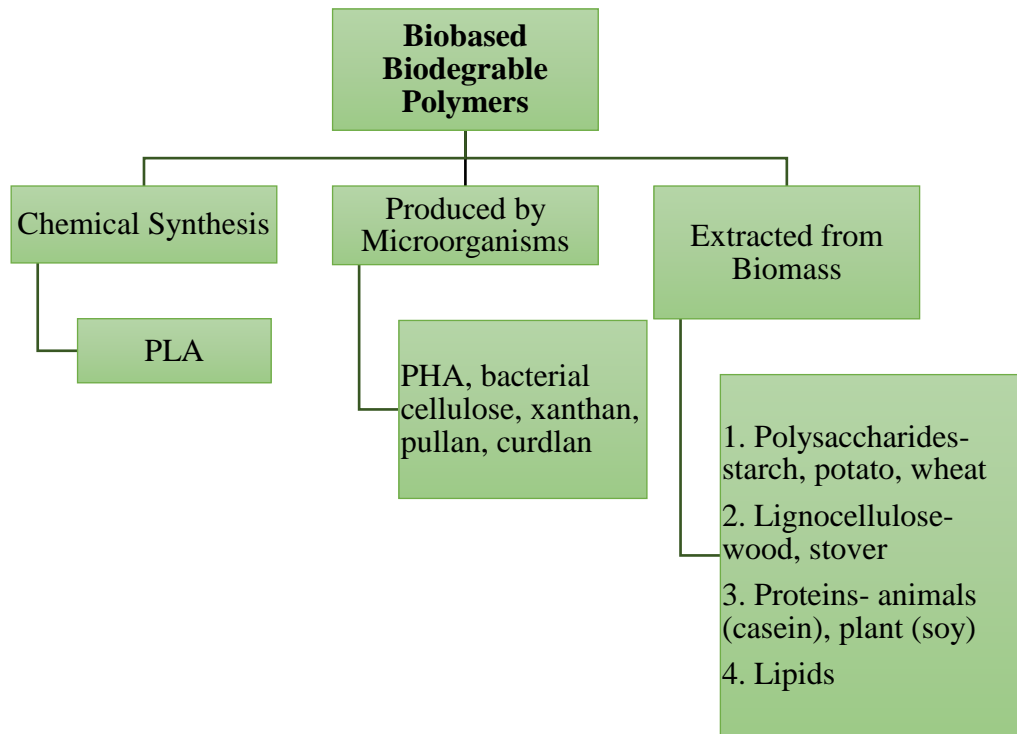


Figure 1.2. Origin of Biobased Biodegradable Polymers (adapted from Madbouly et al., 2012)

Poly(lactic acid) (PLA) is the most widely used biobased and biodegradable polymer. It is obtained by polymerization of lactic acid, which is a sugar fermentation product from corn, sugar beets/cane, or potatoes. The two methods that are currently used in producing PLA are polycondensation of lactic acid, and via lactic ring opening. Since glass transition temperature (T_g) and melting temperature (T_m) of PLA are between 55-65°C and 150-175°C, it is appropriate for injection molding, blow molding, extrusion, and film forming operations (Bessadok et al., 2010; Mukherjee & Kao, 2011; Petinakis, Simon, Dean, & Yu, 2013).

Other commonly used biopolymers are Polyhydroxybutyrate (PHB) and poly(3-hydroxybutyrate-co-3-hydroxyvalerate) (PHBV), which are important types of Polyhydroxyalkanoate (PHA) biopolymers. The PHAs are produced in nature by bacterial fermentation of sugar or lipids, where PHB is accumulated as a reserve of carbon and energy by

a number of bacteria. The PHBV copolymer is produced by incorporating 3-hydroxyvalerate (3HV) units into PHB segments (Rutkowska et al., 2008). During degradation, PHA polymer is too large in size to be conveyed directly through the bacterial cell wall, so it should be permuted into corresponding hydroxyl acid monomers (Gilmore, Fuller, & Lenz, 1990). Monomers are soluble in water and small enough to diffuse through the cell wall. Under aerobic conditions they produce CO₂ and water by being metabolized by β -oxidation and tricarboxylic acid cycle. Under anaerobic conditions, methane is also produced (Shah, Hasan, Hameed, & Ahmed, 2008).

Starch is the most common, abundant and cheap biopolymer. It is mainly extracted from potatoes, corn, wheat and rice. Starch is biodegraded via hydrolysis of acetal link by enzymes. Starch is usually used as a thermoplastic. Thermoplastic starch (TPS) is produced by plasticizing starch through destructurement of molecules that are capable of hydrogen bonding with hydroxyl groups of starch. However, TPS tend to have poor mechanical properties as it is highly sensitive to humidity and water content. Nevertheless, due to its low cost and widespread availability, starch has been incorporated into many products.

Degradation

There are many types of polymer degradation mechanisms: thermal, mechanical, chemical, biological and chemical degradation (Schnabel, 1981). According to ASTM definition, “degradable plastics are the plastics that are designed to undergo a significant change in its chemical structure under specific environmental conditions, resulting in a loss of some properties that may vary as measured by standard methods appropriate to the plastic and the application in a period of time that determines its classification” (Müller, 2005). This definition can be applied to many polymer degradation types (Hamid, 2000).

Biodegradation: Degradation of the polymers due to the microorganism attacks.

Chemical degradation: Occurs when the polymers brought into contact with chemicals such as acids, bases, solvents, etc.

Thermal degradation: It is the molecular deterioration of polymer due to heat. For thermoplastic polymers, this occurs at the melting temperature of the polymer, where the state of the polymer is transformed from solid to liquid. The components of the polymer backbone chain detach (molecular scission) and react with each other changing the properties of the polymer.

Mechanical degradation: Macroscopic changes occur in polymer material due to compression, tension, and shear forces.

Photodegradation: When polymers undergo physical and chemical changes due to ultraviolet light or visible light, inducing in Norrish reactions and/or crosslinking reactions.

Hygrothermal degradation: Substantial loss of weight and mechanical properties of a material due to the effects of moisture and temperature (Balakrishnan, Hassan, Imran, & Wahit, 2011).

Biodegradation

Since this chapter focuses on biobased biodegradable polymers, it is important to understand the biodegradation process. During biodegradation, living organism breakdown the organic substances to smaller and simpler structures resulting in chemical structure changes of the material (Figure 1.3). These smaller structures of monomers are mineralized to CO₂, H₂O, or CH₄ as end products (Shah et al., 2008). Abiotic parameters are useful factors in initiating the biodegradation process, as these parameters help to weaken the polymer structures (Jakubowicz, Yarahmadi, & Petersen, 2006; Lucas et al., 2008). Degraded products are entirely assimilated as a food source by soil microorganisms during biodegradation. It returns carbon into the ecosystem safely and effectively. Initial breakdown of the polymers prompts different kinds of physical

forces to occur such as heating/cooling, freezing/thawing, or wetting/drying, which results in mechanical damage in the polymer such as the cracking (Shah et al., 2008). Biodegradation of polymers includes the following steps, and the process could stop at any stage (Lucas et al., 2008).

- (a) *Biodeterioration*: Microbial and other decomposer organisms or/and abiotic factors break the biodegradable materials into small fractions.
- (b) *Depolymerization*: Microorganisms produces catalytic agents (enzymes and free radicals) that could cleave polymeric molecules reducing their molecular weight. This process generates units such as oligomers, dimers and monomers, that are small in size to transfer through the semi-permeable outer bacterial membranes (Shah et al., 2008).
- (c) *Assimilation*: Transferred molecules are exploited by microbes as carbon and energy sources in the cytoplasm to produce storage, vesicles energy, new biomass, and many types of metabolites that helps in maintaining cellular activity, structure, and reproduction. Thus, microorganisms grow while reproducing and consuming nutrient substrate from the environment.
- (d) *Mineralization*: It is possible for metabolites to be excreted and reach the extracellular surroundings. Molecules such as CO₂, N₂, CH₄ and H₂O are released to the environment. When O₂ is available, aerobic microorganisms produce microbial biomass, CO₂ and H₂O. Under anoxic conditions, anaerobic microorganisms produce microbial biomass, CO₂, CH₄, and H₂O as end products (Shah et al., 2008).

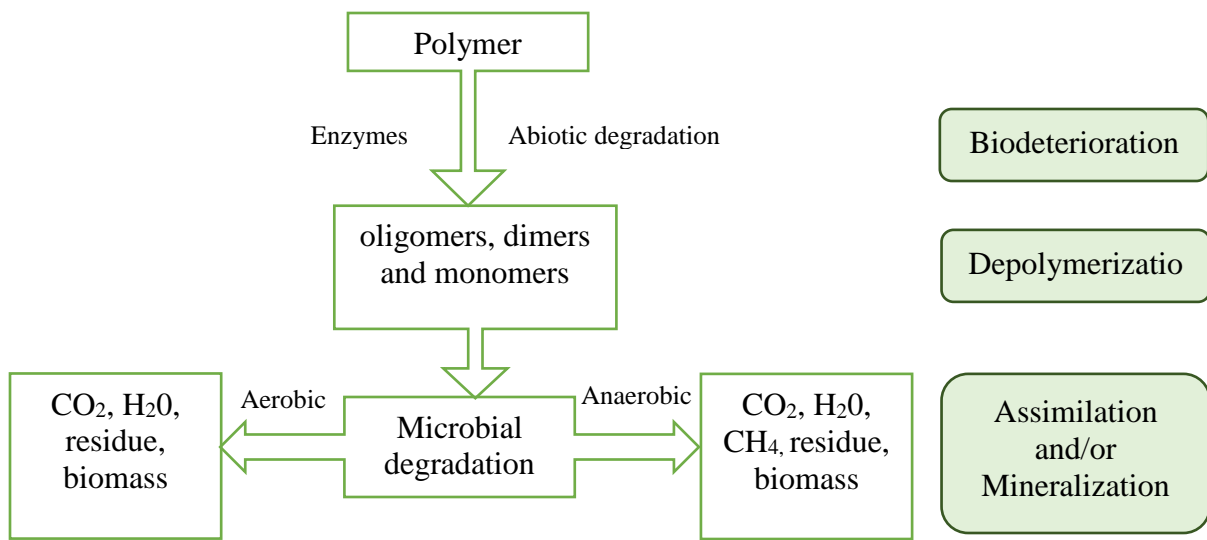


Figure 1.3. General mechanism of plastic biodegradation under aerobic and anaerobic conditions

Biodegradation Characteristics of Biopolymer Composites

Depending on the properties of the biopolymer, the biodegradation of plastics proceeds actively under different soil conditions as the microorganisms have their own optimal growth conditions in the soil (Shah et al., 2008). Results of soil biodegradation of PHA films and pellets in tropical Vietnamese soils revealed that the degradation of PHA depends on polymer chemical composition, specimen shape and microbial characteristics (Boyandin et al., 2013). The average mass loss rates were 0.04-0.33% and 0.02-0.18% per day for films and for compact pellets, respectively. Higher degradation of PHA film was attributed to the availability of larger surface area of films as it allowed better attachment of microorganisms and quicker formation of biofilms. When PHA was subjected degradation in natural environment in water reservoirs, it was revealed that biodegradation of polymer depends on the environment temperature and inorganic composition of water (Voinova, Gladyshev, & Volova, 2008). After 49 days at 19°C of water temperature, polymers degraded almost completely, having a residual weight of 2.3-5.2% of the initial value. Half-life of PHA at 19°C was 32 days, while it was 55 days at 5°C.

Biodegradability of manila hemp fiber reinforced starch-based plastics were studied in natural soil (only half buried in soil) and in compost soil (completely buried). The biodegradability and mechanical properties of the parts of specimens that were under soil changed significantly, while it was insignificant in the part exposed to atmosphere (Ochi, 2011). Tensile strength of composites decreased by 80% after 20 days in compost soil and 90 days in natural soil. Composted specimens lost 30% of weight at 90°C in 30 days, while the natural soil buried specimens had the same weight loss in 180 days, indicating accelerated degradation at elevated temperatures. When the specimen interaction with microbes is higher, significant loss of weight and strength can be observed.

Investigation on biodegradability of PLA/kenaf bast fiber (KBF) study showed that the decompositions of the composites were faster than pure PLA (Maizatunisa, Nor Azowa, Ruzaidi, Mohd Nazarudin, & Zahurin, 2012). Higher the addition of fiber to the PLA matrix, higher the micropore surface area of the PLA/KBF biocomposites were. Thus, the biodegradation rate was higher at higher fiber content. Similarly, for PHBV/peach palm particles (PPp) composites, soil biodegradation increased with increased content of PPp (Batista et al., 2010). Distance between the PPp and matrix in the composites amplified as the PPp content was increased. Higher the PPp content in the composites, higher the moisture absorption and microbial attack due to poor adhesion between PPp and the polymer matrix.

Sugar palm fiber (SPF) is used as a reinforcement material due to its high durability and resistance to seawater. At the end of 72 h of soil burial, sugar palm starch (SPS) lost 63.58% of its weight while it was 56.73% for SPF reinforced SPS composites (Sahari, Sapuan, Zainudin, & Maleque, 2014). The biodegradation rate of SPS was higher compared to the SPF/SPS biocomposites due to higher water intake of SPS, which made it more prone to microorganism

attack. Similarly, 8-month soil biodegradation of PHB and potato peel waste fermentation residue (PPW-FR) composites showed absolute debonding at higher filler content (50 wt%), while for lower (<50 wt%) fiber content composites only exhibited partial degradation (Wei et al., 2015). First component that was degraded was PPW-FR, resulting higher amount of PHB and holes on the surface of the specimens. In case of PHB, amorphous regions were degraded first followed by crystalline regions.

When PLA/silk fiber 5 wt% composites were immersed in Phosphate Buffered Saline (PBs) solution, moisture absorption increased due to hydrophilic properties of the silk, resulting in higher biodegradability and reduction in mechanical properties compared to neat PLA (Ho, Lau, Wang, & Bhattacharyya, 2011). Tensile strengths of both PLA and composites decreased from 70 MPa to 35-40 MPa and to 55-60 MPa, respectively. Another biodegradability study of PLA/silk fiber composites that was conducted using PBs (pH 7.4) showed that there were no significant differences between the weight loss for both pure PLA and silk/PLA biocomposites (Cheung, Lau, Pow, Zhao, & Hui, 2010). After 16 weeks, tensile strengths of the composite and neat PLA decreased from 65 MPa to 60 MPa, and from 61 MPa to 42 MPa, respectively. The higher property loss in the composites with respect to neat PLA was attributed to higher water intake of the composites due to increase in the area available for hydrolysis with the reinforcement of hydrophilic silk fiber.

The enzymatic biodegradation of PLA/cuphea fiber and PLA/lesquerella fiber composites revealed that extruded composites were more biodegradable than extruded and injection molded composites (Mohamed, Finkenstadt, Rayas-Duarte, Debra, & Gordon, 2009). Extruded composites exhibited 5-6% weight loss, while it was only 1-2% in extruded and injection molded composites. Unlike extruded composites, extruded and injection molded specimens had a better

fiber encapsulation on the surface. Consequently, enzymes only had access from the cut edges of the extruded and injection molded specimens.

When TPS/modified cellulose biocomposites were aged in Baltic Sea at Nordic Wharf of Gdynia harbor, samples showed a clear erosion of the surface and weight loss (Rutkowska & Heimowska, 2008). Modified cellulose was more affected by microbial attacks in sea water than TPS. Film form of starch/modified cellulose composites showed a more distinct weight changes than its sheet form due to large surface development at phase boundary.

Effect of Compatibilization on Biodegradation

Mechanical properties of composites strongly depend on the quality of the fiber-matrix interface (Batista et al., 2010). The main reason for poor interfacial adhesion between the polymer matrix and fibers is the hydroxyl and other polar groups of natural fibers which makes them hydrophilic in nature (Spiridon et al., 2013). Hemicelluloses and lignin in natural fibers are amorphous with high affinity for water. The hydrophilic fractions of the fibers with their free hydroxyl group makes it incompatible with the hydrophobic polymer matrix (Azwa et al., 2013). This leads to poor mechanical performance of the composites (Shah et al., 2008; C. S. Wu, 2012). However, mechanical properties of the biopolymer composites can be enhanced by introducing reactive functional groups such as compatibilizers and coupling agents [36, 39]. They form both hydrogen and covalent bonds with hydroxyl groups of fiber and molecular entanglement with polymer. When sisal fibers (SF 20 wt%) were blended with PLA (PLA/SF), and also with acrylic acid-grafted PLA (AA-g-PLA/SF), AA-g-PLA/SF showed higher tensile strength, water resistance, and lower biodegradability compared to PLA/SF due to the greater compatibility and adhesion (C. S. Wu, 2012). The rate of weight loss of the composites increased with increased SF content. Similar results were obtained for green coconut fiber (GCF) blended

PLA (PLA/GCF), and maleic anhydride (MA) grafted PLA/GCF composites (C.-S. Wu, 2009). After exposing the composites to *Burkholderia cepacia* bacterium, it was found that biodegradation rate of PLA-g-MA/GCF was higher than PLA, but lower than PLA/GCF, and the rate increased with addition of GCF. After 21 days, weight loss% of PLA, PLA/GCF and MA-g-PLA/GCF were about 15%, 80% and 75%, respectively.

Aerobic biodegradation of PLA/Coir natural fibers with thermoplastic starch (TPS) composite with maleic anhydride (MA) under controlled composting conditions was measured by the percentage of CO₂ produced (Iovino, Zullo, Rao, Cassar, & Gianfreda, 2008). At the end of aging period, TPS completely biodegraded due to the microorganism attacks on TPS domains. The amount of CO₂ produced for uncompatibilized composites was 101.5 g, while it was 95.3 g for composites with MA. This was attributed to hindered water or microorganism penetration due to improved interface interaction between matrix and fiber (Iovino et al., 2008).

Similar studies have been conducted for compatibilized PHB composites. Three different biocomposites of PHB with hemp, jute and lyocell fibers exhibited decreased melt flow index, impact and tensile strength with the addition of fibers (Gunning et al., 2013). After composting the samples (30 wt% fiber) using a rotary aerated composter, PHB/jute composites exhibited the highest level of biodegradation due to increased water absorption. When MA grafted PHB was used with the same fiber types, composites showed improved mechanical properties, but lower biodegradation rates (Gunning et al., 2014). However, when the temperature increased to 60°C in later weeks in the composter, the biodegradation rate of the composites with MA was higher than those without. After 12 weeks at rotary aerated composter, PHB, PHB/jute and MA-g-PHB/jute showed a weight loss of 35%, 50% and 80%, respectively. The MA increased fiber dispersion in the matrix compared to uncompatibilized ones. Thus, when the fiber debonded from the matrix at

higher temperatures, it increased the area available for microbial attack accelerating the degradation rate.

Acrylic acid (AA) grafted PHB/wood flour (Wf) composites subjected to soil and enzymatic biodegradation environments showed lower degradation than PHB/Wf, but higher than neat PHB (C. S. Wu, 2006). After 12 weeks, residual weight % of PHB/Wf and AA-g-PHB/Wf in soil was about 72% and 78%, respectively. As the wood flour content was increased, degradation rate of the composites increased due to increased difficulty in forming polymer chain arrangements. Water resistance was higher in AA-g-PHB/Wf than PHB/Wf composites, but lower than neat PHB. Hydrophilic nature of Wf and hydrophobic PHB caused the poor adhesion, which increased the water absorption resulting in increased rate of degradation.

Degradation of Biopolymer Composites due to Weathering

In order to use biodegradable biopolymer composites in outdoor applications, it is important to study the degradation behavior of these biocomposites under long-term weathering. To evaluate the weathering characteristics of biocomposites, materials are subjected to different weathering environments.

Accelerated Weathering

Due to the long-time duration of natural weathering, accelerated weathering is more commonly used. In accelerated weathering, the materials are aged in chambers that simulate natural environment. To transpire the damages that occurs during the long term outdoor exposure, weathering chambers induce harsh conditions with ultraviolet radiation, moisture and heat in a controlled manner. The PHB and PHB/hemp fiber composites subjected to accelerated weathering for 1998 h exhibited mass loss and fading (Michel & Billington, 2012). The fading was a result of absorbing UV by chromophores of hemp fibers and PHB. Mass loss of neat PHB

was due to surface erosion and reduction in molecular weight occurred due to UV photo-oxidative and cyclic hygrothermal degradation mechanism. Mass loss of PHB/hemp composites was attributed to weakened adhesion between the matrix and fiber due to different coefficients of thermal expansion of the polymer matrix and the fiber. The decline in tensile strength was 30% for PHB and 47% for the composites.

Impact of 600 h accelerated weathering on PLA/chitosan/keratin composites was investigated by Spiridon et al (Spiridon, Paduraru, Zaltariov, & Darie, 2013). Upon weathering, impact and tensile strength of PLA decreased from 11 to 4 kJ/m², and from 59 to 13 MPa, respectively. For PLA/chitosan and PLA/chitosan/keratin composites, tensile strength changed from 36 to 5 MPa and from 50 to 10 MPa. Impact strength remained constant at 8 kJ/m² for composites with keratin, while for PLA/chitosan it changed 7 to 5 kJ/m². Composites with no keratin exhibited higher property loss as a result of swelling of material due to water penetration into the hydrophobic matrix and the hydrophilic interface. Another accelerated weathering study conducted by Spiridon et al (Spiridon, Leluk, Resmerita, & Darie, 2015) for PLA with softwood lignin (LB), and with hardwood lignin (LO) showed deterioration of mechanical properties. Before weathering, the composites exhibited a good adhesion with improved thermal and mechanical properties. After weathering, Young modulus of the composites exhibited about 8% increase, while it decreased by 25% for neat PLA. Weathering decreased impact strength by 17% in composites and 60% in neat PLA. Decrease in properties was due to lessened PLA macromolecules lengths. Increase in modulus was due to recrystallization of material with weathering conditions.

Applications

A majority of biobased polymers are biodegradable and have the ability to replace the synthetic plastics. Biocomposites have gained a tremendous attention as they provide unique properties that do not exist naturally. Qualities such as biodegradability, air permeability and low temperature sealability of biopolymers lead them to be widely used in packaging applications (Vroman & Tighzert, 2009). Non-renewable and non-degradable synthetic polymers that used in food packaging have many health related issues (Thompson, Moore, Vom Saal, & Swan, 2009). Biobased biodegradable polymers provide containment and protection of food, and maintain quality and safety of food. Biobased polymers not only provide sustainable alternative for packaging but also biodegradability and compostability.

Following is a list of different applications of biobased biodegradable polymers that were discussed in this paper.

PLA

Among biopolymers, application of PLA has increased in the recent past due to its high mechanical strength, easy processability, and thermal stability (Balakrishnan et al., 2011). Due to its lower price and higher biodegradability, its composites have been widely used as packaging materials, paper coatings, planting cups, disposable cups and bottles, take-away food trays, containers and lawn waste bags. Potential markets for PLA include sustained release systems for pesticides and fertilizers, greenhouse films, transparent films for wrapping food and mulch films. Since its physical and melt processing properties similar to conventional packaging resins, it can be used as a commodity resin for general packaging applications (Petinakis et al., 2013).

PLA and kenaf fiber composites are employed in electronic applications, and in panels of car doors and dashboards. By incorporating carbon and kenaf fibers to PLA, NEC Corporation

(Japan) has produced a composite with improved thermal and flame retardancy properties (Babu, O'Connor, & Seeram, 2013). Compact disks and computer cases based on PLA were launched by Pioneer and Sanyo groups, and Fujitsu Company, respectively (Vroman & Tighzert, 2009).

As for its high strength and biocompatibility, PLA is frequently used in biomedical applications such as plates or screws for the treatment of fractures and to fill in bone defects, and as scaffolding to facilitate the formation of new cartilage material in the body. Since it has the ability to degrade in human body, PLA sutures are widely used in surgeries (Luckachan & Pillai, 2011).

PHA

The PHAs are used as an alternate for synthetic polymers such as polypropylene and polyethylene in agricultural applications. They are commonly used in commercial packaging, automotive and construction applications. Also as structural materials in personal hygiene products, and small disposable products like bottles, bags, wrapping film and disposable nappies (Babu et al., 2013). Biodegradability and apparent biocompatibility are main advantages of PHAs (Congress, 1993). Types of PHAs, such as PHB and PHBV are soluble in many solvents and can be processed into different shapes (Vroman & Tighzert, 2009). Also, PHB can degrade in D-3-hydroxybutyrate, which is a natural constituent of human blood. Thus, PHAs are commonly used in medical applications, such as long-term controlled drug release, drug carriers, tissue engineering scaffolds, surgical pins, sutures, and bone and blood vessel replacement (Shah et al., 2008). However, the brittleness of PHB limits its use in biomaterial. Compared to PHB, PHBV is less brittle, which makes PHBV more usable in this area (Congress, 1993).

Starch

Due to excellent biodegradability of starch, it is used in packaging, garbage bags and golf tees. Close to 75% of industrial starch produced is used as adhesives in paper, paperboard and related industries (Congress, 1993). Thermoplastic starch polymers are used in films, such as for overwraps, flushable sanitary product, packing materials, special mulch films, shopping bags and fishing bait bags (Babu et al., 2013). Some fishing hooks are also made from starch based polymers. Since cornstarch can absorb 1000 times its weight in moisture, it is used in disposable diapers, fuel filters to remove water, and as a treatment for burns (Vroman & Tighzert, 2009).

Other

Natural plant fibers like pineapple, sisal, coconut, coir, jute, hemp, ramie, flax, palm, cotton, rice husk, bamboo, banana and wood have been used as fillers and reinforcements in polymer matrix composites due to their light weight and low cost. Natural fiber based composites are extremely useful in the applications where high specific strength and stiffness required, such as in automobile interior components. Interior parts like absorption panels and spare wheel covers of Audi and Ford car models have incorporated jute, sisal and flax fibers (Chen, Li, & Ren, 2011). In addition, biocomposites that include fast degrading biomaterials can be used in agricultural and horticultural applications in crop/plant containers and agricultural mulch films (Wei et al., 2015).

For use in applications in biomedical area, it is necessary for biobased polymers to be biocompatible, bioabsorbable, and to have great mechanical resistance (Vroman & Tighzert, 2009). Hence, proteins are used in haemostatic agents, sutures and scaffolds for tissue engineering and drug delivery systems. Gelatin, which is an animal protein, is used for preparing

biodegradable hydrogels, and for coating and microencapsulating many drugs for biomedical applications.

Bacterial cellulose (BC) is extensively used in foods and acoustic diaphragms for audio speakers and headphones. Large surface area and great liquid absorbance properties of BC make it to use in very low concentrations to form excellent binding, thickening and coating agents (Congress, 1993). Papers that are coated with BC are extremely strong and smooth as the coating protects the underlying fibers from moisture. It is also used in medical applications as wound dressings and artificial skins, artificial blood vessels and tissue engineering scaffolds (Wan et al., 2009). Cellulose acetate is used in packaging, for blisters, skins, transparent rigid containers, and windows in folding or setup boxes. It is also used as a write-on pressure-sensitive tape such as for credit card receipts (Congress, 1993).

Conclusion

Biodegradable biobased polymers have gained much interest recently due to their low impact to the environment. There are several articles that highlights the importance of utilizing polymers and their composites from renewable resources instead of petroleum based polymers. Along with desirable properties, biobased polymers have disadvantageous properties in terms of strength, dimensional stability, and difficulty in processing. However, by blending biopolymers with other natural polymers/fibers, composites can be created with unique properties that do not exist naturally.

When fibers are added to polymers such as PLA, PHB and PHBV, an increase in degradation rate can be observed with increased content of fiber due to higher water absorption. Thus, fibers weaken the mechanical properties such as tensile and impact strength due to poor adhesion between the hydrophobic polymer matrix and the hydrophilic fiber of the composite.

However, a greater adhesion can be achieved by introducing reactive functional groups such as compatibilizers to the composites. Even though compatibilizers improve the properties of the composites they reduce the degradation rate due to higher water resistance. Nevertheless, both compatibilized and uncompatibilized composites have shown a complete debonding of fibers and matrix, and a complete degradation after some time duration. Overall, degradability of polymers depends on many factors such as environmental conditions, polymer chemical composition, specimen shape, processing method, fiber-matrix interaction, and microbial characteristics.

Recent advances in biobased polymers can be found in different sectors such as in biomedical area, agriculture, packaging, automotive, construction, electronic applications, and as binding, thickening and coating agents. It is clear that most biobased polymers can be engineered to have improved physico-mechanical and thermal properties and also can be fully or partially degraded with appropriate environmental conditions.

References

- Azwa, Z., Yousif, B., Manalo, A., & Karunasena, W. (2013). A review on the degradability of polymeric composites based on natural fibres. *Materials & Design*, 47, 424-442.
- Babu, R. P., O'Connor, K., & Seeram, R. (2013). Current progress on bio-based polymers and their future trends. *Progress in Biomaterials*, 2(8), 1-16.
- Balakrishnan, H., Hassan, A., Imran, M., & Wahit, M. U. (2011). Aging of toughened polylactic acid nanocomposites: water absorption, hygrothermal degradation and soil burial analysis. *Journal of Polymers and the Environment*, 19(4), 863-875.
- Batista, K., Silva, D., Coelho, L., Pezzin, S., & Pezzin, A. (2010). Soil biodegradation of PHBV/peach palm particles biocomposites. *Journal of Polymers and the Environment*, 18(3), 346-354.

- Bessadok, A., Belgacem, M. N., Dufresne, A., & Bras, J. (2010). Beneficial Effect of Compatibilization on the Aging of Cellulose-Reinforced Biopolymer Blends. *Macromolecular Materials and Engineering*, 295(8), 774-781.
- Boyandin, A. N., Prudnikova, S. V., Karpov, V. A., Ivonin, V. N., Đỗ, N. L., Nguyễn, T. H., . . . Filipenko, M. L. (2013). Microbial degradation of polyhydroxyalkanoates in tropical soils. *International Biodeterioration & Biodegradation*, 83, 77-84.
- Chen, D., Li, J., & Ren, J. (2011). Influence of fiber surface-treatment on interfacial property of poly (l-lactic acid)/ramie fabric biocomposites under UV-irradiation hydrothermal aging. *Materials Chemistry and Physics*, 126(3), 524-531.
- Cheung, H.-Y., Lau, K.-T., Pow, Y.-F., Zhao, Y.-Q., & Hui, D. (2010). Biodegradation of a silkworm silk/PLA composite. *Composites Part B: Engineering*, 41(3), 223-228.
- Congress, U. (1993). Biopolymers: Making Materials Nature's Way'. *Office of Technological Assessement*, 51-62.
- Gilmore, D. F., Fuller, R. C., & Lenz, R. (1990). Biodegradation of poly (beta-hydroxyalkanoates). *Degradable materials: perspectives, issues and opportunities*. CRC, Boston, 481-514.
- Gunning, M. A., Geever, L. M., Killion, J. A., Lyons, J. G., & Higginbotham, C. L. (2013). Mechanical and biodegradation performance of short natural fibre polyhydroxybutyrate composites. *Polymer Testing*, 32(8), 1603-1611.
- Gunning, M. A., Geever, L. M., Killion, J. A., Lyons, J. G., & Higginbotham, C. L. (2014). Effect of Compatibilizer Content on the Mechanical Properties of Bioplastic Composites via Hot Melt Extrusion. *Polymer-Plastics Technology and Engineering*, 53(12), 1223-1235.

- Hamid, S. (2000). *Handbook of Polymer Degradation* (Second ed.): CRC Press.
- Ho, M.-p., Lau, K.-t., Wang, H., & Bhattacharyya, D. (2011). Characteristics of a silk fibre reinforced biodegradable plastic. *Composites Part B: Engineering*, 42(2), 117-122.
- Iovino, R., Zullo, R., Rao, M., Cassar, L., & Gianfreda, L. (2008). Biodegradation of poly (lactic acid)/starch/coir biocomposites under controlled composting conditions. *Polymer Degradation and Stability*, 93(1), 147-157.
- Jakubowicz, I., Yarahmadi, N., & Petersen, H. (2006). Evaluation of the rate of abiotic degradation of biodegradable polyethylene in various environments. *Polymer degradation and stability*, 91(7), 1556-1562.
- Lucas, N., Bienaime, C., Belloy, C., Queneudec, M., Silvestre, F., & Nava-Saucedo, J.-E. (2008). Polymer biodegradation: Mechanisms and estimation techniques—A review. *Chemosphere*, 73(4), 429-442.
- Luckachan, G. E., & Pillai, C. (2011). Biodegradable polymers-a review on recent trends and emerging perspectives. *Journal of Polymers and the Environment*, 19(3), 637-676.
- Madbouly, S., Schrader, J., Srinivasan, G., Haubric, K., Liu, K., Grewell, D., . . . Kessler, M. (2012). *Bio-based Polymers and Composites for Container Production Materials*. Paper presented at the 2012 Bioplastic Container Cropping Systems Conference, Iowa State University.
- Maizatunisa, O., Nor Azowa, I., Ruzaidi, C. M., Mohd Nazarudin, Z., & Zahurin, H. (2012). *Biodegradability analysis of KBF reinforced poly (lactic acid) biocomposites*. Paper presented at the Advanced Materials Research.

- Michel, A., & Billington, S. (2012). Characterization of poly-hydroxybutyrate films and hemp fiber reinforced composites exposed to accelerated weathering. *Polymer Degradation and Stability*, 97(6), 870-878.
- Mohamed, A., Finkenstadt, V., Rayas-Duarte, P., Debra, E., & Gordon, S. H. (2009). Thermal properties of extruded and injection-molded poly (lactic acid)-based cuphea and lesquerella bio-composites. *Journal of applied polymer science*, 111(1), 114-124.
- Mukherjee, T., & Kao, N. (2011). PLA based biopolymer reinforced with natural fibre: a review. *Journal of Polymers and the Environment*, 19(3), 714-725.
- Ochi, S. (2011). Durability of starch based biodegradable plastics reinforced with Manila hemp fibers. *Materials*, 4(3), 457-468.
- Petinakis, E., Simon, G., Dean, K., & Yu, L. (2013). *Natural Fibre Bio-Composites Incorporating Poly (Lactic Acid)*: INTECH Open Access Publisher.
- Rutkowska, M., & Heimowska, A. (2008). Degradation of Naturally Occurring Polymeric Materials in Sea Water Environment. *Polimery*, 53(11-12), 854-864.
- Rutkowska, M., Krasowska, K., Heimowska, A., Adamus, G., Sobota, M., Musioł, M., . . . Żagar, E. (2008). Environmental degradation of blends of atactic poly [(R, S)-3-hydroxybutyrate] with natural PHBV in Baltic Sea water and compost with activated sludge. *Journal of Polymers and the Environment*, 16(3), 183-191.
- Sahari, J., Sapuan, S. M., Zainudin, E. S., & Maleque, M. A. (2014). Degradation characteristics of SPF/SPS biocomposites. *Fibres & Textiles in Eastern Europe*.
- Schnabel, W. (1981). *Polymer Degradation*: Macmillan Publishing.
- Shah, A. A., Hasan, F., Hameed, A., & Ahmed, S. (2008). Biological degradation of plastics: a comprehensive review. *Biotechnology advances*, 26(3), 246-265.

- Spiridon, I., Leluk, K., Resmerita, A. M., & Darie, R. N. (2015). Evaluation of PLA–lignin bioplastics properties before and after accelerated weathering. *Composites Part B: Engineering*, *69*, 342-349.
- Spiridon, I., Paduraru, O. M., Zaltariov, M. F., & Darie, R. N. (2013). Influence of keratin on polylactic acid/chitosan composite properties. Behavior upon accelerated weathering. *Industrial & Engineering Chemistry Research*, *52*(29), 9822-9833.
- Thompson, R. C., Moore, C. J., Vom Saal, F. S., & Swan, S. H. (2009). Plastics, the environment and human health: current consensus and future trends. *Philosophical Transactions of the Royal Society of London B: Biological Sciences*, *364*(1526), 2153-2166.
- Voinova, O., Gladyshev, M., & Volova, T. G. (2008). *Comparative study of PHA degradation in natural reservoirs having various types of ecosystems*. Paper presented at the Macromolecular symposia.
- Vroman, I., & Tighzert, L. (2009). Biodegradable polymers. *Materials*, *2*(2), 307-344.
- Wan, Y., Luo, H., He, F., Liang, H., Huang, Y., & Li, X. (2009). Mechanical, moisture absorption, and biodegradation behaviours of bacterial cellulose fibre-reinforced starch biocomposites. *Composites Science and Technology*, *69*(7), 1212-1217.
- Wei, L., Liang, S., & McDonald, A. G. (2015). Thermophysical properties and biodegradation behavior of green composites made from polyhydroxybutyrate and potato peel waste fermentation residue. *Industrial Crops and Products*, *69*, 91-103.
- Wu, C.-S. (2009). Renewable resource-based composites of recycled natural fibers and maleated polylactide bioplastic: Characterization and biodegradability. *Polymer Degradation and Stability*, *94*(7), 1076-1084.

Wu, C. S. (2006). Assessing biodegradability and mechanical, thermal, and morphological properties of an acrylic acid-modified poly (3-hydroxybutyric acid)/wood flours biocomposite. *Journal of applied polymer science*, 102(4), 3565-3574.

Wu, C. S. (2012). Preparation, characterization, and biodegradability of renewable resource-based composites from recycled polylactide bioplastic and sisal fibers. *Journal of Applied Polymer Science*, 123(1), 347-355.

CHAPTER 2. COMPATIBILIZATION IMPROVES PHYSICO-MECHANICAL PROPERTIES OF BIODEGRADABLE BIOBASED POLYMER COMPOSITES

Abstract

Biodegradable biobased polymer composites have the advantage of low environmental impact and high sustainability. However, these biocomposites exhibit poor mechanical properties due to poor fiber-matrix interfacial interaction. This study evaluated the effect of compatibilization of five biocomposites on their physico-mechanical properties. Composites were prepared with 30 wt% wood fiber and one of the five biodegradable biopolymer: poly(lactic acid) (PLA), polyhydroxybutyrate (PHB), poly(3-hydroxybutyrate-co-3-hydroxyvalerate) (PHBV), Bioflex (PLA blend), or Solanyl (starch-based). The composites were compatibilized with 2-3 wt% maleic anhydride, and evaluated for melt flow index, water uptake, hardness, flexural, compressive, impact and thermal properties. Melt flow index was reduced by 10-16% for compatibilized composites implying the crosslinking of the polymer. Compatibilized composites of PLA, Bioflex and PHBV exhibited improved thermal and strength properties, and reduced water absorption. These improvements were attributed to the enhanced fiber-matrix interfacial interaction caused by the compatibilizer. However, compatibilization did not work in PHB and Solanyl.

Introduction

Biodegradable polymers produced from renewable and biobased resources reduce waste accumulation, do not contribute to CO₂ emissions and ease dependency on petroleum-based fuels and products. Along with their positive impact to environment, biodegradable biobased polymers have many other desirable properties such as biocompatibility, bioactivity, chemical inertness, high stiffness and strength, good film-forming properties and low toxicity (Bessadok, Belgacem,

Dufresne, & Bras, 2010; Suryanegara, Nakagaito, & Yano, 2009). Although biobased polymers have numerous benefits compared to conventional plastics, they usually have high cost, higher crystallinity, sensitivity to thermal degradation, and poor mechanical properties (W. Srubar et al., 2012; Suryanegara et al., 2009).

By blending biobased polymers with other biodegradable natural fillers to create a composite, the overall mechanical and degradation properties can be improved while reducing cost (Gunning, Geever, Killion, Lyons, & Higginbotham, 2013; Petinakis, Yu, Simon, & Dean, 2013). Despite higher mechanical properties of synthetic fibers such as glass fibers, natural fibers are attractive due to growing concern over environmental and ecological impacts and societal preferences. For example, wood fiber (WF) is an inexpensive and readily available byproduct from furniture manufacturing and other wood processing businesses that is reused as a filler in polymer composites (Shah, Selke, Walters, & Heiden, 2008). Properties such as specific strength, ease of separation, low density, and carbon dioxide seizure are beneficial characteristics of natural fibers over synthetic fibers such as glass or carbon fibers (Mukherjee & Kao, 2011). Natural fibers serve as good reinforcements and fillers in biocomposites for a myriad of reasons including low cost, fewer health hazards during processing, less abrasiveness to processing equipment, and good specific strength, electric and acoustic properties (Batista, Silva, Coelho, Pezzin, & Pezzin, 2010).

Poor interfacial adhesion between the hydrophobic polymer and hydrophilic natural fibers causes decrease in some mechanical strength properties and increase affinity to water of the composites (Gunning et al., 2013). Mechanical properties of polymer composites can be improved by introducing reactive functional groups such as compatibilizers and coupling agents (Gunning, Geever, Killion, Lyons, & Higginbotham, 2014). Grafting a compatibilizer into a

polymer enhances the miscibility between the polymer and natural fiber, which improves the overall mechanical and thermal properties. One of the most commonly used compatibilizers, maleic anhydride (MA), forms hydrogen and covalent bonds with hydroxyl groups of the fiber and induce molecular entanglement with the polymer. These bonds improve the adhesion between the polymer and the fiber, and a better dispersion of fibers in the polymer matrix. Even though there are many studies conducted with several different natural fiber-polymer composites, there is only limited research reported on the effect of compatibilization on biodegradable biobased polymer composites with wood fiber (WF) as a filler (W. V. Srubar et al., 2012). Therefore, a study was conducted to understand the impact of wood fiber fillers and compatibilizer on five biodegradable biopolymers. The following questions were asked in this study.

1. How does incorporating wood fiber filler into five different biobased biodegradable polymers affect their mechanical, thermal, and water absorption properties?
2. Does compatibilization of the biopolymer-natural fiber composites with MA improve their mechanical, thermal, and water absorption properties?

In this study, five types of MA-compatibilized biocomposites were prepared by compounding wood fiber (WF) with five different types of biopolymers: poly(lactic acid) (PLA), Bioflex (BF, PLA blend), Solanyl (SL, starch-based), poly(3-hydroxybutyric acid) (PHB), and poly(3-hydroxybutyrate-co-3-hydroxyvalerate) (PHBV). The effect of WF loading and compatibilization on mechanical and physical properties was evaluated using tests for water absorption, melt flow index, hardness, impact fracture energy, compressive strength, and flexural strength and modulus. The influence of compatibilization and WF loading on the melting

behavior and crystallinity of biocomposites was studied using Differential scanning calorimetry (DSC).

Experimental Procedure

Materials

PLA used in this study was type 2003D from NatureWorks LLC (Minnetonka, MN). PLA is produced by polymerization of lactic acid. Lactic acid is a sugar fermentation product from corn, sugar beets, sugar cane, or potatoes. The PHB (ENMAT Y3000P) and PHBV (ENMAT Y1000P) were supplied by TianAN Biopolymer (Ningbo City, Zhejiang Province, China). Both PHB and PHBV are examples of polyhydroxyalkanoates (PHA). Polyhydroxyalkanoates are produced by bacterial fermentation of sugar or lipids. Bioflex (BF) biopolymer (Bio-Flex® F2110) was obtained from FKUR Plastics (Willich, Germany). Solanyl (SL) biopolymer (Solanyl® C2201) was purchased from Rodenburg Biopolymers (Oosterhout, Netherlands). The SL is made from potato starch reclaimed from the food processing industry, while BF is a PLA blend. Maleic anhydride (63200), Luperox® P: tert-Butyl peroxybenzoate (TBPB), benzoyl peroxide (BP), and Luperox 101: 2,5-bis(tert-butylperoxy)-2,5-dimethylhexane (L101) were purchased from Sigma-Aldrich Chemical Co. (St. Louis, MO). The WF used in this study was from oak wood.

Polymer Composite Manufacturing

Preparation of Grafted Polymer

The procedure for biopolymer grafting included mixing each of the polymer with MA and an initiator, and then extruding them with a micro 18 lab-scale twin screw extruder with a 40/1 length to diameter ratio (Leistritz Ltd., Somerville, NJ). It is a high shear force extruder with two co-rotating screws. It is mostly used for blending components. The diameter of the die

that was used is about 3 mm. Prior to extrusion, all the polymer pellets were dried according to recommended conditions provided by the supplier. The PHB and PHBV polymers were dried at 80°C for 2 hours (h), PLA at 80°C for 6 h, SL at 45°C for 4 h, and BF at 60°C for 3 h. For grafting, 2-3 wt% of Maleic anhydride (MA) and 0.5-1 wt% of a specific initiator (TBPB, BP, or L101) were hand-mixed with each polymer in a zip-lock plastic bag (Table 2.1). The mixture was then compounded via extrusion, cut into pellets, and dried at 80°C in an oven for 12 h. Extrusion temperature profiles used for PLA, BF, SL, PHB and PHBV were all different as shown in Table 2.2.

Table 2.1. Compositions of maleic anhydride (MA) grafted Polymers.

Polymer Formulations	Amount of polymer, MA and initiator used in grafting (wt %)									
	PLA	BF	SL	PHB	PHBV	MA	L101	TBPB	BP	
MA-g-PLA	97.5					2	0.5			
MA-g-BF		97.5				2	0.5			
MA-g-SL			97.5			2				0.5
MA-g-PHB				96		3			1	
MA-g-PHBV					96	3			1	

Table 2.2. Temperature profile used for extrusion for grafting with maleic anhydride (MA) and compounding of polymer with wood fiber (WF).

Polymer	Extruder Temperature (°C)									Screw RPM
	Zone 1	Zone 2	Zone 3	Zone 4	Zone 5	Zone 6	Zone 7	Zone 8	Die	
PLA	140	150	160	170	180	190	200	190	180	150
PHB	130	135	140	145	150	155	160	155	150	200
PHBV	140	145	150	155	160	170	180	170	160	200
BF	150	155	160	165	170	175	180	170	160	150
SL	130	135	140	145	150	150	160	150	140	120

Preparation of WF composites

All the composites were manufactured with 30 (wt%) WF loading. For compatibilized composites, WF was hand mixed with grafted polymer and neat polymer pellets according to compositions shown in Table 2.3. For uncompatibilized composites, the WF was hand mixed only with neat polymer (Table 2.3). The mixture of WF, polymer, and/or MA grafted polymer were then compounded using the same twin screw extruder used for the preparation of grafted polymer composites, using the same temperature setting shown in Table 2.2. All the extruded strands were water cooled, cut into pellets, and dried at 80°C in an oven for 24 h.

Table 2.3. Compositions of biocomposites made with five different biopolymers with wood fiber (WF), and with and without maleic anhydride (MA).

Treatment No	Composite treatments	Amount of each ingredient in composite (wt %)		
		Polymer	MA grafted polymer	Wood Fiber
1	PLA/WF	70	0	30
2	BF/WF	70	0	30
3	SL/WF	70	0	30
4	PHB/WF	70	0	30
5	PHBV/WF	70	0	30
6	MA-g-PLA/WF	66	4	30
7	MA-g-BF/WF	66	4	30
8	MA-g-SL/WF	66	4	30
9	MA-g-PHB/WF	65	5	30
10	MA-g-PHBV/WF	65	5	30

Compression Molding

After drying, composite pellets were compression molded into 150 mm square, 5 mm thick sheets using a Carver hot press (model 3856, Carver Inc., Wabash, IN) at 50 atm pressure. The molding temperature was maintained at 180°C for all polymers except SL, which was kept at

150°C. The molding time was also different for different polymers (Table 2.4). The molded sheets were allowed to cool slowly under ambient conditions to prevent cracking.

Table 2.4. Temperature profile used for compression molding.

	Temperature (°C)	Time held at 50 atm (min.)
PLA and composites	180	7
BF and composites	180	10
SL and composites	150	10
PHB and composites	180	8
PHBV and composites	180	7

Characterization of Composites

Differential scanning calorimetry

To determine the thermal properties of composites, approximately 8 mg of each sample was characterized using a Q20 Dynamic Scanning Calorimeter (TA Instruments, New Castle, DE). All samples were first equilibrated at 25°C, then heated from 25°C up to 200 °C at the rate of 10°C/min under N₂ atmosphere. From the heating scan, glass transition temperature (T_g), cold crystallization temperature (T_{cc}), melt temperature (T_m), crystallization enthalpy (ΔH_c), and melting enthalpy (ΔH_m) were determined. The degree of crystallinity (X%) of the samples was evaluated as follows, (Eq. 2.1):

$$X\% = \frac{\Delta H_m - \Delta H_c}{\Delta H_m^0(w_p)} 100\% \quad (\text{Eq. 2.1})$$

where, w_p is the polymer fraction in the composites, and ΔH_m⁰ is the estimated melting enthalpies of their respected pure polymer, which is 93.7 J/g for PLA and BF, and 146 J/g for PHB and PHBV (Abdulkhani, Hosseinzadeh, Dadashi, & Mousavi, 2015; W. Srubar et al., 2012).

Melt Flow Index (MFI)

To measure the changes in MFI that occurred due to fiber loading and compatibilization, composite pellet samples were evaluated using a Tinius Olsen melt flow indexer (model MP1200, Tinius Olsen, Horsham, PA) according to ASTM D1238 standard (D. ASTM, 2004) with a fixed weight of 2.16 kg at melting temperatures provided in the standard and also by the polymer supplier (Table 2.5).

Table 2.5. Temperatures at which MFI was calculated for each polymer.

Polymer	Temperature (°C)
PLA	210
PHB	180
PHBV	180
BF	190
SL	170

Water Absorption

To measure the water absorption of samples, Eq. 2.2 was used as specified by ASTM D570 standard ("ASTM D570," 2010). All the test specimens were 38.1 mm long and wide, and 5 mm in thickness. Weights were measured every 24 h for 5 weeks.

$$\% \text{Increase in weight } (M_t) = \frac{\text{wet weight} - \text{conditioned weight}}{\text{conditioned weight}} \times 100 \quad (\text{Eq. 2.2})$$

Diffusivity (D) was analyzed with the hypothesis of a Fickian mechanism- Fick's second law of diffusion, which is given by Eq. 2.3 (Balakrishnan, Hassan, Imran, & Wahit, 2011):

$$\frac{M_t}{M_m} = 1 - \frac{8}{\pi^2} \exp \left[- \left(\frac{D_t}{h^2} \right) \pi \right] \quad (\text{Eq. 2.3})$$

where, 't' is the time, 'h' is the thickness of the sample, and M_m is the maximum water absorption capacity. The M_m was calculated by taking the average of several consecutive

measurements once the sample weight has stabilized. Diffusivity (D) was calculated using Eq. 2.4 (Balakrishnan et al., 2011):

$$D = \frac{\pi h^2 (M_2 - M_1)^2}{16 M_m^2 (\sqrt{t_2} - \sqrt{t_1})^2} \quad (\text{Eq. 2.4})$$

where, M_1 and M_2 are the % weight gain at times t_1 and t_2 , respectively.

Mechanical Properties

Following mechanical properties of the polymers and composites were evaluated (Table 2.6). Five specimens from each batch were used in each property testing.

Table 2.6. Evaluated mechanical properties.

Mechanical property tested	Standard used	Equipment used	Other
Impact fracture energy (notched)	ASTM D256 ("ASTM D256," 2010) method A	Tinius Olsen Impact tester (model IT504, Tinius Olsen, Horsham, PA)	Pendulum with 4.497 N of weight and 334.949 mm of radius. Notch of 2.54 mm was made on each sample.
Flexural modulus and strength	ASTM D790 (I. ASTM, 2007)	Instron 5567 load frame (Instron, Norwood, MA)	2kN load cell was used with a cross head rate of 2 mm/min.
Surface Hardness	ASTM D2240 (D. ASTM, 2000) (manual operation method)	type D durometer (Model 409, S/N 02015, Davis Instrumentation, Vernon Hills, IL)	Eq. 2.5 was used to calculate force. Force, N = (0.4445) HD (Eq. 2.5) HD is the hardness reading on durometer.
Compressive strength	ASTM D695 (International, 2010)	Instron 5567 load frame (Instron, Norwood, MA)	30kN load cell was used with a cross head rate of 1.3 mm/min.

Fourier transform infrared spectroscopy (FTIR)

FTIR spectroscopy testing of PHB and SL samples was conducted using a Nicolet Magna spectrometer (Modal Nicolet 8700, Thermo Scientific, Waltham, MA) and MTEC photoacoustic

detector (Model 300, MTEC Photoacoustic Inc., Ames, IA). Analysis was performed with 32 scans in wavenumbers ranging from 4000 to 650 cm^{-1} for a spectral resolution of 4 cm^{-1} .

Gel permeation chromatography (GPC)

The molecular weight of neat SL and composites was analyzed by a gel permeation chromatography (GPC) system (EcoSEC HLC-8320GPC, Tosoh Bioscience, Tokyo, Japan) with a differential refractometer (DRI) detector. Tetrahydrofuran (THF) was used as the solvent at a flow rate of 0.4 mL/min. The detector temperature was 40°C. The sample concentration was 1.0 mg/mL in THF, and the injection volume was 20 μL . Separations were performed using two TSKgel SuperHM-L 6.00 mm ID \times 15 cm columns. Calibration was conducted using PS standards (Agilent EasiVial PS-H 4ml).

Data Analysis

Tukey's test of multiple comparisons ($P < 0.05$) was applied to determine significant differences between the mechanical properties of neat polymers and composites. Data analysis was performed with Minitab software (version 18, Minitab Inc., PA).

Cost Analysis

The cost of the neat and composites produced was calculated using Eq. 2.6. Prices for polymers and fibers were calculated at the cost per kg for 1 ton of material. Prices of the polymers and fiber are in \$/kg.

$$\text{Price per kg} = \%F(Fc) + \%P(Pc) + \%MA(MAc) + \%IN(INc) \quad (\text{Eq. 2.6})$$

Where, %F is the percentage of fiber used, Fc is the cost of fiber per kg, %P is the percentage of polymer used, Pc is the cost of the polymer per kg, %MA is the percentage of MA used, MAc is the cost of MA per kg, %IN is the percentage of initiator used, and INc is the cost of initiator per kg.

Results and Discussion

Thermal Properties

Thermal behavior is a crucial factor in physico-mechanical behavior of polymers as it influences the arrangement of amorphous/crystalline phase. Overall, compatibilized composites exhibited improved thermal properties compared to the uncompatibilized composites (Table 2.7).

Table 2.7. Thermal properties of the composites with and without compatibilizer, in relation to that of neat polymer used in the study. Here, T_g is glass transition temperature, T_{cc} is cold crystallization temperature, T_m is melting temperature, ΔH_c is crystallization enthalpy, ΔH_m is melting enthalpy and X (%) is crystallinity of the specimens.

Composition	T_g (°C)	T_{g2} (°C)	T_{cc} (°C)	ΔH_c (J/g)	T_{m1} (°C)	T_m (°C)	ΔH_m (J/g)	X (%)
PLA	64.2		135.44	3.09		167.8	21.4	19.54
PLA/WF	61.12		145.45	3.38		164.66	30.77	41.77
MA-g-PLA/WF	62.52		145.55	3.33		165.33	31.55	43.08
BF	60.2		101.7	2.61		147.7	5.67	3.26
BF/WF	59.76		98.05	3.75		146.88	3.98	0.35
MA-g-BF/WF	62.59	83.78	136.47	0.48		147.14	3.47	4.57
SL	54		92.8	11.04	137.97	148.49	15.77	
SL/WF	55					152.99	13.87	
MA-g-SL/WF	55.1					149.8	11.53	
PHB	1.07					178.9	100.3	68.7
PHB/WF	-1.97					172.19	61.22	59.9
MA-g-PHB/WF	-4.06					171.8	62.14	59.6
PHBV	-0.33					170.4	110.2	75.48
PHBV/WF	1.84					160.8	72.4	70.8
MA-g-PHBV/WF	1.92					161	73.2	71.83

The MA grafted PLA, BF and PHBV composites exhibited an increase in glass transition temperature (T_g) compared to uncompatibilized composites, which is in agreement with the results obtained by Wu et al (Wu, 2009) for the acrylic acid-grafted PLA composites. The addition of WF reduced T_g in PLA, BF, PHB and PHBV compared to the neat polymers due to

weak interaction between WF and the polymer matrix. Since the mobility of polymeric chains is one of the important factors affecting T_g , the slight increase in T_g in compatibilized composites compared to uncompatibilized ones can be ascribed to improved fiber-matrix interactions.

Grafting MA carboxyl groups to the polymer resulted in restricting the mobility of the polymer chains near the fibers due to reduced space available for molecular motion (Wu, 2009). Maleic anhydride interacts mainly with hydroxyl groups (-OH) of cellulose to form covalent or hydrogen bonding (Babu, O'Connor, & Seeram, 2013). However, T_g of MA grafted PHB composites is lower than PHB/WF, which could be an indication of weak fiber-matrix interaction in compatibilized composites. The SL/WF composites exhibited higher T_g compared to neat SL, but compatibilization did not affect the T_g in SL composite. Starch is a hydrophilic material, and SL is a starch based polymer. Thus, there is good compatibility and hydrogen bonding interactions between the hydrophilic starch and natural fibers due to chemical similarities (Wan et al., 2009). Consequently, the increase in T_g could be due to the intermolecular interactions occurring between the starch and WF, which restricted the mobility of the amorphous starch chains in contact with WF (Cao, Chen, Chang, Stumborg, & Huneault, 2008). Compatibilized BF composites exhibited two glass transition temperatures. This could be due to the immiscibility of the composite. Miscibility of the binary polymer blends can be investigated by the number of glass transitions (Bourara, Hadjout, Benabdelghani, & Etxeberria, 2014).

Neat SL exhibited a bimodal melting peak, in which the first melting peak (T_{m1}) occurred at 137.97°C. Polymers exhibit multiple melting peaks due to partial melting, recrystallization, and melting of crystals with different lamellar thickness (Gunaratne & Shanks, 2008). With the incorporation of WF, the T_{m1} peak and cold crystallization diminished. Except for SL, the T_m of all the composites with no MA decreased slightly, indicating a weak interaction between WF and

the polymer matrix (Abdulkhani et al., 2015). The SL/WF composite exhibited a 4.5 °C increase in T_m compared to neat SL, signifying strong interaction between SL and WF, as expected when both matrix and fiber are hydrophilic in nature. On the other hand, the MA grafted PLA, BF and PHBV composites exhibited increase in T_m , compared to uncompatibilized composites.

Addition of WF to neat polymers decreased the crystallinity ($X\%$). This could be a result of change in the crystalline structure of the pure polymer matrix due to steric effect, wherein the hydrophilic nature of WF led to poor adhesion with hydrophobic polymer matrix (Wu, 2009). The compatibilized PLA, BF and PHBV composites showed higher crystallinity compared to their uncompatibilized ones. This can be attributed to the nucleating effect of MA, which can assist in forming more crystals in the polymer structure (Roumeli et al., 2015). Crystallinity of SL could not be determined due to limited availability of necessary information to calculate the degree of crystallinity. The higher crystallinity of PLA composites compared to neat PLA showed that the presence of WF accelerates the crystallization of PLA (Suryanegara et al., 2009). Reduced ΔH_m suggests a less perfect arrangement of polymer crystal structures as WF was added to the polymer matrices. Similar results can be seen in the literature for microcrystalline cellulose, microfibrillated cellulose, and pulp fiber reinforcements (Mathew, Oksman, & Sain, 2005; Suryanegara et al., 2009).

Melt Flow Index (MFI)

Compatibilized composites exhibited a decrease in MFI compared to their neat polymers and composites with no compatibilizer (Figure 2.1). Compatibilized BF, PHB and PHBV composites showed about 16% decrease in MFI, while compatibilized PLA and SL exhibited 10% decrease in MFI compared to their uncompatibilized composites. MFI decreases uniformly with increase in degree of crosslinking (Tamboli, Mhaske, & Kale, 2004). MA is an α , β -

unsaturated carbonyl compound, which has a conjugated structure with a carbon-carbon double bond and two carboxylate groups. When an initiator is added, this structure significantly increases the graft reactivity of the C=C bond with the polymer matrix, resulting in crosslinking or strong interfacial adhesion (Lu, Wu, & McNabb, 2007). Zig-zag structure of a cross linked polymer provides the elastic property, thus, increasing the impact properties of the composite (Tamboli et al., 2004). In contrast, a previous study has shown that compatibilization of PHB increased its MFI due to increased interaction between the polymer and the fiber, as a result of MA side chains (Gunning et al., 2014).

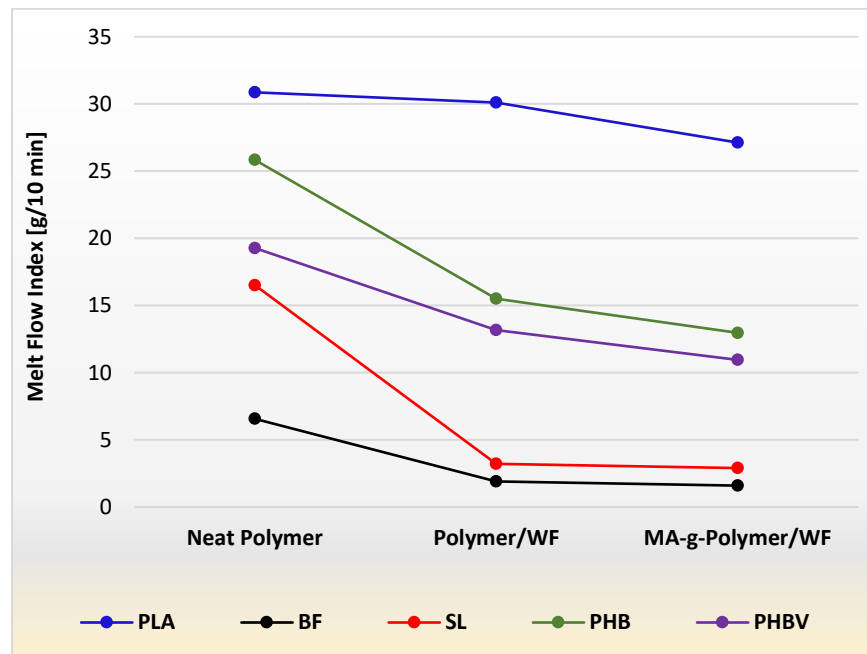


Figure 2.1. Melt flow index of the neat, uncompatibilized and MA compatibilized polymer specimens (PLA, BF, SL, PHB and PHBV).

Water Absorption

The water absorption of the composites was many times higher than the corresponding neat polymers (Table 2.8). The SL and its composites exhibited the highest water absorption compared to other polymers due to the high hydrophilicity of the starch based SL polymer. The

addition of MA decreased the water absorption of composites. The diffusion coefficient (D) determines the ability of the solvent to move along the polymer segment. The higher M_m (maximum moisture content) values show the increased equilibrium moisture absorption while the smaller D values show the decreased moisture diffusion rate (Table 2.8). Higher M_m values were observed for PLA, BF and PHBV composites with no compatibilizer. Use of MA resulted in reductions in M_m and D for PLA, BF and PHBV composites, as also observed by other researchers (Gunning et al., 2014; Wu, 2009). Decrease in M_m in compatibilized composites was due to reduced diffusion rate. When compatibilized, improved adhesion between matrix and fibers causes to lower the diffusional rate process as there are fewer gaps available in the interfacial region. This results in lower water accumulation in the interfacial voids, thus, preventing water from entering to natural fiber (Arbelaiz et al., 2005). On the other hand, addition of MA to SL and PHB composites did not reduce the M_m and D values with respect to their uncompatibilized composites. Instead, those values were slightly higher than that of uncompatibilized composites.

Table 2.8. Equilibrium water content (M_m) and diffusivity (D) of the neat biopolymer and composite specimens.

Composition	M_m	D ($\times 10^{-6}$ mm ² /s)
PLA	0.87	4.87
PLA/WF	11.86	1.3
MA-g-PLA/WF	7.86	0.88
BF	1.04	5.71
BF/WF	7.82	2.11
MA-g-BF/WF	7.73	1.94
SL	17.99	2.79
SL/WF	34.32	9.85
MA-g-SL/WF	37.29	12.78
PHB	0.61	2.85
PHB/WF	10.15	0.84
MA-g-PHB/WF	11.23	0.86
PHBV	0.69	1.46
PHBV/WF	8.64	0.83
MA-g-PHBV/WF	7.4	0.77

Mechanical Properties

Impact Properties

The impact toughness of polymer composites is dependent on the fiber, polymer matrix, and their interfacial bonding strength. Addition of WF to neat polymer matrix caused a significant decrease in its impact properties for PLA, BF, SL and PHBV (Figure 2.2). Similar results were obtained by Gunning et al (Gunning et al., 2013) for fiber reinforced PHB composites. However, grafting MA to the polymer significantly improved the impact properties of the PLA and BF composites. Compatibilized PLA, BF and PHBV composites exhibited a 24%, 203% and 24% improvement in impact fracture energies compared to their composites with no compatibilizer. This can be ascribed to increased resistance to crack propagation during impact due to improved adhesion between the fiber and the matrix (Spiridon, Leluk, Resmerita,

& Darie, 2015). The increase in crosslinking in compatibilized composites, as evidenced by the decreased MFI, explains the improvements in the impact properties of compatibilized composites (Tamboli et al., 2004). On the other hand, MA-g-SL/WF did not exhibit any improvement in impact fracture energy compared to SL/WF. MA grafted PHB composites showed 67% decrease, with respect to PHB/WF. This can be attributed to reduced compatibility between WF and the polymer as evidenced by the higher M_m and D values in water absorption for MA grafted PHB composites.

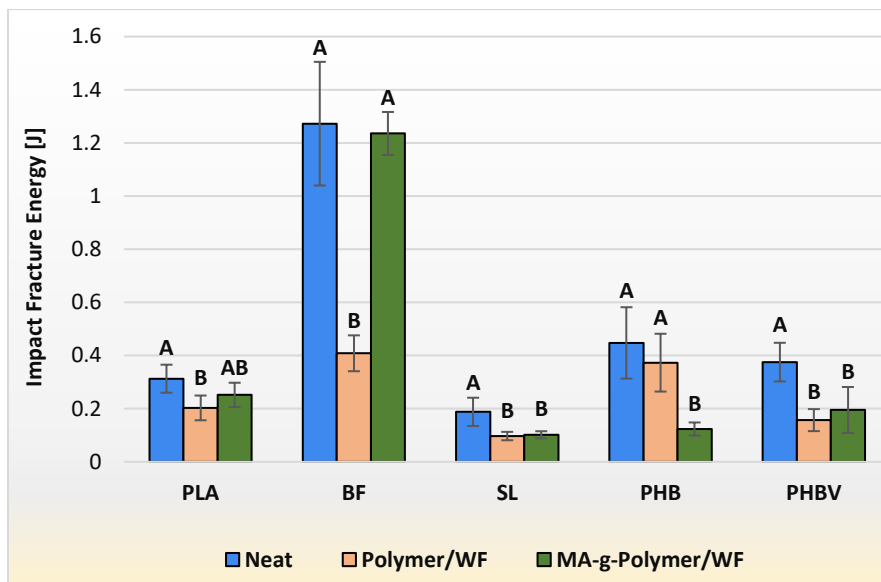


Figure 2.2. Impact fracture energy of the neat biopolymer and composite specimens. The error bars indicate standard deviation. Different letters above the bars indicate statistically significant differences at $P < 0.05$.

Flexural Properties

Compatibilization increased flexural strength significantly in PLA composites compared to PLA/WF (Figure 2.3). Compatibilized PLA and PHBV composites showed 24% and 11% increase over the respective uncompatibilized composites. Compatibilized BF composite exhibited an increase of 58% in flexural strength compared to neat BF, and 19% over uncompatibilized blends. These improvements were caused by the stronger interface between the

fiber and the matrix in MA grafted composites. Similar behavior of compatibilized composites can be found in literature (Gunning et al., 2014). The SL was an exception, where fiber fillers increased flexural strength by 33% over neat polymer, while MA grafted composites showed only 16% increase over neat polymer.

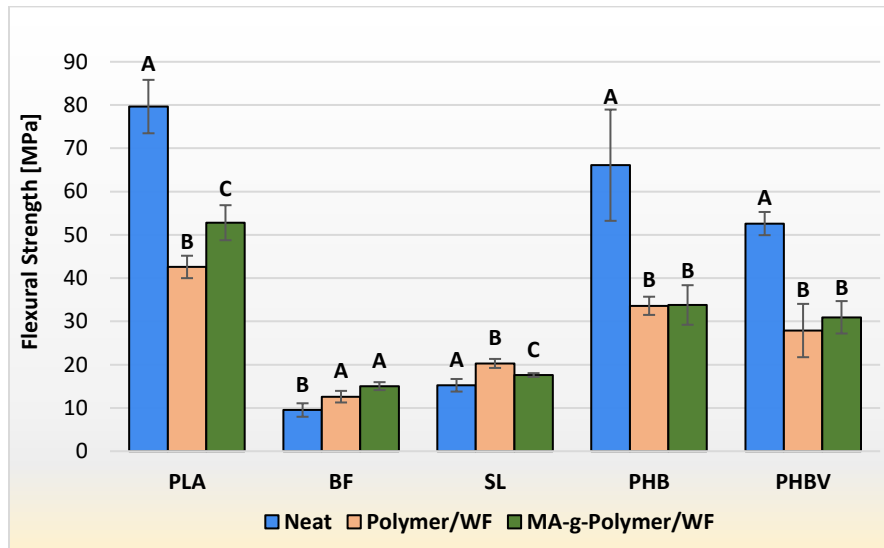


Figure 2.3. Flexural strength of all the 15 biopolymer compositions. The error bars indicate standard deviation. Different letters above the bars indicate statistically significant differences at $P < 0.05$.

Addition of WF caused a substantial increase in the modulus of the polymer composite matrix compared to neat polymer (Figure 2.4). Uncompatibilized PLA, BF, SL and PHBV composites exhibited 27%, 92%, 119% and 33% increase in flexural modulus, over the neat polymer. Overall, compatibilization did not affect flexural modulus of the biopolymer composites. These results are contradictory to the findings of Nyambo et al (Nyambo, Mohanty, & Misra, 2011) that reported a slight decrease in flexural modulus of PLA/wheat straw when compatibilized with 5 phr MA-g-PLA. In contrast, Avella et al (Buzarovska et al., 2007) observed significant improvement in flexural modulus for MA compatibilized PHBV/kenaf composites compared to neat and uncompatibilized composites.

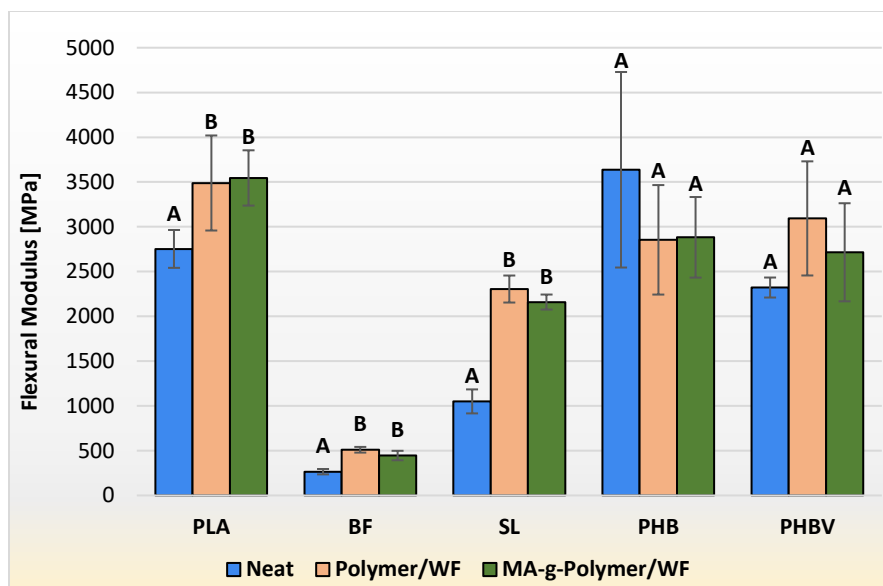


Figure 2.4. Flexural modulus of all the 15 biopolymer compositions. The error bars indicate standard deviation. Different letters above the bars indicate statistically significant differences at $P < 0.05$.

Surface Hardness

In PLA and PHBV biopolymers, addition of WF decreased the surface hardness, but the compatibilization significantly increased it to values similar to the neat polymer (Figure 2.5). Both the BF/WF and MA-g-BF/WF composites showed about 14% increase in hardness with respect to the neat polymer. In the case of PHB, hardness of compatibilized composites decreased by 9% compared to PHB/WF, and by 15% compared to neat PHB. The SL/WF showed a 15% increase over neat SL, but no significant difference was observed due to compatibilization. Hardness is the resistance of the material surface against the indentation, which decreases with the flexibility and mobility of the polymer chain structure. Grafting of MA leads to a reduction in chain mobility, thus, increasing the hardness (Mandal, Chakraborty, & Siddhanta, 2014).

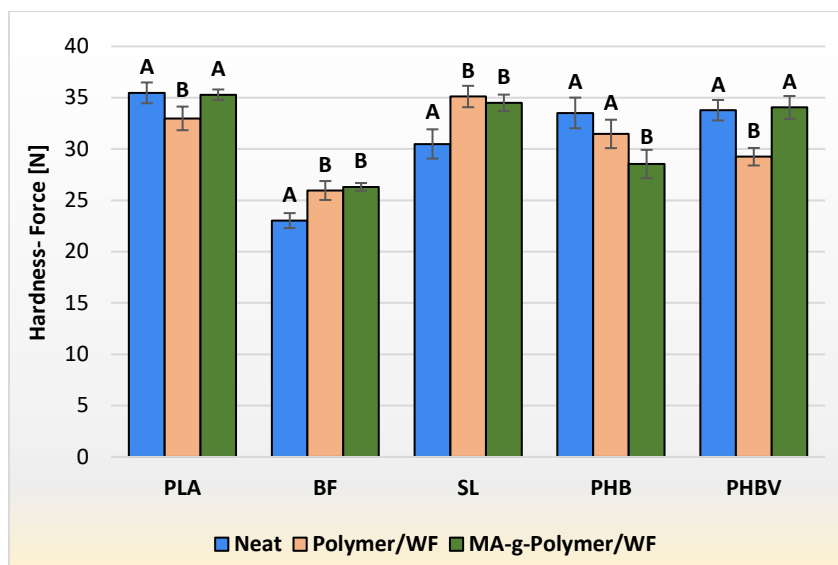


Figure 2.5. Surface hardness of the composite and neat biopolymer specimens. The error bars indicate standard deviation. Different letters above the bars indicate statistically significant differences at $P < 0.05$.

Compressive Strength

For BF and SL, addition of WF increased the compressive strength by 54%, while the addition of MA had no effect on the composites (Figure 2.6). When MA was added to PLA/WF, compressive strength increased from 78.7 to 90.7 MPa, which is slightly higher than that of neat PLA (87.2 MPa). Compatibilized PHBV exhibited a 22% increase compared to the PHBV/WF. However, compatibilization had no significant effect on the compressive strength of all five biopolymer composites. Observed reduction in compressive strength in uncompatibilized composites with respect to the neat biopolymer can be attributed to voids that generated due to poor bonding strength between hydrophobic polymer matrix and the hydrophilic fiber.

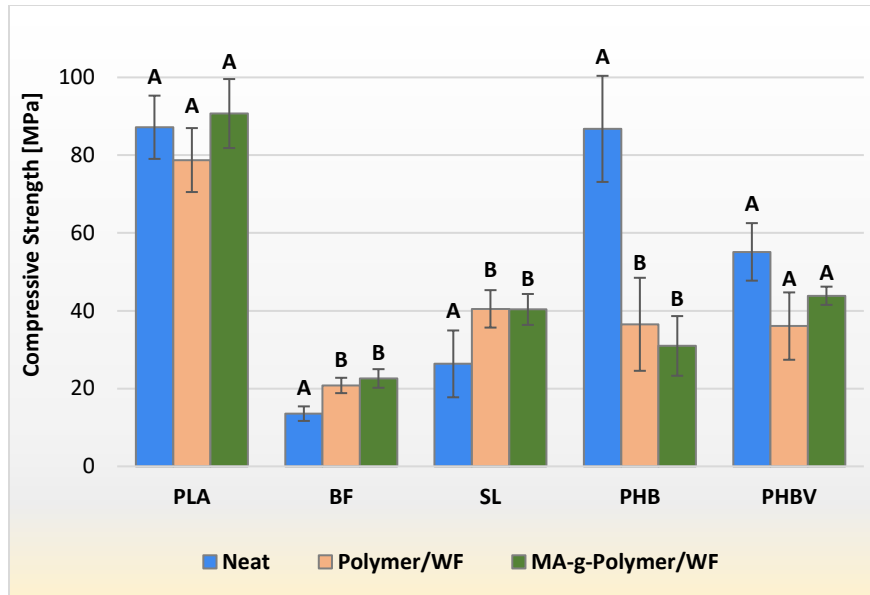


Figure 2.6. Compressive strength of the biopolymer compositions. The error bars indicate standard deviation. Letters above the bars indicate statistically significant differences at $P < 0.05$.

Cost Analysis

The price differences between the neat polymers and the composites are substantial (Figure 2.7). However, the difference between the cost of composites with and without MA is negligible.

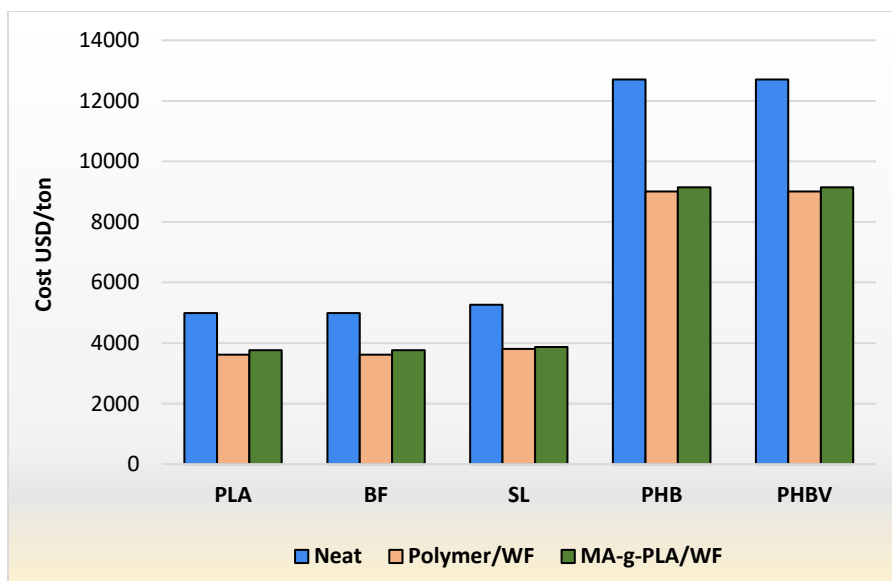


Figure 2.7. Cost of all the neat polymers and their composites with and without compatibilizer.

Effect of MA Grafting on Biopolymer- Discussion

Most thermoplastics are hydrophobic substances that are not compatible with hydrophilic WF, thus results in poor adhesion between polymer matrix and WF. Compatibilized biopolymer/natural fiber composites are fabricated to increase the interfacial adhesion between the hydrophobic polymer matrix and the hydrophilic fibers. When MA is melt mixed with an initiator and the polymer via reactive extrusion, the initiator attacks the backbone of the polymer and removes a hydrogen molecule to create a radical, so MA can graft. Subsequently, MA increases the bonding between the polymer and the fiber, acting as a bridge that links WF and thermoplastic polymers by covalent bonding and/or polymer chain entanglement (Gunning et al., 2014). As can be seen from the results, compatibilized PLA, BF and PHBV composites exhibited improved thermal and physico-mechanical properties compared to their uncompatibilized composites due to improved interfacial fiber-matrix adhesion.

Solanyl and PHB composites did not show improvements in thermal and physico-mechanical properties with compatibilization, as expected. Solanyl used in the study (Solanyl® C2201) is certified according to Vinçotte (EN 13432) OK Compost and Vinçotte OK (#3) Biobased. Further analysis of SL composites with GPC indicated that both compatibilized and uncompatibilized SL composites had similar weight average molecular weight, M_w (Table 2.9). The M_w is a good measure of statistical size of the polymer. Higher the molecular weight is, higher the mechanical properties of the polymer are.

Table 2.9. Weight-average molecular weight (M_w) of SL, SL/WF, and MA-g-SL/WF.

Sample	M_w (g/mol)
SL	61,709
SL/WF	56,259
MA-g-SL/WF	56,357

MA could be grafted onto the starch backbone, which creates a starch ester bearing a free carboxylic acid group. However, the MA moieties grafted onto the starch backbone could promote hydrolysis (Raquez, Nabar, Narayan, & Dubois, 2008). Maleation of starch introduce maleinates onto starch chains, which contain hydrophilic carboxyl groups, thus significantly enhancing hydrophilicity of starch (Zhu & Wang, 2014). This clarifies the increase in water absorption in MA grafted SL composites. When WF was added to SL, increase in strength and thermal properties (T_m and T_g) were observed due to the intrinsic adhesion of the fiber–matrix interface caused by the chemical similarity of both hydrophilic starch and WF, as observed in the literature (Ma, Yu, & Kennedy, 2005).

The similarity between SL and starch, and the effect of grafting of MA onto PHB were also analyzed with FTIR spectroscopy. FTIR spectrum of PHB composites was obtained by using a Magna spectrometer, while for neat PHB and SL a photoacoustic detector was used due to unavailability of Nicolet Magna spectrometer at the time. The FTIR spectral of SL polymer was similar to that of yam starch (Figure 2.8) (Ogunmolasuyi, Egwim, Adewoyin, & Awoyinka, 2016), with similar peaks. Both SL and starch spectra showed distinctive peaks and bands including a broad band in the range of $3780\text{--}3010\text{ cm}^{-1}$ for hydrogen bonded hydroxyl groups, C–H asymmetric stretching of $\text{--CH}_2\text{--}$ at $2995\text{--}2850\text{ cm}^{-1}$, C=O stretching at $1650\text{--}1750\text{ cm}^{-1}$, characteristic for $\text{--CH}_2\text{--}$ folding between 1450 and 1370 cm^{-1} , CH_2OH side chain at the peaks around 1250 cm^{-1} , O–C stretching in the range of $1180\text{--}960\text{ cm}^{-1}$, and anhydroglucose ring stretching vibrations at $861\text{--}575\text{ cm}^{-1}$. This indicates that SL biopolymer was very similar to starch.

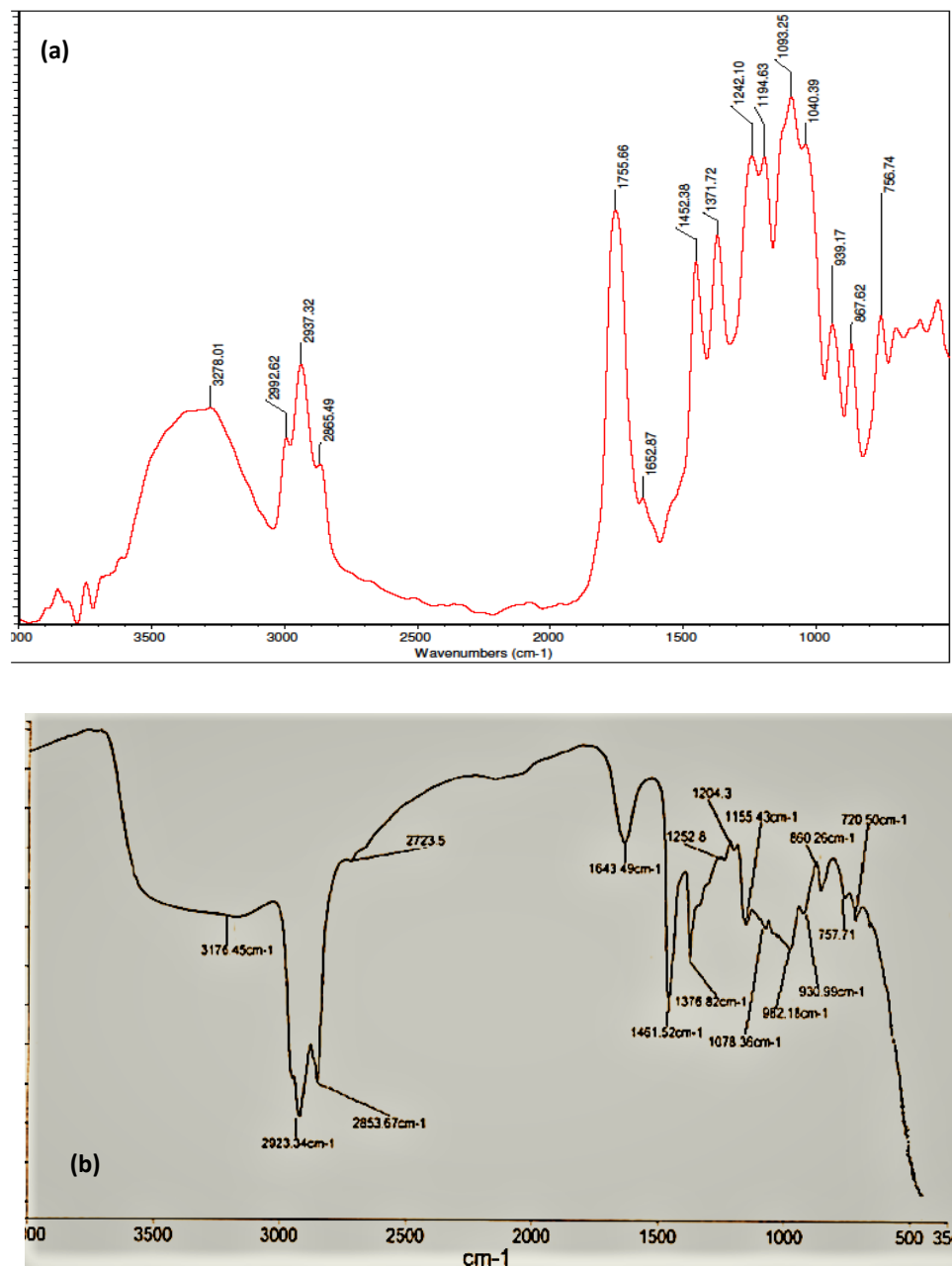


Figure 2.8. FTIR spectra of (a) SL and (b) Yam starch (Copyright Wiley-VCH Verlag GmbH & Co. KGaA. Reproduced with permission (*Ogunmolasuyi et al., 2016*)).

FTIR spectroscopy was used to investigate the grafting of MA onto PHB (Figure 2.9). FTIR spectra of PHB samples (PHB, MA-g-PHB, PHB/WF, MA-g-PHB/WF) showed characteristic peaks of PHB at 2800–3200, 1700–1750, and 600–1500 cm^{-1} . Large peak at 1720 cm^{-1} was present in all samples, which represents carbonyl groups in the crystalline region of

PHB. An extra shoulder should be present at 1700-1800 peak in MA grafted composites compared to neat PHB, as reported at 1790 cm^{-1} with 3% MA (Gunning et al., 2014). The extra peak is due to a product of free acid from the modified polymer, which exhibits the presence of MA. There was no such extra shoulder present for the compatibilized samples in this study, indicating that the MA was not grafted to PHB successfully. This can explain why there was no improvement shown when MA was added to PHB composite.

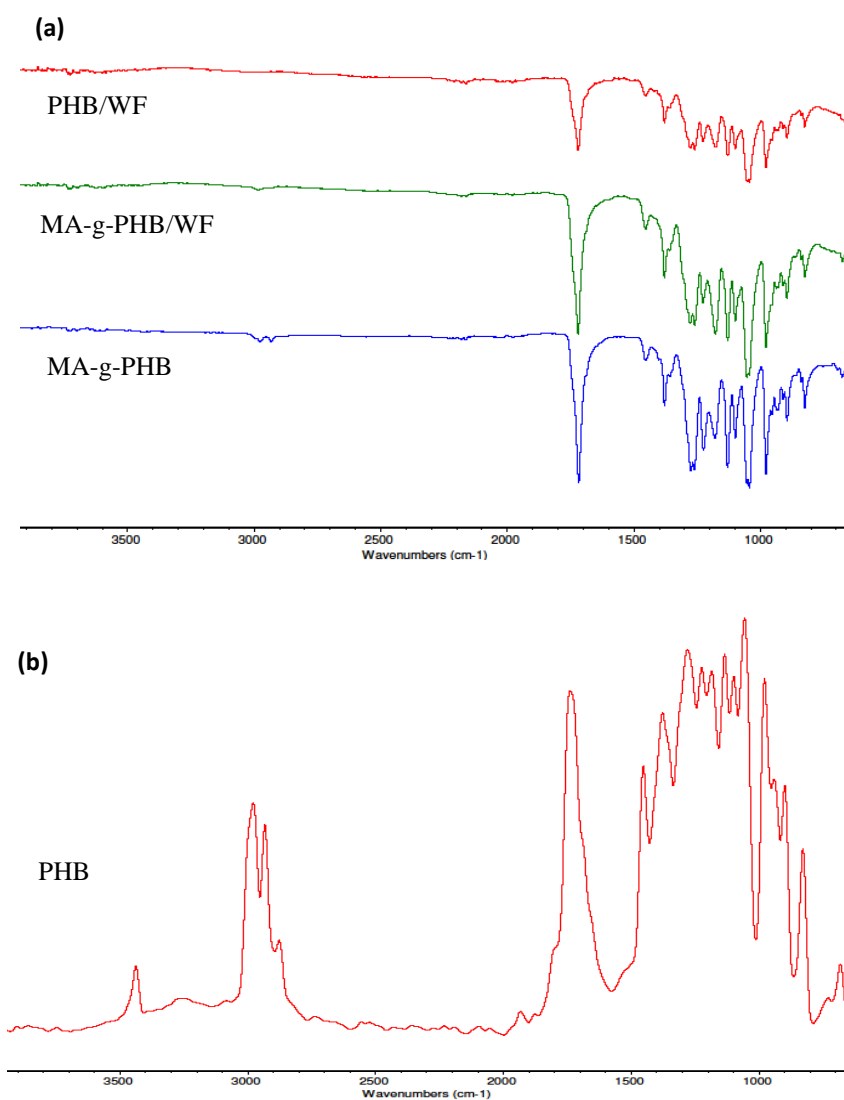


Figure 2.9. FTIR spectra of PHB composites. (a): MA-g-PHB, MA-g-PHB/WF, PHB/WF from Magna spectrometer; (b) PHB from photoacoustic detector.

Conclusion

Compatibilization with maleic anhydride (MA) improved thermal properties such as glass transition temperature, melting temperature and crystallinity in PLA, Bioflex (BF, PLA blend) and PHBV composites indicating better adhesion between the polymer matrix and wood fiber (WF). Melt flow index of compatibilized composites decreased, indicating polymer crosslinking. Compatibilized composites of PLA, BF and PHBV showed decreased water absorption. Increased resistance to water is a beneficial characteristic, as the water uptake in natural fibers composites causes dimensional instability and poor mechanical properties. Mechanical properties of MA grafted PLA, BF and PHBV composites increased due to compatibilization as it improved fiber-matrix interfacial adhesion. Both Solanyl (SL, starch-based) and BF composites did not show any improvements due to compatibilization. A failure to graft MA to PHB successfully, and the similarity of molecular weight of grafted and ungrafted SL explain why these composites behaved differently.

References

- Abdulkhani, A., Hosseinzadeh, J., Dadashi, S., & Mousavi, M. (2015). A study of morphological, thermal, mechanical and barrier properties of PLA based biocomposites prepared with micro and nano sized cellulosic fibers. *Cell Chem Technol*, 49(7-8), 597-605.
- Arbelaiz, A., Fernandez, B., Ramos, J., Retegi, A., Llano-Ponte, R., & Mondragon, I. (2005). Mechanical properties of short flax fibre bundle/polypropylene composites: Influence of matrix/fibre modification, fibre content, water uptake and recycling. *Composites Science and Technology*, 65(10), 1582-1592.

- ASTM D256. (2010). In *ASTM D256: Standard Test Methods for Determining the Izod Pendulum Impact Resistance of Plastics*: American Society for Testing and Materials.
- ASTM D570. (2010). In *Standard Test Method for Water Absorption of Plastics*: American Society for Testing and Materials.
- ASTM, D. (2000). 2240, Standard Test Method for Rubber Property-Durometer Hardness. *Figure S. left column shows visual surface degradation of the polyurethane after (top to bottom), 18.*
- ASTM, D. (2004). 1238-04c—Standard Test Method for Melt Flow Rates of Thermoplastics by Extrusion Plastometer. *Current edition approved Dec, 1, 1-14.*
- ASTM, I. (2007). Standard test methods for flexural properties of unreinforced and reinforced plastics and electrical insulating materials. *ASTM D790-07.*
- Babu, R. P., O'Connor, K., & Seeram, R. (2013). Current progress on bio-based polymers and their future trends. *Progress in Biomaterials*, 2(8), 1-16.
- Balakrishnan, H., Hassan, A., Imran, M., & Wahit, M. U. (2011). Aging of toughened polylactic acid nanocomposites: water absorption, hygrothermal degradation and soil burial analysis. *Journal of Polymers and the Environment*, 19(4), 863-875.
- Batista, K., Silva, D., Coelho, L., Pezzin, S., & Pezzin, A. (2010). Soil biodegradation of PHBV/peach palm particles biocomposites. *Journal of Polymers and the Environment*, 18(3), 346-354.
- Bessadok, A., Belgacem, M. N., Dufresne, A., & Bras, J. (2010). Beneficial Effect of Compatibilization on the Aging of Cellulose-Reinforced Biopolymer Blends. *Macromolecular Materials and Engineering*, 295(8), 774-781.

- Bourara, H., Hadjout, S., Benabdelghani, Z., & Etxeberria, A. (2014). Miscibility and hydrogen bonding in blends of poly (4-vinylphenol)/poly (vinyl methyl ketone). *Polymers*, 6(11), 2752-2763.
- Buzarovska, A., Bogoeva-Gaceva, G., Grozdanov, A., Avella, M., Gentile, G., & Errico, M. (2007). Crystallization behavior of poly (hydroxybutyrate-co-valerate) in model and bulk PHBV/kenaf fiber composites. *Journal of materials science*, 42(16), 6501-6509.
- Cao, X., Chen, Y., Chang, P. R., Stumborg, M., & Huneault, M. A. (2008). Green composites reinforced with hemp nanocrystals in plasticized starch. *Journal of Applied Polymer Science*, 109(6), 3804-3810.
- Gunaratne, L., & Shanks, R. (2008). Miscibility, melting, and crystallization behavior of poly (hydroxybutyrate) and poly (D, L-lactic acid) blends. *Polymer Engineering & Science*, 48(9), 1683-1692.
- Gunning, M. A., Geever, L. M., Killion, J. A., Lyons, J. G., & Higginbotham, C. L. (2013). Mechanical and biodegradation performance of short natural fibre polyhydroxybutyrate composites. *Polymer Testing*, 32(8), 1603-1611.
- Gunning, M. A., Geever, L. M., Killion, J. A., Lyons, J. G., & Higginbotham, C. L. (2014). Effect of Compatibilizer Content on the Mechanical Properties of Bioplastic Composites via Hot Melt Extrusion. *Polymer-Plastics Technology and Engineering*, 53(12), 1223-1235.
- International, A. (2010). *Standard Test Method for Compressive Properties of Rigid Plastics*: ASTM International.

- Lu, J. Z., Wu, Q., & McNabb, H. S. (2007). Chemical coupling in wood fiber and polymer composites: A review of coupling agents and treatments. *Wood and Fiber Science*, 32(1), 88-104.
- Ma, X., Yu, J., & Kennedy, J. F. (2005). Studies on the properties of natural fibers-reinforced thermoplastic starch composites. *Carbohydrate Polymers*, 62(1), 19-24.
- Mandal, A. K., Chakraborty, D., & Siddhanta, S. K. (2014). Effect of the compatibilizer, on the engineering properties of TPV based on Hypalon® and PP prepared by dynamic vulcanization. *Journal of Applied Polymer Science*, 131(11).
- Mathew, A. P., Oksman, K., & Sain, M. (2005). Mechanical properties of biodegradable composites from poly lactic acid (PLA) and microcrystalline cellulose (MCC). *Journal of applied polymer science*, 97(5), 2014-2025.
- Mukherjee, T., & Kao, N. (2011). PLA based biopolymer reinforced with natural fibre: a review. *Journal of Polymers and the Environment*, 19(3), 714-725.
- Nyambo, C., Mohanty, A. K., & Misra, M. (2011). Effect of maleated compatibilizer on performance of PLA/wheat Straw-Based green composites. *Macromolecular Materials and Engineering*, 296(8), 710-718.
- Ogunmolasuyi, A. M., Egwim, E. C., Adewoyin, M. A., & Awoyinka, O. (2016). A comparative study of functional and structural properties of starch extracted from *Dioscorea rotundata* and *Colocasia esculenta*. *Starch-Stärke*, 68(7-8), 771-777.
- Petinakis, E., Yu, L., Simon, G., & Dean, K. (2013). Natural fibre bio-composites incorporating poly (lactic acid). In *Fiber Reinforced Polymers-The Technology Applied for Concrete Repair*: InTech.

- Raquez, J. M., Nabar, Y., Narayan, R., & Dubois, P. (2008). In situ compatibilization of maleated thermoplastic starch/polyester melt-blends by reactive extrusion. *Polymer Engineering & Science*, 48(9), 1747-1754.
- Roumeli, E., Terzopoulou, Z., Pavlidou, E., Chrissafis, K., Papadopoulou, E., Athanasiadou, E., . . . Bikiaris, D. N. (2015). Effect of maleic anhydride on the mechanical and thermal properties of hemp/high-density polyethylene green composites. *Journal of Thermal Analysis and Calorimetry*, 121(1), 93-105.
- Shah, B. L., Selke, S. E., Walters, M. B., & Heiden, P. A. (2008). Effects of wood flour and chitosan on mechanical, chemical, and thermal properties of polylactide. *Polymer Composites*, 29(6), 655-663.
- Spiridon, I., Leluk, K., Resmerita, A. M., & Darie, R. N. (2015). Evaluation of PLA–lignin bioplastics properties before and after accelerated weathering. *Composites Part B: Engineering*, 69, 342-349.
- Srubar, W., Wright, Z., Tsui, A., Michel, A., Billington, S., & Frank, C. (2012). Characterizing the effects of ambient aging on the mechanical and physical properties of two commercially available bacterial thermoplastics. *Polymer Degradation and Stability*, 97(10), 1922-1929.
- Srubar, W. V., Pilla, S., Wright, Z. C., Ryan, C. A., Greene, J. P., Frank, C. W., & Billington, S. L. (2012). Mechanisms and impact of fiber–matrix compatibilization techniques on the material characterization of PHBV/oak wood flour engineered biobased composites. *Composites Science and Technology*, 72(6), 708-715.

- Suryanegara, L., Nakagaito, A. N., & Yano, H. (2009). The effect of crystallization of PLA on the thermal and mechanical properties of microfibrillated cellulose-reinforced PLA composites. *Composites Science and Technology*, *69*(7), 1187-1192.
- Tamboli, S., Mhaske, S., & Kale, D. (2004). Crosslinked polyethylene. *Indian journal of chemical technology*, *11*(6), 853-864.
- Thiré, R. M. d. S. M., Arruda, L. C., & Barreto, L. S. (2011). Morphology and thermal properties of poly (3-hydroxybutyrate-co-3-hydroxyvalerate)/attapulgitite nanocomposites. *Materials Research*, *14*(3), 340-344.
- Wan, Y., Luo, H., He, F., Liang, H., Huang, Y., & Li, X. (2009). Mechanical, moisture absorption, and biodegradation behaviours of bacterial cellulose fibre-reinforced starch biocomposites. *Composites Science and Technology*, *69*(7), 1212-1217.
- Wu, C.-S. (2009). Renewable resource-based composites of recycled natural fibers and maleated polylactide bioplastic: Characterization and biodegradability. *Polymer Degradation and Stability*, *94*(7), 1076-1084.
- Zhu, Z., & Wang, M. (2014). Effects of starch maleation and sulfosuccination on the adhesion of starch to cotton and polyester fibers. *Journal of Adhesion Science and Technology*, *28*(10), 935-949.

**CHAPTER 3. COMPATIBILIZATION IMPROVES PERFORMANCE OF
BIODEGRADABLE BIOPOLYMER COMPOSITES WITHOUT AFFECTING UV
WEATHERING CHARACTERISTICS**

Abstract

With growing interest in the use of eco-friendly composite materials, biodegradable polymers and composites from renewable resources are gaining popularity for use in commercial applications. However, the long-term performance of these composites and the effect of compatibilization on their weathering characteristics are unknown. In this study, five biodegradable biopolymer composites were compatibilized with 1-2 wt% maleic anhydride (MA), and the effect of accelerated UV weathering on their performance was evaluated against composites without MA. The composite samples were prepared with 30 wt% wood fiber and one of the five biodegradable biobased polymer: poly(lactic) acid (PLA), polyhydroxybutyrate (PHB), poly(3-hydroxybutyrate-co-3-hydroxyvalerate) (PHBV), Bioflex (PLA blend), or Solanyl (starch based). The composites were UV weathered for 2000 hours (h), and characterized for morphological, physical, thermal and mechanical properties at 0, 1000 and 2000 h of weathering. Blends containing MA grafted polymers exhibited improved properties due to increased interfacial adhesion between the fiber and matrix. Upon accelerated weathering, overall thermal and mechanical properties decreased. Surfaces of the specimens were roughened, and drastic color changes were observed. Water absorption increased with increased weathering exposure. Even though the compatibilization is shown to improve composite properties before weathering, after weathering, no considerable differences in properties were exhibited for the composites with MA and without MA. The results suggest that compatibilization improves properties of biodegradable biobased composites without affecting its UV degradation properties.

Introduction

Petroleum-based polymers create substantial environmental problems at disposal due to low degradation rates and harmful degradation products such as carbon dioxide. These polymers make up about a fifth by volume of all waste generated in the U.S. every year, and contribute to global warming (Madbouly et al., 2012). Petroleum is a limited resource that can only last for another 50– 60 years at the current rate of consumption (Bronzino, 1999). Due to the environmental concerns associated with petroleum-based plastics and the uncertainty in supplies of fossil fuels, there is a great impetus on replacing conventional plastics with green/biobased biodegradable alternatives.

Biobased polymers are blended with other biodegradable natural fibers to create composites to customize its properties such as crystallinity, thermal degradation and dimensional stability (Gunning, Geever, Killion, Lyons, & Higginbotham, 2014; W. Srubar et al., 2012; Suryanegara, Nakagaito, & Yano, 2009). Natural fibers serve as good reinforcements and fillers in biocomposites for a myriad of reasons including good thermal, electric and acoustic properties, fewer health hazards during processing, and less abrasiveness to processing equipment compared to conventional inorganic fillers (Batista, Silva, Coelho, Pezzin, & Pezzin, 2010). In addition to low cost and biodegradability, properties such as specific strength and specific stiffness of natural fibers are similar to those of glass fibers due to the lower density of natural fibers. Thus, natural fibers are preferred over glass and carbon fibers in some applications such as panels of car doors and dashboards, compact disks and computer cases (Vroman & Tighzert, 2009).

Even though the addition of natural fibers to biopolymers can be cost-effective and improve some properties, it can weaken other properties such as flexural, impact and tensile

strengths due to poor interfacial adhesion between the hydrophobic polymer matrix and the hydrophilic fiber (Wei, Liang, & McDonald, 2015). Polymer matrix-fiber compatibility can be improved by introducing reactive functional groups such as compatibilizers (Gunning et al., 2014). Maleic anhydride (MA) is a commonly used compatibilizer. It forms hydrogen and covalent bonds with hydroxyl groups of the fiber, and molecular entanglement with the polymer, resulting in improved adhesion between the polymer and the fiber (W. V. Srubar et al., 2012). It is important to study the long-term behavior of compatibilized biodegradable biopolymer composites under accelerated weathering conditions to understand their behavior in degrading environments such as the outdoors. Very few studies have addressed the effect of the addition of compatibilizers to green composites, and their behavior under accelerated weathering (Michel & Billington, 2012; Sahari, Sapuan, Zainudin, & Maleque, 2014; Spiridon, Leluk, Resmerita, & Darie, 2015; Spiridon, Paduraru, Zaltariov, & Darie, 2013).

The objectives of this study are to 1) quantify changes in the physical, mechanical, thermal and visual properties of biobased biodegradable polymers and composites under accelerated UV weathering, and 2) understand whether the compatibilization affects the long-term performance of biobased biodegradable polymers with weathering exposure. To the extent of our knowledge no research has been presented so far regarding the behavior of these materials under accelerated weathering.

Experimental Procedure

In this study, composites of five types of biodegradable biopolymers were prepared by compounding them with 30 wt% oak-wood fiber (WF) filler with and without 1-2% compatibilizer. The five biodegradable biopolymers were poly(lactic acid) (PLA), Bioflex (BF), Solanyl (SL), poly(3-hydroxybutyric acid) (PHB), and poly(3-hydroxybutyrate-co-3-

hydroxyvalerate) (PHBV). The effect of WF filler and compatibilization on thermal, mechanical and physical properties were evaluated. To investigate the effects of weathering on morphological, mechanical, thermal and physical properties, composite samples were exposed to accelerated weathering up to 2000 h. Morphological changes were characterized by using optical microscopic images and by measuring color changes. The influence of weathering on the crystallinity and melting behavior of biocomposites was studied using Differential scanning calorimetry (DSC). Thermogravimetric analysis (TGA) was used to determine degradation temperatures. Physical and mechanical properties such as water absorption, flexural strength and modulus, impact fracture energy and hardness were evaluated.

Materials

The PLA was type 2003D from NatureWorks LLC (Minnetonka, MN). The PHB (ENMAT Y3000P) and PHBV (ENMAT Y1000P) were supplied by TianAN Biopolymer (Ningbo City, Zhejiang Province, China). Both PHB and PHBV are polyhydroxyalkanoates (PHA). Bioflex (BF) biopolymer (Bio-Flex® F2110) is a PLA blend, and was obtained from FKUR Plastics (Willich, Germany). Solanyl (SL) biopolymer (Solanyl® C2201) was from Rodenburg Biopolymers (Oosterhout, Netherlands). The SL is made from potato starch reclaimed from the food processing industry. Maleic anhydride (63200), Luperox® P: tert-Butyl peroxybenzoate (TBPB), benzoyl peroxide (BP), and Luperox 101: 2,5-bis(tert-butylperoxy)-2,5-dimethylhexane (L101) were purchased from Sigma-Aldrich Chemical Co. (St. Louis, MO).

Polymer Composite Manufacturing

Preparation of Grafted Polymer

All the polymer pellets were pre-dried according to the recommendation provided by the supplier. The PHB and PHBV polymers were dried at 80°C for 2 h, PLA at 80°C for 6 h, SL at

45°C for 4 h, and BF at 60°C for 3 h. To graft biopolymers, first, each of the polymer was hand-mixed with MA (2 or 3 wt%) and an initiator (0.5-1 wt%) in a zip-lock plastic bag (Table 2.1). Mixture was then extruded using a micro 18 lab-scale twin screw extruder (Leistritz Ltd., Somerville, NJ) with a 40/1 length to diameter ratio (Table 2.2). Extruded pellets were dried at 80°C in an oven for 12 h.

Preparation of biodegradable biopolymer composites with wood fiber

The WF was hand mixed with neat polymer for uncompatibilized composites. For MA compatibilized composites, grafted polymer was hand mixed with WF and neat polymer in a zip-lock bag (Table 2.3). Each of the mixtures (with or without MA grafted polymer) were then extruded (Table 2.2), water cooled, cut into pellets and dried at 80°C in an oven for 24 h.

Compression Molding

Dried extruded pellets were compression molded into 150 mm square, 5 mm thick sheets using a Carver hot press (model 3856, Carver Inc., Wabash, IN) (Table 2.4). The pressure was maintained at 50 atm. The molded sheets were cooled slowly under ambient conditions.

Accelerated Weathering

All polymer specimens were placed in a QUV accelerated weathering tester (QUV/Spray, Q-Lab Co., OH, USA) according to ASTM G154 standard ("ASTM G154," 2012) for a total of 2000 h. Each 12 h weathering cycle consisted of 8 h of UV exposure at 60°C and 4 h condensation cycle at 45°C. Characterization of the materials were done after 1000 h of weathering, and again after 2000 h of weathering.

Characterization of Composites

The composite materials were characterized before weathering, after 1000 h of weathering, and again after 2000 h of weathering. However, since the Solanyl composites (SL/WF and MA-g-SL/WF) deteriorated after 884 h and 1479 h of weathering, all the characterizations were done at 884 h for SL/WF instead of 1000 h, and at 1479 h for MA-g-SL/WF instead of 2000 h.

Water Absorption

The water absorption of samples were measured with Eq. 3.1 specified by ASTM D570 standard ("ASTM D570," 2010). All the test specimens were 38.1 mm long and wide, while maintaining the original thickness of 5 mm. To obtain conditioned weight, samples were dried in an oven for 24 h at 50°C and weighed to the nearest 0.001 g. Specimens were then immersed in water at room temperature and weights were measured periodically for 5 weeks. Maximum moisture content (M_m), which is the maximum water absorption capacity, was calculated by taking the average of several consecutive measurements once the sample weight has stabilized.

$$\% \text{Increase in weight } (M_t) = \frac{\text{wet weight} - \text{conditioned weight}}{\text{conditioned weight}} \times 100 \quad (\text{Eq. 3.1})$$

Differential scanning calorimetry

Thermal properties such as glass transition temperature (T_g), melt temperature (T_m), crystallization enthalpy (ΔH_c), and melting enthalpy (ΔH_m) were determined using Q20 Dynamic Scanning Calorimeter (TA Instruments, New Castle, DE). About 8 mg of each sample was first equilibrated at 25°C, then heated from 25°C up to 200°C at the rate of 10°C/min. The degree of crystallinity (X%) was evaluated according to Eq. 3.2:

$$X\% = \frac{\Delta H_m - \Delta H_c}{\Delta H_m^0 * (w_p)} 100\% \quad (\text{Eq. 3.2})$$

where, w_p is the polymer fraction in the composites, and ΔH_m^0 is the estimated melting enthalpies of their respected pure polymer. ΔH_m^0 of PLA and BF is 93.7 J/g, and for PHB and PHBV it is 146 J/g (Abdulkhani, Hosseinzadeh, Dadashi, & Mousavi, 2015; W. Srubar et al., 2012).

Thermogravimetric analysis (TGA)

Thermogravimetric analysis was performed using a Q500 Thermogravimetric Analyzer (TA Instruments, New Castle, DE) under a constant nitrogen flow of 40 mL/min, with a heating rate of 20°C/min. About 5-8 mg of each samples were used to perform the heating scans in the 25–800°C range. The range of temperatures for the thermal degradation was estimated from the first derivative (DTG) curves, while the weight loss was determined from the TG plot.

Optical Microscopy

Surfaces of all the specimens before and after weathering were observed using OMAX AMSCOPE microscope (S7M7045/SZM7045TR, Omax, yeonggi-do, Korea) fitted with OMAX A3590U video camera (D/N: UCMOSO9000KPB, P/N: TP609000B) for collecting images. Images at 30X magnification were collected and examined using the ToupView 3.7 software that came with the camera.

Color Measurement

The surface colors of the weathered and non-weathered samples were measured using X-Rite Spectrophotometer (Model SP62, S/N 000737, X-Rite, Grandville, MI) according to the CIELAB color system with L^* , a^* , b^* coordinates. The color parameter L^* is for the lightness coordinate and has a range of 100 (white) to 0 (dark); a^* is for the coordinate of red ($+a^*$) to green ($-a^*$); and b^* for the yellow ($+b^*$) to blue ($-b^*$) coordinate. The color difference (ΔE^*) was calculated as specified in ASTM D2244 standard (D. ASTM, 2003) using Eq. 3.3:

$$\Delta E^* = \sqrt{(\Delta L^*)^2 + (\Delta a^*)^2 + (\Delta b^*)^2} \quad (\text{Eq. 3.3})$$

where, ΔL^* , Δa^* , and Δb^* represent the change in initial values of L^* , a^* , and b^* , by the end of weathering period, respectively.

Impact Testing

To calculate impact fracture energy, impact tests were performed according to ASTM D256 standard ("ASTM D256," 2010) method A. Tinius Olsen Impact tester (model IT504, Tinius Olsen, Horsham, PA) was used with a pendulum of 4.497 N weight and 334.949 mm radius. Five specimens per batch were tested, and a notch of 2.54 mm was made on each sample to ensure failure.

Flexural Testing

To calculate flexural strength and modulus, three-point bending tests were performed according to ASTM D790 standard (I. ASTM, 2007) procedure A with an Instron 5567 load frame (Instron, Norwood, MA). A 2kN load cell was used at a cross head rate of 2 mm/min. Test specimens were 12.7 mm wide and 152.4 mm long with 5 mm thickness. Five specimens from each batch were tested.

Hardness

A type D durometer (Model 409, S/N 02015, Davis Instrumentation, Vernon Hills, IL) was used to measure the surface hardness of the composite samples. In this method, the resistance force of the penetration of durometer pin into the test specimen is measured. Five readings were taken for each batch to obtain an average value. As indicated in ASTM D2240 (D. ASTM, 2000) (manual operation method), Eq. 3.4 was used to calculate force:

$$\text{Force, N} = (0.4445)HD \quad (\text{Eq. 3.4})$$

where, HD is the hardness reading on type D durometer.

Data Analysis

Tukey's test of multiple comparisons was applied to determine significant differences between the mechanical properties of neat polymers and composites at each of the weathering period. $P < 0.05$ was used to determine statistical significance. Data analysis was performed with Minitab software (version 18, Minitab Inc., PA).

Results and Discussion

Optical Microscopy

Micrographs of the composite samples before UV weathering showed that all the neat polymers and their composites had even color distribution with smooth polymer layers on top (Table 3.1-3.3) exhibiting decent encapsulation of fibers (Krehula et al., 2014). With weathering exposure, all the specimens showed roughened surfaces due to matrix degradation. Matrix degradation occurs under UV weathering through polymer chain scission, which leads to more crystalline regions in the polymer structure (Rahman et al., 2011). The cracking can be observed on these formed crystalline regions during weathering. Formation of cracks in the specimen with weathering is a result of chemicrystallization (due to photo-oxidation), in which the scission of polymer chain occur in amorphous regions, and then released and crystallized onto pre-existing crystals (Fabiya, McDonald, Wolcott, & Griffiths, 2008). For instance, at 1000 h, PLA only had a few voids on the surface (Table 3.1). Those voids developed into cracks on the surface after 2000 h, where PLA had an extreme brittleness with a glassy texture, which was broken down into pieces eventually.

Table 3.1. Comparison of surface morphology of the specimens before and after weathering at 1000h and 2000h for five biopolymers, and their composites with and without compatibilizer: PLA, PLA/WF, MA-g-PLA/WF, BF, BF/WF, MA-g-BF/WF.





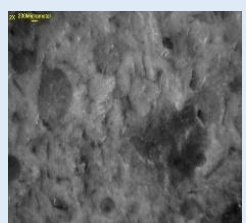
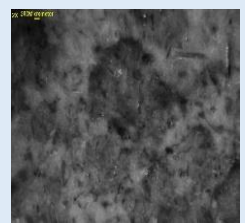
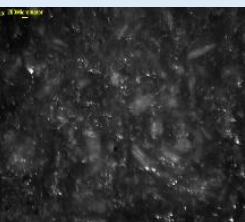
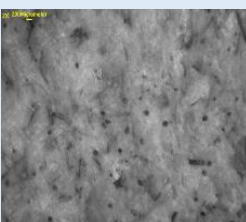
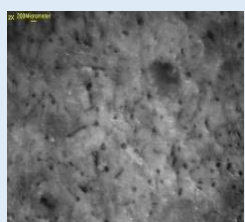



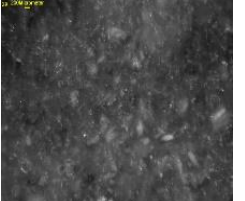
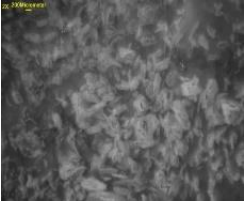

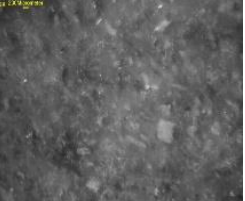
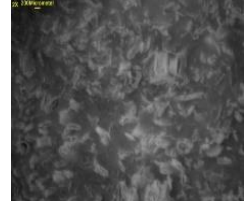

Composition	Weathering exposure		
	0 h	1000 h	2000 h
PLA			
PLA/WF			
MA-g-PLA/WF			
BF			
BF/WF			
MA-g-BF/WF			

Table 3.2. Comparison of surface morphology of the specimens before and after weathering at 1000h and 2000h: PHB, PHB/WF, MA-g-PHB/WF, PHBV, PHBV/WF, MA-g-PHBV/WF.



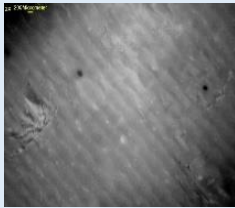


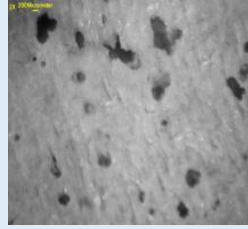
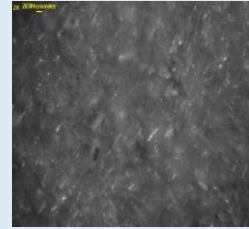



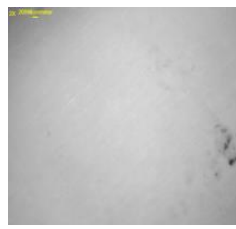

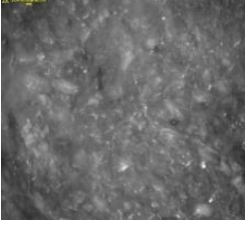

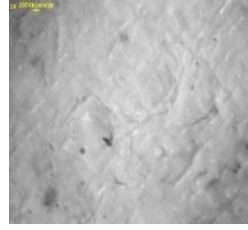
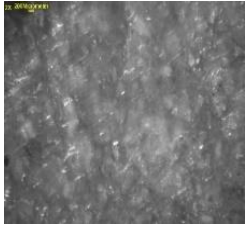
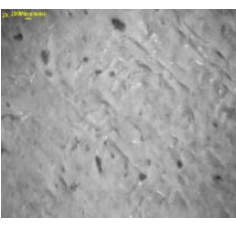
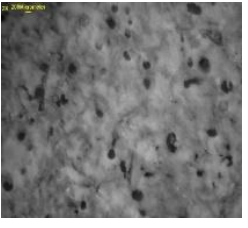



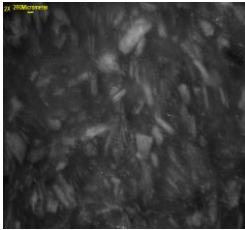
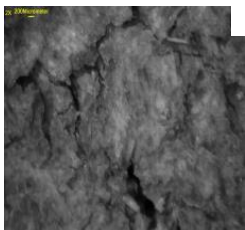
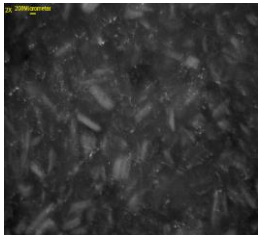
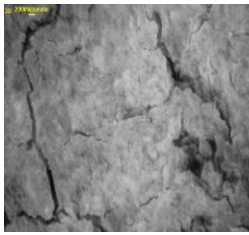
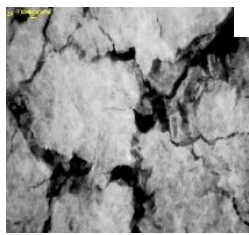
Composition	Weathering exposure		
	0 h	1000 h	2000 h
PHB			
PHB/WF			
MA-g-PHB/WF			
PHBV			
PHBV/WF			
MA-g-PHBV/WF			

Table 3.3. Comparison of surface morphology of the specimens before and after weathering at 1000h and 2000h: SL, SL/WF, MA-g-SL/WF.

Composition	Weathering exposure		
	0 h	1000 h	2000 h
SL			
SL/WF			
MA-g-SL/WF			

* Taken after 884 h of weathering. **Taken after 1479 h of weathering.

For all the composites, the cracks were formed in between the polymer matrix and the wood fibers (WF). Most noticeably, protrusion of WF from the surface can be seen in the composites (Table 3.3). This can be ascribed to swelling and shrinking of the WF due to the higher moisture absorption of hydrophilic WF compared to the matrix during the repeated moisture-UV cycles. When polymer matrix is subjected to UV, it accelerates the matrix degradation, resulting detachment of WF and the polymer matrix. The cracks generated on the specimens can also be due to both polymer photo-degradation and fiber swelling (Butylina, Hyvärinen, & Kärki, 2012). From Table 3.1-3.3, it can clearly be seen that only a few cavities and/or cracks occurred after 1000 h of weathering on all the polymer specimens. For example,

BF only had a very few number of cavities at 1000 h, however the number of cracks dramatically increased after 2000 h of weathering (Table 3.1). As the surface matrix layer cracked under the combined action of UV radiation and water, both degradation agents penetrated deeper into the composite, resulting in more degradation and deterioration of interfacial properties.

Surface Color of Composite Material

Lightness (ΔL^*) of all the specimens increased with increased weathering time except for BF and SL (Figure 3.1). Before weathering, SL and BF exhibited pure white color. After weathering exposure, BF turned to a yellowish color, while SL exhibited dark spots on the surface. At 2000 h, BF was the only specimen that had a positive Δb^* value, which indicated its yellowness. Black mold spots of SL can be the cause for its lower ΔL^* values. Whitening of all other specimens can be attributed to increased diffuse reflectance due to increased surface roughness, and photo-oxidation that occurred as a result of polymer degradation by UV (Michel & Billington, 2012; Rahman et al., 2011). Color change of all the composites can be attributed to photo-degradation of conjugated structure of WF under UV and condensation cycles, and to the photo-oxidation of lignin (Chen, Stark, Tshabalala, Gao, & Fan, 2016; Peng, Liu, Cao, & Chen, 2014). Photodegradation of lignin is initiated by UV absorbance, forming free radicals and chromophore groups, which results in color changes after weathering (Peng et al., 2014).

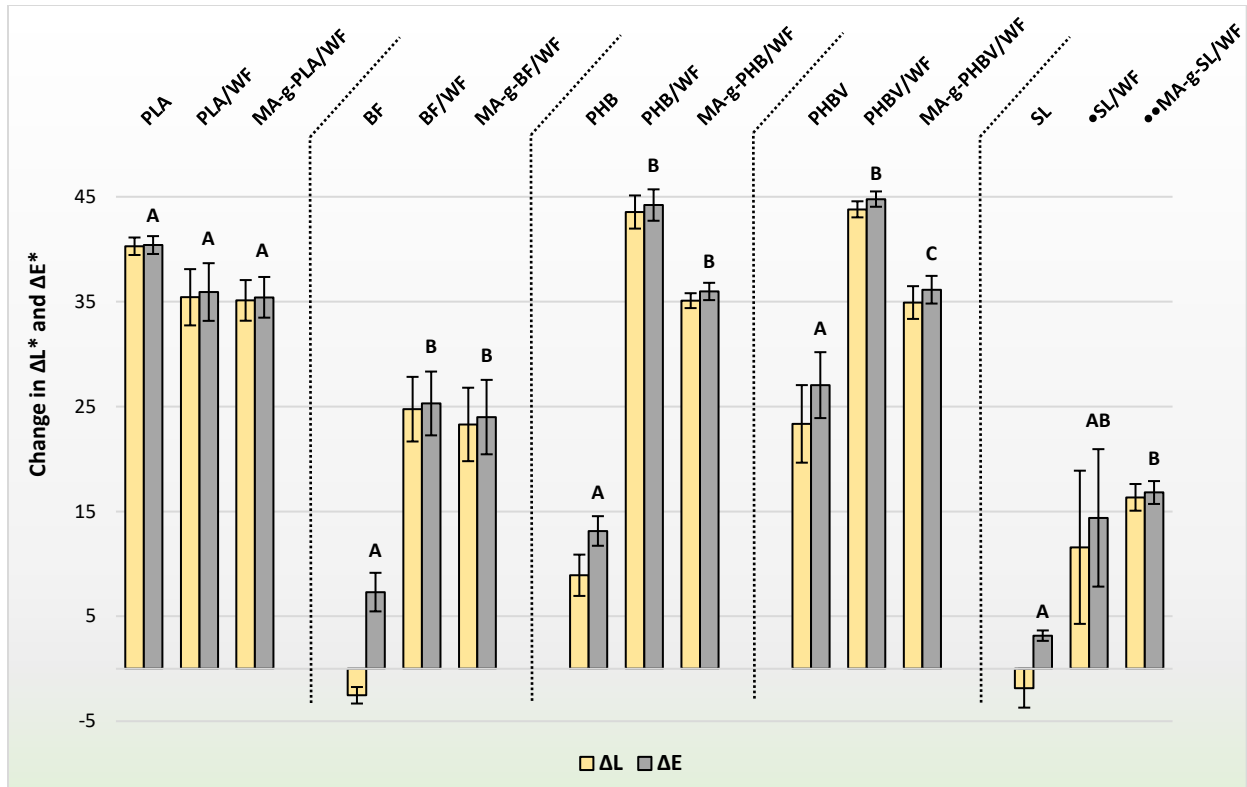


Figure 3.1. The lightness (ΔL^*) and total color changes (ΔE^*) of the specimens after 2000h of accelerated weathering. Different letters above the bars indicate statistically significant differences type at $P < 0.05$ between the specimens in each polymer type. The error bars show standard deviation.

NOTE: • Measured after 884 h of weathering, and •• Measured after 1479 h of weathering.

Even though ΔE^* of compatibilized composites were slightly lower than their uncompatibilized composites by the end of 2000 h, according to Tukey's test ($P > 0.05$), there is no significant difference between ΔE^* of compatibilized and uncompatibilized composites except for PHBV (Figure 3.1). Interestingly, at 1000 h, all the uncompatibilized composites exhibited lower or similar ΔE^* values with respect to their compatibilized composites (Figure 3.2). For instance, from 1000 h to 2000 h, ΔE^* of PHBV/WF changed from 29 to 44, while for MA-g-PHBV/WF, it was from 32 to 36 (Figure 3.2b). Except for PLA composites, overall color change was more significant in the composites compared to neat polymers (Figure 3.1). This result is in agreement with a similar study on polypropylene composites, where the color change

increased with increasing content of wood in the composites (Butylina et al., 2012). The color of neat PLA was transparent before weathering, but turned into white with weathering exposure. This could be the reason for exhibiting higher color change in neat PLA compared to its composites. For all the specimens, rate of color change was higher during the first 1000 h (Figure 3.2). Similar behavior was observed by other researchers (Butylina et al., 2012; Peng et al., 2014; Rahman et al., 2011).

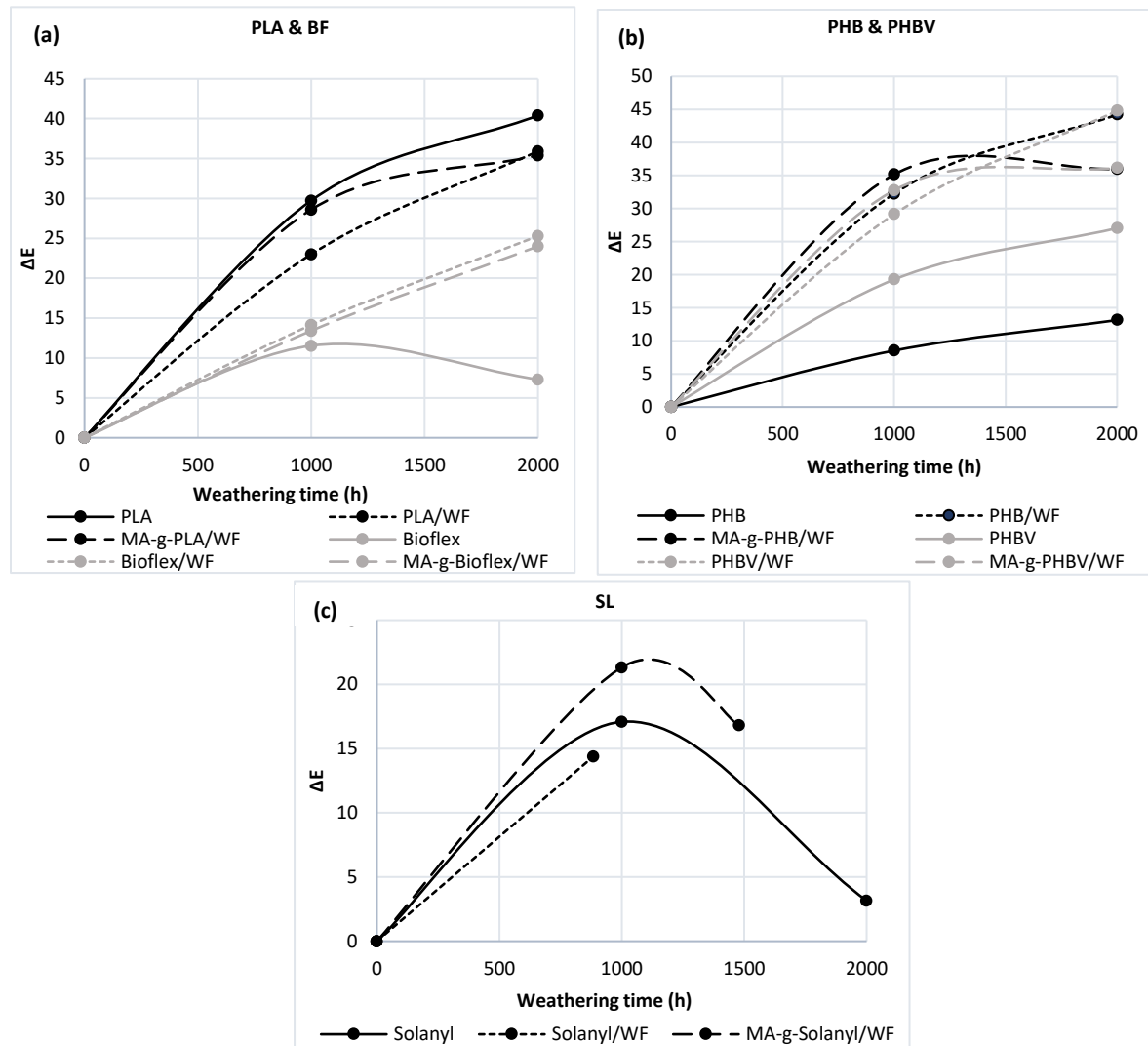


Figure 3.2. The total color change (ΔE^*) of the 15 biopolymer compositions during 2000 h of weathering: (a) PLA, PLA/WF, MA-g-PLA/WF, BF, BF/WF, MA-g-BF/WF; (b) PHB, PHB/WF, MA-g-PHB/WF, PHBV, PHBV/WF, MA-g-PHBV/WF; (c) SL, SL/WF, MA-g-SL/WF.

Water Absorption

Water absorption is a critical factor affecting dimensional stability, material degradation and long-term performance. Higher the water absorption, higher the degradation rate of a material is (Wan et al., 2009).

As the samples degraded under UV weathering, water absorption of all the specimens increased (Figure 3.3). The SL had the highest water absorption, having the highest M_m of 51.28%, which indicated its higher hydrophilicity than other polymers (Table 3.4). The SL/WF and MA-g-SL/WF lasted only for 884 h and for 1479 h of weathering, respectively. At 884 h, SL/WF had a M_m of 36.58%, while MA-g-SL/WF had 30.76% at 1000 h. These were the highest M_m exhibited at half way of weathering. Higher moisture absorbance of SL composites due to hydrophilicity of both SL and WF can be the reason for early deterioration of these composites.

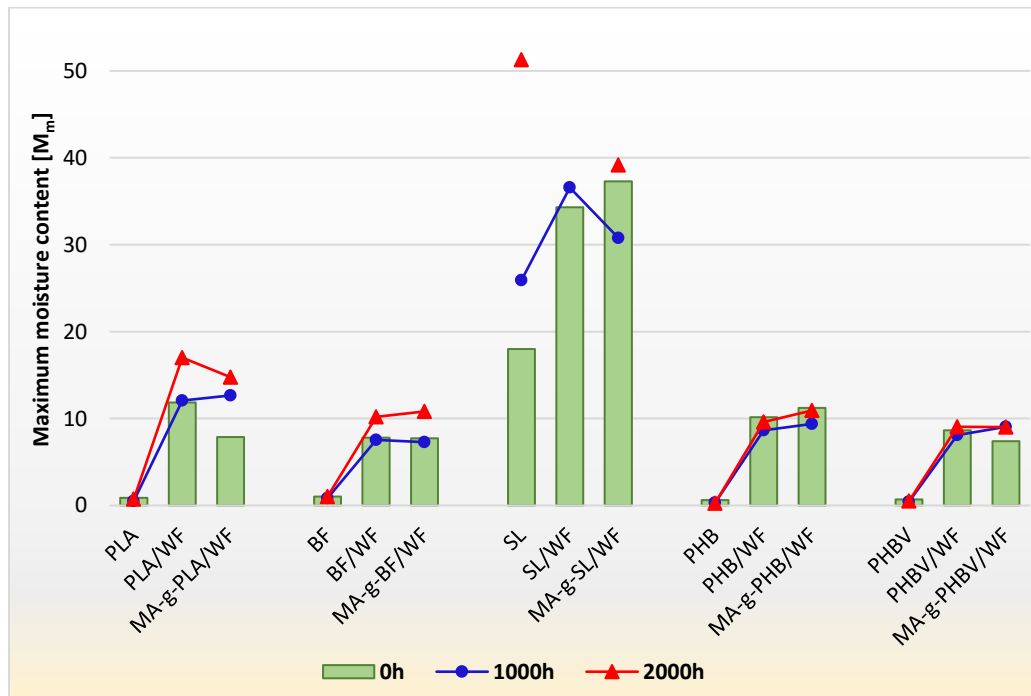


Figure 3.3. Maximum moisture (M_m) content of the 15 biopolymer compositions before weathering, and after 1000 h and 2000 h weathering (884 h instead of 1000 h for SL/WF, and 1479 h instead of 2000 h for MA-g-SL/WF).

NOTE: Reduced M_m with weathering is due to the destruction of the material few days after subjecting the samples to water absorption.

Table 3.4. Maximum moisture content (M_m) and standard deviation of the composite and neat biopolymer specimens before weathering, and 1000h and 2000h after weathering.

Composition	0 h		1000 h		2000 h	
	M_m	SD_{\pm}	M_m	SD_{\pm}	M_m	SD_{\pm}
PLA	0.87	0.05	0.50	0.03	0.73	0.12
PLA/WF	11.86	2.60	12.06	0.52	17.01	0.58
MA-g-PLA/WF	7.86	0.19	12.66	1.11	14.74	0.30
BF	1.04	0.15	0.83	0.05	1.04	0.05
BF/WF	7.82	0.60	7.56	0.52	10.18	0.20
MA-g-BF/WF	7.73	0.17	7.30	0.28	10.84	1.66
SL	17.99	0.12	25.90	0.54	51.28	2.81
SL/WF	34.32	0.38	36.58*	1.84		
MA-g-SL/WF	37.29	1.11	30.76	1.89	39.16**	2.00
PHB	0.61	0.08	0.31	0.03	0.26	0.10
PHB/WF	10.15	0.67	8.65	0.19	9.62	0.57
MA-g-PHB/WF	11.23	1.49	9.40	0.26	10.95	0.50
PHBV	0.69	0.09	0.43	0.04	0.51	0.06
PHBV/WF	8.64	0.51	8.09	0.27	9.07	0.22
MA-g-PHBV/WF	7.40	0.60	9.06	0.21	9.01	0.41

* Measured after 884 h of weathering, and **Measured after 1479 h of weathering.

The higher water absorption of the composites compared to the neat polymers was also due to the degradation of WF with weathering exposure, in addition to the hydrophilicity of WF. The low water absorption after 1000 h of weathering is an indication of surface degradation of the composite instead of the bulk. With time, surface degradation develops and prompts microcracks in the composite, resulting in higher water absorption (Krehula, Katančić, Siročić, & Hrnjak-Murčić, 2014). Microspores are also formed at the fiber-matrix interface due to weakened interfacial adhesion in composites. Microspores allow water to be diffused into the matrix easily (Balakrishnan, Hassan, Imran, & Wahit, 2011). For instance, at 1000 h, M_m of PLA/WF was 12.06% while it increased to 17.01% by the end of 2000 h of weathering. The PLA, BF, MA-g-SL/WF, PHB, PHB/WF and PHBV exhibited an irregular pattern of M_m

(increased and then decreased) with increased weathering time. For example, 0.69% M_m of PHBV was decreased to 0.43% after 1000 h of weathering, and then it increased to 0.51% at 2000 h. Reduced M_m values with weathering can be due to deterioration of those specimens in water after one week of time, which resulted in lower specimen weight values. Except for PLA, no considerable difference was shown for the composites with and without MA after 2000 h of weathering.

Differential scanning calorimetry (DSC)

With weathering exposure, overall, T_g shifted slightly to lower temperatures for all the specimens except for MA-g-PLA/WF and BF (Table 3.5). The reduction can be attributed to plasticization effect of absorbed water. Water is a key factor in aging. When water enters in between the polymer chains, the mobility of the polymer chains increases, decreasing the T_g . Another reason for the shift of T_g is the degradation effect of water on amorphous and crystalline regions of the material (Niaounakis, Kontou, & Xanthis, 2011). Degradation can take place mainly in the amorphous regions of the polymer by chain scission, whereas the UV prompted crosslinking can occur in the imperfect crystalline regions (Spiridon et al.). In addition, plasticization effect of water prompts the growth of crystals. Higher the water absorption, higher the plasticization effect is, which results in higher crystallinity ($X\%$) (Acioli-Moura & Sun, 2008). Amount of increase in $X\%$ in uncompatibilized composites was higher than the compatibilized composites. In the case of BF/WF, UV weathering increased the crystallinity by $\approx 2400\%$ (from 0.35 to 8.86%) after 2000 h, while it was only a 62% increase for MA-g-BF/WF (from 4.57% to 7.41%). This can be attributed to improved fiber-matrix interaction with the addition of MA, which reduced the water absorption of composites. However, there were no

considerable differences in $X(\%)$ between the compatibilized and uncompatibilized composites by the end of 2000 h of weathering except for PLA composites.

Table 3.5. Thermal properties of the unweathered composite specimens with and without compatibilizer, in relation to neat polymer, for the five biopolymers used in the study. Here, T_g is glass transition temperature, T_m is melting temperature, and $X(\%)$ is crystallinity of the specimens.

Composition	0 h			1000 h			2000 h		
	T_g (°C)	T_m (°C)	X (%)	T_g (°C)	T_m (°C)	X (%)	T_g (°C)	T_m (°C)	X (%)
PLA	64.2	167.8	19.54	59.98	166.88	24.4	61.56	151.24	63.52
PLA/WF	61.12	164.66	41.77	62.66	164.49	50.87	60.46	165.53	50
MA-g-PLA/WF	62.52	165.33	43.08	62.7	163.99	46.5	65.8	165.48	42.97
BF	60.2	147.7	3.26	60.25	149.65	6.8	61.33	151.85	7.34
BF/WF	59.76	146.88	0.35	61.54	148.25	7.24	57.85	151.02	8.86
MA-g-BF/WF	62.59	147.14	4.57	59.35	153.11	10.71	60.65	150.31	7.41
SL	54	148.49	***	51.83	148.25	***	51.44	148.54	***
SL/WF	55	152.99	***	53.4*	152.35*	***			***
MA-g-SL/WF	55.1	149.8	***	56.22	153.65	***	54.2**	153.11**	***
PHB	1.07	178.9	68.7	0.39	169.11	56.25	-1.08	162.88	65.14
PHB/WF	-1.97	172.19	59.9	-2.06	173.61	53.94	-1.72	168.43	62.29
MA-g-PHB/WF	-4.06	171.8	59.6	-2.44	168.65	58.72	-3.66	172.58	63.91
PHBV	-0.33	170.4	75.48	-1.36	173.23	65.34	-0.45	172.42	68.42
PHBV/WF	1.84	160.8	70.8	1.52	167.3	71.07	0.88	166.54	68.16
MA-g-PHBV/WF	1.92	161	71.83	0.72	172.39	61.44	-0.56	165.84	69.38

* Measured after 884 h of weathering, and **Measured after 1479 h of weathering.

*** Crystallinity of SL, could not be determined due to limited availability of necessary information to calculate the degree of crystallinity.

Unlike PLA or BF polymers/composites, neat PHB and PHBV and their composites only had a slight change in crystallinity. For instance, crystallinity of neat PLA increased from 19.5% to 63.5%, whereas PHB only changed by 5% by the end 2000 h weathering exposure. As Srubar

et al (W. Srubar et al., 2012) explained, with aging, PHB and PHBV exhibit a gradual rearrangement of the inter-lamellar amorphous regions only with slight changes in crystalline structure and its stability. Both PHB and PHBV undergo long-term degradation/aging period in amorphous region (W. Srubar et al., 2012).

Most of the specimens showed slightly lower melting temperatures with weathering. This was a result of both enhanced mobility of chains combined with higher crystal formation with lower melting points (Niaounakis et al., 2011). Chain scission of the polymers increases the mobility of the polymer chains, which can be result in modifications in crystalline region. These split chains rearranged into more organized structure (Iovino, Zullo, Rao, Cassar, & Gianfreda, 2008). Hence, the reduction in T_m can be attributed to consequent molecular weight reduction and breakage of polymer chains (Iovino et al., 2008). Photodegradation of polymers after exposure to weathering can be one other reason for lower T_m as well as for lower T_g (Spiridon et al.). However, after 2000 h, T_m of all the BF specimens increased by 5°C.

Thermo-Gravimetric Analysis (TGA)

TGA delivers a good insight of the polymer behavior during oxidation or thermal degradation. The thermogravimetric parameters determined from differential thermo-gravimetric (DTG) curve included the starting thermal degradation temperature (T_{onset}), the temperature corresponding to the maximum mass loss (T_{peak}), and the temperature corresponding to the end of the thermal degradation stage (T_{endset}). The total weight loss (W%) was also determined from the TG plots (Table 3.6).

Table 3.6. Starting thermal degradation temperature (T_{onset}), the temperature corresponding to the maximum mass loss (T_{peak}), the temperature corresponding to the end of the thermal degradation stage (T_{endset}), and the total weight loss (W%) for the five biopolymers and their composites, derived from thermo-gravimetric analysis.

Sample	T_{onset1} (°C)	T_{peak1} (°C)	T_{endset1} (°C)	T_{onset2} (°C)	T_{peak2} (°C)	T_{endset2} (°C)	W%
PLA	282.57	355	368				98.55
PLA/WF	251.06	345	396				87.5
MA-g-PLA/WF	263.66	363	402				91.07
BF	309.58	366	379	379	408	455	88.92
BF/WF	251.06	355	367	367	403	452	84.79
MA-g-BF/WF	265.46	352	371	371	398	454	86.12
SL	254	341	405	405	453	484	92
SL/WF	243	352	410	410	446	478	86.29
MA-g-SL/WF	245	348	401	401	446	485	87.28
PHB	238.04	264	287				92.78
PHB/WF	249.67	302	336	336	376	402	91.92
MA-g-PHB/WF	242.96	307.26	337.16	337.16	366.12	398.79	90.62
PHBV	261.43	293	305				97.1
PHBV/WF	246	296	328	328	372	399	90.76
MA-g-PHBV/WF	245	295	327	327	365	397	91.55

The TG data shows that the decomposition of PLA started at 282.6°C and completed at 368°C. During PLA degradation, many gaseous products such as cyclic oligomers, lactide molecules, acetaldehyde, carbon monoxide, and CO₂ are released (Spiridon et al., 2013). The total weight loss (W%) for PLA was 98.6%. However, it was about 10% less for PLA composites. Overall, the W% of every composite was lower than their neat polymers. For all the PLA composites, DTG curves only showed one peak, with different T_{peak} values (Figure 3.4a). The addition of MA substantially increased the thermal stability of PLA and BF composites. When WF was added to PLA and BF, the thermal degradation (T_{onset1}) started about 30°C and 50°C earlier. With the incorporation of MA, T_{onset1} increased by about 12-15°C for both PLA and BF. This can be attributed to improved fiber-matrix interfacial adhesion. With MA, it requires a

larger amount of energy to decompose the matter due to improved interfacial adhesion between the matrix and fiber (Acioli-Moura & Sun, 2008; Wong, Shanks, & Hodzic, 2004).

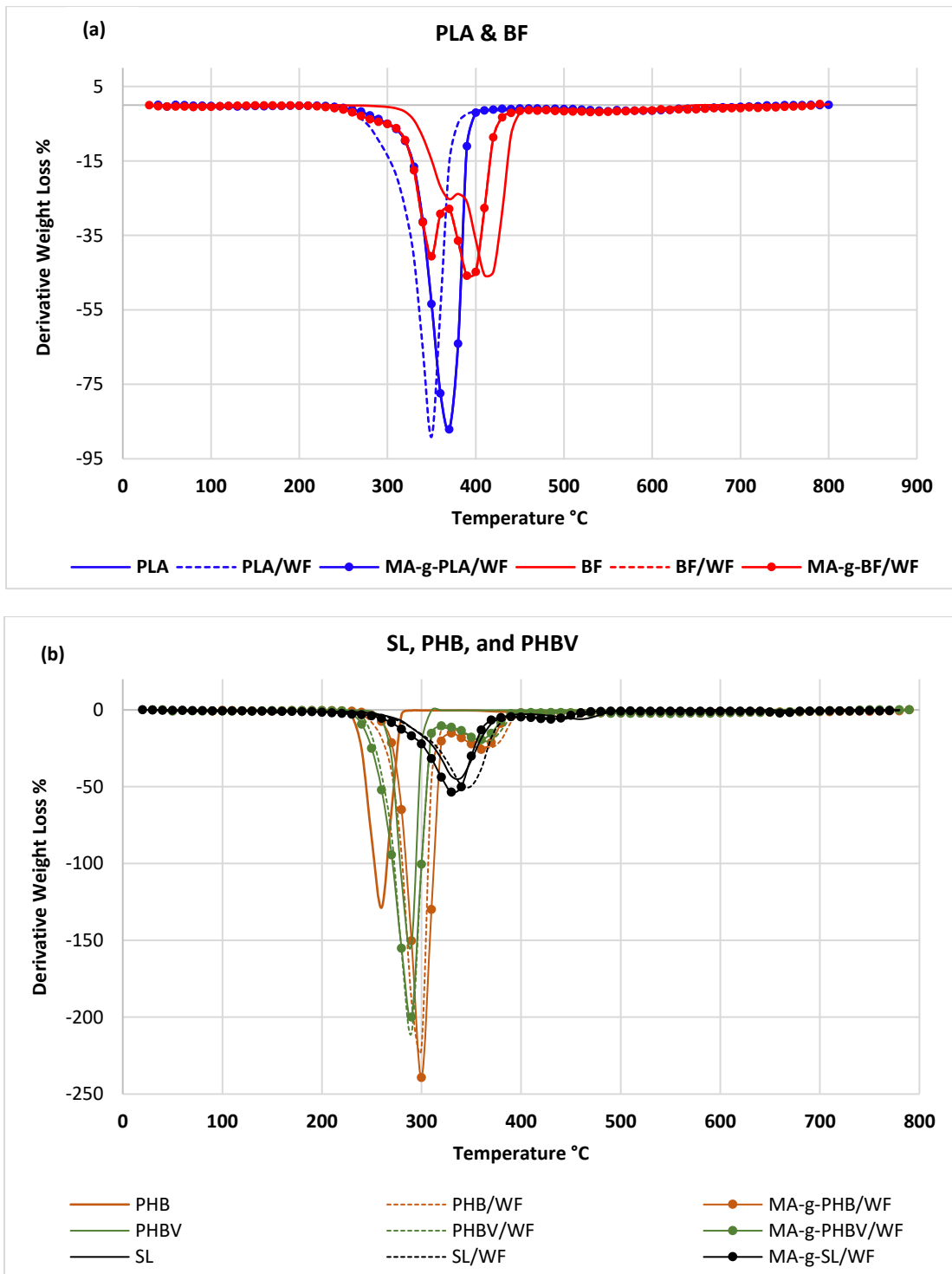


Figure 3.4. First derivative thermo-gravimetric (DTG) curves of (a) PLA and BF specimens (b) SL, PHB, and PHBV specimens.

With the addition of WF to PHB and PHBV, two stages of mass loss occurred. For both PHB/WF and PHBV/WF, the 1st peak was around 300°C, while the 2nd peak was around 370°C (Figure 3.4b). Similar results of two peaks in the derivative spectra were observed by Wong et al (Wong et al., 2004), when flax fibers were added to PHB. Neat PHB showed a single T_{peak} at 264°C, while it was at 293°C for neat PHBV. This single derivative peak of PHB and PHBV was due to degradation of the neat polymers by polymer chain scission. In this stage, crotonic acid and its oligomers are produced as degradation products (Wong et al., 2004). For PHBV, the addition of WF decreased the T_{onset} by 15°C. The PHBV degradation consists of chain scission and hydrolysis (Batista et al., 2010), which results in molecular weight reduction, and crotonic acid as a degradation product. When fiber is added, it increases the moisture in the matter, thus increasing the hydrolytic degradation of the polymer. In PHB and PHBV composites, first T_{peak} can be ascribed to degradation of the neat polymer, while the second peak corresponds to fiber degradation. There were no major differences in degradation temperatures (T_{onset}) of PHBV/WF and MA-g-PHBV/WF. On the other hand, T_{onset} of PHB/WF were slightly shifted to a lower value when MA was added.

For all SL specimens, an initial mass loss was observed in between 100-200°C (Figure 3.4b) due to moisture loss (Acioli-Moura & Sun, 2008). No significant moisture losses were apparent for the PHB and PHBV specimens. Slight moisture losses were observed for PLA/WF, BF/WF, and MA-g-BF/WF between 50-150°C. All the SL and BF specimens exhibited multiple degradation stages.

Mechanical Properties

Grafting MA to the polymers significantly improved the impact, flexural and hardness properties of PLA, BF and PHBV composites due to increased interfacial adhesion between the

fiber and the matrix in MA grafted composites (Table 3.7- 3.8). On the other hand, compatibilized PHB and SL did not exhibit any significant improvement in strength properties with respect to the uncompatibilized composites.

Table 3.7. Flexural strength and modulus all the specimens at 0, 1000 and 2000 h of UV weathering. Different letters indicate statistically significant differences at $P < 0.05$ between the specimens in each polymer type.

	Flexural Strength [MPa]						Flexural Modulus [MPa]					
	0 h		1000 h		2000 h		0 h		1000 h		2000 h	
PLA	79.65 ± 6.17	A*	10.16 ± 1.56	A*	0.91 ± 0.39	A*	2753.05 ± 211.4	A*	2886.72 ± 339.86	A*		*
PLA/WF	42.58 ± 2.59	B	26.03 ± 4.88	B	13.79 ± 0.86	B	3489.18 ± 530.57	B	2289.34 ± 236.12	B	1828.08 ± 146.71	A
MA-g-PLA/WF	52.8 ± 4.05	C	18.78 ± 1.37	C	13.5 ± 0.07	B	3545.6 ± 308.67	B	2267.96 ± 156.26	B	1900.75 ± 73.09	A
BF	9.52 ± 1.56	B	5.88 ± 0.5	A	2.98 ± 0.31	A	265.31 ± 30.16	A	337.86 ± 17.34	A	220.59 ± 43.42	A
BF/WF	12.6 ± 1.34	A	9.75 ± 0.28	B	5.43 ± 1.48	B	510.32 ± 31.68	B	360.93 ± 37.68	A	467.94 ± 23.25	B
MA-g-BF/WF	15.04 ± 0.92	A	10.52 ± 0.96	B	4.69 ± 1.56	AB	445.79 ± 52.57	B	398.55 ± 57.04	A	423.78 ± 16.9	B
SL	15.24 ± 1.45	A	2.22 ± 0.96	A	1.38 ± 0.33	A	1050.34 ± 134.06	A	265.18 ± 113.8	A	252.75 ± 104.85	A
SL/WF	20.45 ± 1.05	B	•3.89 ± 0.76	A			2305.08 ± 150.76	B	•446.49 ± 55.92	A		
MA-g-SL/WF	17.7 ± 0.38	C	2.77 ± 0.71	A	••0.63 ± 0.31	B	2159.8 ± 83.89	B	399.8 ± 154.43	A	••79.55 ± 33.87	B
PHB	66.1 ± 12.86	A	50.33 ± 2.66	A	27.84 ± 3.13	A	3636.83 ± 1091.73	A	3659.64 ± 307.19	A	2970.64 ± 687.85	A
PHB/WF	33.6 ± 3.88	B	32.73 ± 1.88	B	23.64 ± 5.29	AB	2854.63 ± 611.49	A	2619.27 ± 303.92	B	2294.72 ± 663.09	A
MA-g-PHB/WF	33.79 ± 4.57	B	25.9 ± 1.56	C	16.7 ± 2.76	B	2882.48 ± 449.97	A	2347.41 ± 121.31	B	2444.18 ± 314.37	A
PHBV	52.61 ± 2.68	A	41.21 ± 7.81	A	22.34 ± 5.11	A	2321.89 ± 111.66	A	3432.75 ± 150.54	A	3209.27 ± 376.4	A
PHBV/WF	27.88 ± 6.16	B	24.9 ± 5.25	B	20.51 ± 3.47	A	3093.76 ± 637.26	A	2180.01 ± 490.87	B	2260.82 ± 315.05	B
MA-g-PHBV/WF	30.95 ± 3.75	B	25.26 ± 3.76	B	17 ± 1.37	A	2715.47 ± 547.68	A	2231.47 ± 265.46	B	2270.88 ± 174.46	B

* Tukey multiple comparison ($P > 0.05$) of the effects of WF and MA content on each polymer type. •Measured after 884 h of weathering, and ••Measured after 1479 h of weathering.

Table 3.8. Impact fracture energy and hardness of all the specimens before weathering and after weathering (1000h and 2000h). Different letters indicate statistically significant differences type at $P < 0.05$ between the specimens in each polymer type.

	Impact Fracture Energy [J]						Hardness [Force, N]					
	0 h		1000 h		2000 h		0 h		1000 h		2000 h	
PLA	0.31 ± 0.05	A*	0.17 ± 0.05	A*	0.03 ± 0.01	A*	35.47 ± 1.01	A*	34.98 ± 1.16	A*	31.95 ± 2.92	A*
PLA/WF	0.20 ± 0.05	B	0.16 ± 0.05	A	0.14 ± 0.06	B	32.98 ± 1.15	B	35.07 ± 1.15	A	34.18 ± 1.15	A
MA-g-PLA/WF	0.25 ± 0.05	AB	0.14 ± 0.05	A	0.13 ± 0.05	B	35.29 ± 0.51	A	33.91 ± 1.19	A	34.71 ± 1.19	A
BF	1.27 ± 0.23	A	0.23 ± 0.05	A	0.10 ± 0.02	A	23.03 ± 0.73	A	23.05 ± 1.27	A	22.25 ± 1.13	A
BF/WF	0.41 ± 0.07	B	0.24 ± 0.02	A	0.11 ± 0.01	A	25.96 ± 0.92	B	24.65 ± 1.02	A	24.3 ± 0.4	B
MA-g-BF/WF	1.24 ± 0.08	A	0.20 ± 0.01	A	0.09 ± 0.01	A	26.31 ± 0.38	B	24.39 ± 0.96	A	21.36 ± 0.31	A
SL	0.19 ± 0.05	A	0.07 ± 0.01	A	0.06 ± 0.02	A	30.49 ± 1.43	A	29.01 ± 3.2	A	24.92 ± 1.81	A
SL/WF	0.10 ± 0.02	B	•0.12 ± 0.02	B			35.12 ± 1.04	B	•23.2 ± 1.9	B		
MA-g-SL/WF	0.10 ± 0.01	B	0.11 ± 0.01	B	••0.07 ± 0.01	A	34.49 ± 0.81	B	27.23 ± 1.39	A	••22.3 ± 1.39	B
PHB	0.45 ± 0.13	A	0.26 ± 0.05	A	0.24 ± 0.03	A	33.52 ± 1.49	A	33.02 ± 1.62	A	34 ± 0.74	A
PHB/WF	0.37 ± 0.11	A	0.10 ± 0.01	B	0.08 ± 0.01	B	31.47 ± 1.38	A	30.44 ± 1.02	A	31.6 ± 2.16	A
MA-g-PHB/WF	0.12 ± 0.02	B	0.10 ± 0.01	B	0.07 ± 0.01	B	28.54 ± 1.38	B	30.53 ± 2.45	A	33.29 ± 1.76	A
PHBV	0.38 ± 0.07	A	0.21 ± 0.04	A	0.15 ± 0.07	A	33.78 ± 0.99	A	33.46 ± 0.52	A	33.38 ± 1.64	A
PHBV/WF	0.16 ± 0.04	B	0.12 ± 0.04	B	0.10 ± 0.02	A	29.25 ± 0.73	B	34.35 ± 0.73	A	32.93 ± 2.59	A
MA-g-PHBV/WF	0.20 ± 0.09	B	0.09 ± 0.01	B	0.09 ± 0.02	A	34.05 ± 1.12	A	34 ± 1.74	A	31.33 ± 1.43	A

* Tukey multiple comparison ($P > 0.05$) of the effects of WF and MA content on each polymer type. •Measured after 884 h of weathering, and ••Measured after 1479 h of weathering.

All the polymer specimens showed decrease in mechanical strength with increased weathering exposure. A considerable drop of impact fracture energy and flexural strength can be observed for most of the polymer specimens after 2000 h of weathering (Figure 3.5-3.6). Impact fracture energy of 0.45 J decreased by 47% by the end of 2000 h weathering for neat PHB (Table

3.8). PLA exhibited substantial reduction in flexural strength from 79.7 MPa to 10.2 MPa by 1000 h, and then to 0.9 MPa by 2000 h of weathering (Table 3.7). Main mechanism of degradation of PLA is the hydrolysis, and higher temperatures ($>50^{\circ}\text{C}$) increase the rate of the hydrolysis process (Niaounakis et al., 2011). Hydrolysis first occurs in amorphous region, and then progresses into crystalline region, which results in lower molecular weight ensuing in reduced strength properties. Compared to neat PLA, loss of strength was notably lower for PLA/WF and MA-g-PLA/WF (Figure 3.5-3.6). This can be ascribed to antioxidant properties of lignin in wood fiber of the composites. Lignin assists in stabilization of the material against photo and thermooxidation during weathering (Peng et al., 2014; Spiridon et al., 2015; Spiridon et al., 2013).

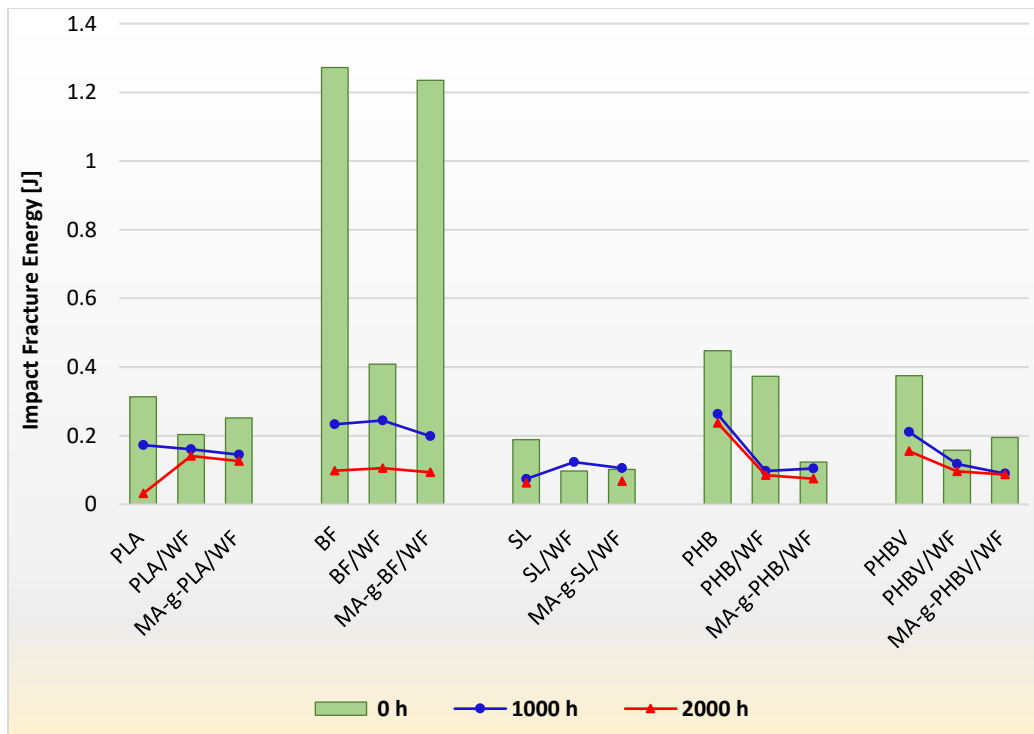


Figure 3.5. Impact fracture energy of the neat biopolymer and composite specimens before weathering, and after 1000 h and 2000 h of weathering (884 h instead of 1000 h for SL/WF, and 1479 h instead of 2000 h for MA-g-SL/WF).

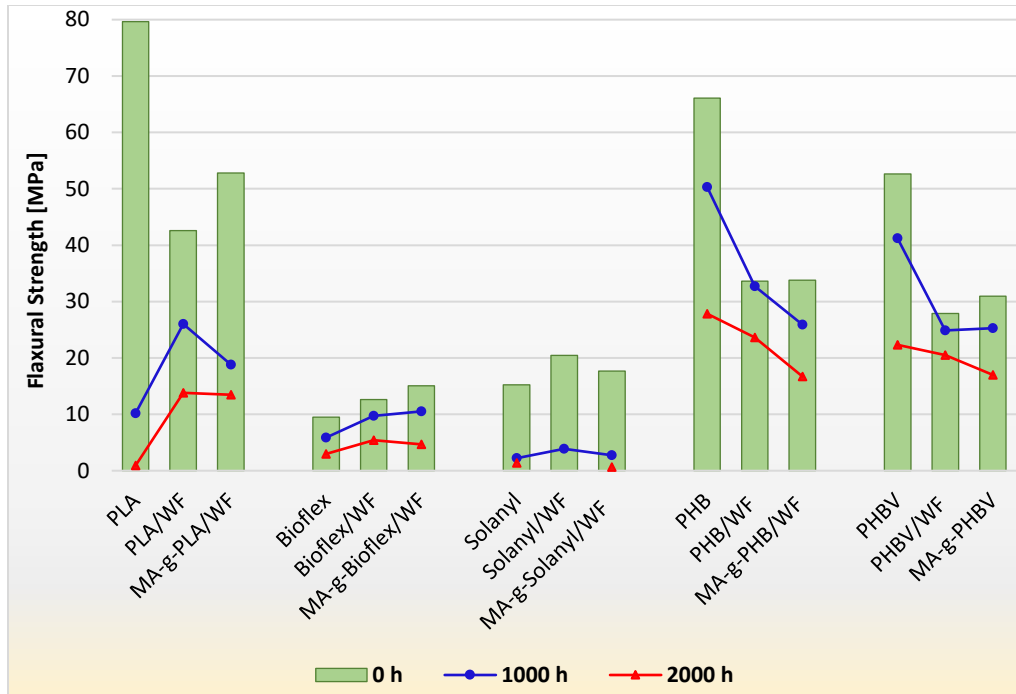


Figure 3.6. Flexural strength of the neat biopolymer and composite specimens before weathering, and after 1000 h and 2000 h of weathering (884 h instead of 1000 h for SL/WF, and 1479 h instead of 2000 h for MA-g-SL/WF).

Flexural modulus reduced with weathering for most of the specimens (Figure 3.7).

Highest reduction of 96% was shown for MA-g-SL/WF after 1479 h (Table 3.7). No considerable reduction was shown for PHBV/WF, and compatibilized BF, PHB and PHBV composites between 1000 h and 2000 h of weathering (Figure 3.7). For instance, modulus of MA-g-PHBV/WF reduced to 2231.5 MPa from 2715.5 by 1000 h, and then slightly increased to 2270.9 MPa by 2000 h. For the specimens that exhibited an increase of the property with weathering, Tukey's pairwise method was conducted to test the significance of the increase at each weathering period. The decreased modulus of BF/WF at 1000 h exhibited a significant increase by the end of 2000 h (Figure 3.7). At 1000 h, modulus of BF and PHBV significantly increased by 27% and 48%, respectively. It should be stated that the flexural modulus of neat PLA at 2000 h could not be obtained by the test method due to its extreme brittleness.

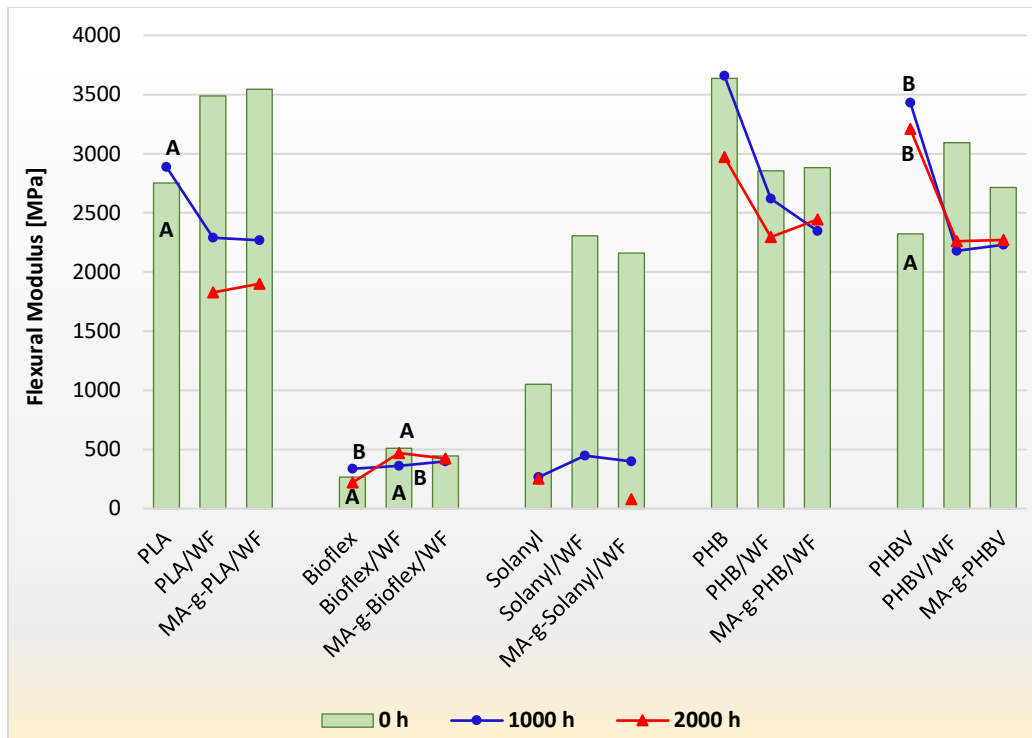


Figure 3.7. Flexural modulus of the neat biopolymer and composite specimens before weathering, and after 1000 h and 2000 h of weathering (884 h instead of 1000 h for SL/WF, and 1479 h instead of 2000 h for MA-g-SL/WF). Different letters indicate statistically significant difference of the specimen on the property at each weathering exposure.

Hardness is the resistance of the material surface against the indentation, which decreases with the flexibility and mobility of the polymer chain structure (Mandal, Chakraborty, & Siddhanta, 2014). It is apparent, that hardness properties were affected to lesser degree by the weathering exposure (Figure 3.8). The highest reduction of 35% can be seen in for MA-g-SL/WF after 1479 h of weathering (Table 3.8). On the other hand, hardness of PLA/WF, MA-g-PHB/WF, and PHBV/WF significantly increased with weathering. This can be attributed to increased degree of crystallinity of the polymer specimens.

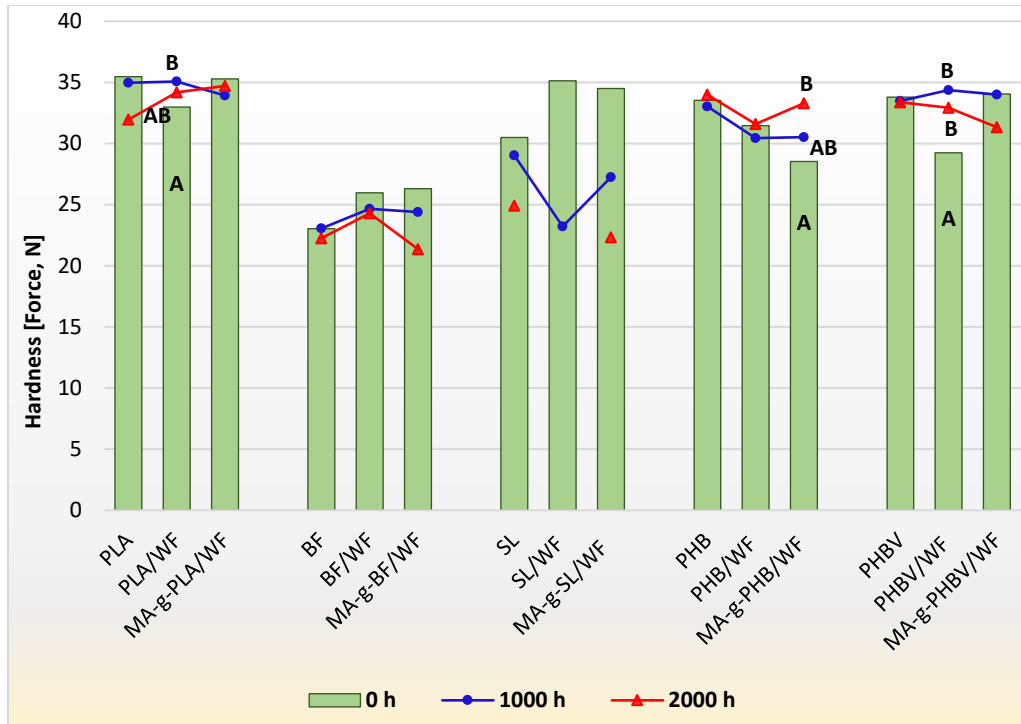


Figure 3.8. Hardness of the neat biopolymer and composite specimens before weathering, and after 1000 h and 2000 h of weathering (884 h instead of 1000 h for SL/WF, and 1479 h instead of 2000 h for MA-g-SL/WF). Different letters indicate statistically significant difference of the specimen on the property at each weathering exposure.

Overall, strength property loss during weathering was due to the formed shorter polymer chains as a result of continuous polymer chain scission, which lead to reduction of macromolecules length and higher degree of crystallinity. Even though the crystallinity increased as evident in DSC results, these formed crystalline regions were weaker due to the shortness of the chains, which resulted in decreased strength properties (Peng et al., 2014). For instance, though the crystallinity of BF increased by $\approx 2400\%$ after 2000 h of weathering, its impact fracture energy decreased by 74% (Table 3.5, Figure 3.5).

For the composites, change in strength properties also depend on fiber-matrix interaction. With weathering, fiber–matrix interaction decreased, and cracks were formed due to swelling of WF because of moisture absorbance property of hydrophilic WF. Consequently, deterioration of the mechanical properties of the material can be observed due to reduction of stress transfer from

fiber to matrix (Butylina et al., 2012; Chen et al., 2016). UV radiation, relative humidity and temperature are the fundamental factors causing deterioration of composites with natural fiber (Islam et al., 2013). Overall, with increased weathering exposure, compatibilized composites did not seem to have any significant difference in mechanical property loss compared to the uncompatibilized composites (Table 3.7-3.8).

Conclusion

Five different types of biodegradable biobased composites were prepared by blending wood fiber with biopolymers: PLA, Bioflex (PLA blend), Solanyl (starch based), PHB, or PHBV. Maleic Anhydride was used to compatibilize the composites. Compatibilization improved physical, thermal and mechanical properties of PLA, Bioflex (BF) and PHBV composites. With increased weathering exposure, increased surface degradation was evident through surface color change and microcracks in the specimens, which led to higher water absorption. After weathering, smooth surfaces of the specimen roughened due to matrix degradation that occurred because of polymer chain scission. Color change of the samples was attributed to photo-degradation, photo-oxidation, and increased diffuse reflectance. Overall, glass transition temperature shifted slightly to lower temperatures with weathering. This reduction was attributed to the plasticization and degradation effect of absorbed water. Reduced melting temperature of weathered specimens was a result of both enhanced mobility of chains combined with higher crystal formation at lower melting points. Even though the crystallinity increased due to chain scission of the polymers, these formed crystalline regions were mechanically weaker because of the shorter polymer chains. Most the polymer specimens showed decrease in impact, flexural and hardness properties with increased weathering exposure due to decrease in molecular weight, intensive chain scission, and decreased fiber-matrix interaction. Some

polymer materials exhibited significant improvements in flexural modulus and hardness with weathering. Even though the compatibilized composites showed improved properties before weathering, there were no differences between compatibilized and uncompatibilized composites on how weathering impacted thermal, physical and mechanical properties. The study indicates that there is an opportunity to design sustainable green composites with better strength properties by adding compatibilizers, without affecting their UV weathering properties.

References

- Abdulkhani, A., Hosseinzadeh, J., Dadashi, S., & Mousavi, M. (2015). A study of morphological, thermal, mechanical and barrier properties of PLA based biocomposites prepared with micro and nano sized cellulosic fibers. *Cell Chem Technol*, 49(7-8), 597-605.
- Acioli-Moura, R., & Sun, X. S. (2008). Thermal degradation and physical aging of poly (lactic acid) and its blends with starch. *Polymer Engineering & Science*, 48(4), 829-836.
- ASTM D256. (2010). In *ASTM D256: Standard Test Methods for Determining the Izod Pendulum Impact Resistance of Plastics*: American Society for Testing and Materials.
- ASTM D570. (2010). In *Standard Test Method for Water Absorption of Plastics*: American Society for Testing and Materials.
- ASTM, D. (2000). 2240, Standard Test Method for Rubber Property-Durometer Hardness. *Figure S. left column shows visual surbet'degradation of the ont'-compont'nt urethane after (top to bottom), 18.*
- ASTM, D. (2003). 2244:“Standard Practice for Calculation of Color Tolerances and Color Differences from Instrumentally Measured Color Coordinates”. *American Society for Testing and Materials, West Conshohocken, PA.*

- ASTM G154. (2012). In *Standard Practice for Operating Fluorescent Ultraviolet (UV) Lamp Apparatus for Exposure of Nonmetallic Materials*.
- ASTM, I. (2007). Standard test methods for flexural properties of unreinforced and reinforced plastics and electrical insulating materials. *ASTM D790-07*.
- Balakrishnan, H., Hassan, A., Imran, M., & Wahit, M. U. (2011). Aging of toughened polylactic acid nanocomposites: water absorption, hygrothermal degradation and soil burial analysis. *Journal of Polymers and the Environment*, 19(4), 863-875.
- Batista, K., Silva, D., Coelho, L., Pezzin, S., & Pezzin, A. (2010). Soil biodegradation of PHBV/peach palm particles biocomposites. *Journal of Polymers and the Environment*, 18(3), 346-354.
- Bronzino, J. D. (1999). *Biomedical engineering handbook* (2 Sub edition ed. Vol. 1): CRC Press.
- Butylina, S., Hyvärinen, M., & Kärki, T. (2012). A study of surface changes of wood-polypropylene composites as the result of exterior weathering. *Polymer Degradation and Stability*, 97(3), 337-345.
- Chen, Y., Stark, N. M., Tshabalala, M. A., Gao, J., & Fan, Y. (2016). Weathering characteristics of wood plastic composites reinforced with extracted or delignified wood flour. *Materials*, 9(8), 610.
- Fabiyi, J. S., McDonald, A. G., Wolcott, M. P., & Griffiths, P. R. (2008). Wood plastic composites weathering: Visual appearance and chemical changes. *Polymer Degradation and Stability*, 93(8), 1405-1414.
- Gunning, M. A., Geever, L. M., Killion, J. A., Lyons, J. G., & Higginbotham, C. L. (2014). Effect of Compatibilizer Content on the Mechanical Properties of Bioplastic Composites

- via Hot Melt Extrusion. *Polymer-Plastics Technology and Engineering*, 53(12), 1223-1235.
- Iovino, R., Zullo, R., Rao, M., Cassar, L., & Gianfreda, L. (2008). Biodegradation of poly (lactic acid)/starch/coir biocomposites under controlled composting conditions. *Polymer Degradation and Stability*, 93(1), 147-157.
- Islam, M. N., Dungani, R., Khalil, H. A., Alwani, M. S., Nadirah, W. W., & Fizree, H. M. (2013). Natural weathering studies of oil palm trunk lumber (OPTL) green polymer composites enhanced with oil palm shell (OPS) nanoparticles. *SpringerPlus*, 2(1), 592.
- Krehula, L. K., Katančić, Z., Siročić, A. P., & Hrnjak-Murgić, Z. (2014). Weathering of high-density polyethylene-wood plastic composites. *Journal of Wood Chemistry and Technology*, 34(1), 39-54.
- Madbouly, S., Schrader, J., Srinivasan, G., Haubric, K., Liu, K., Grewell, D., . . . Kessler, M. (2012). *Bio-based Polymers and Composites for Container Production Materials*. Paper presented at the 2012 Bioplastic Container Cropping Systems Conference, Iowa State University.
- Mandal, A. K., Chakraborty, D., & Siddhanta, S. K. (2014). Effect of the compatibilizer, on the engineering properties of TPV based on Hypalon® and PP prepared by dynamic vulcanization. *Journal of Applied Polymer Science*, 131(11).
- Michel, A., & Billington, S. (2012). Characterization of poly-hydroxybutyrate films and hemp fiber reinforced composites exposed to accelerated weathering. *Polymer Degradation and Stability*, 97(6), 870-878.
- Niaounakis, M., Kontou, E., & Xanthis, M. (2011). Effects of aging on the thermomechanical properties of poly (lactic acid). *Journal of Applied Polymer Science*, 119(1), 472-481.

- Peng, Y., Liu, R., Cao, J., & Chen, Y. (2014). Effects of UV weathering on surface properties of polypropylene composites reinforced with wood flour, lignin, and cellulose. *Applied Surface Science*, 317, 385-392.
- Rahman, W. A. W. A., Sin, L. T., Rahmat, A. R., Isa, N., Salleh, M., & Mokhtar, M. (2011). Comparison of rice husk-filled polyethylene composite and natural wood under weathering effects. *Journal of Composite Materials*, 45(13), 1403-1410.
- Sahari, J., Sapuan, S. M., Zainudin, E. S., & Maleque, M. A. (2014). Degradation characteristics of SPF/SPS biocomposites. *Fibres & Textiles in Eastern Europe*.
- Spiridon, I., Leluk, K., Resmerita, A. M., & Darie, R. N. (2015). Evaluation of PLA–lignin bioplastics properties before and after accelerated weathering. *Composites Part B: Engineering*, 69, 342-349.
- Spiridon, I., Paduraru, O. M., Zaltariov, M. F., & Darie, R. N. (2013). Influence of keratin on polylactic acid/chitosan composite properties. Behavior upon accelerated weathering. *Industrial & Engineering Chemistry Research*, 52(29), 9822-9833.
- Srubar, W., Wright, Z., Tsui, A., Michel, A., Billington, S., & Frank, C. (2012). Characterizing the effects of ambient aging on the mechanical and physical properties of two commercially available bacterial thermoplastics. *Polymer Degradation and Stability*, 97(10), 1922-1929.
- Srubar, W. V., Pilla, S., Wright, Z. C., Ryan, C. A., Greene, J. P., Frank, C. W., & Billington, S. L. (2012). Mechanisms and impact of fiber–matrix compatibilization techniques on the material characterization of PHBV/oak wood flour engineered biobased composites. *Composites Science and Technology*, 72(6), 708-715.

- Suryanegara, L., Nakagaito, A. N., & Yano, H. (2009). The effect of crystallization of PLA on the thermal and mechanical properties of microfibrillated cellulose-reinforced PLA composites. *Composites Science and Technology*, *69*(7), 1187-1192.
- Thiré, R. M. d. S. M., Arruda, L. C., & Barreto, L. S. (2011). Morphology and thermal properties of poly (3-hydroxybutyrate-co-3-hydroxyvalerate)/attapulgitite nanocomposites. *Materials Research*, *14*(3), 340-344.
- Vroman, I., & Tighzert, L. (2009). Biodegradable polymers. *Materials*, *2*(2), 307-344.
- Wan, Y., Luo, H., He, F., Liang, H., Huang, Y., & Li, X. (2009). Mechanical, moisture absorption, and biodegradation behaviours of bacterial cellulose fibre-reinforced starch biocomposites. *Composites Science and Technology*, *69*(7), 1212-1217.
- Wei, L., Liang, S., & McDonald, A. G. (2015). Thermophysical properties and biodegradation behavior of green composites made from polyhydroxybutyrate and potato peel waste fermentation residue. *Industrial Crops and Products*, *69*, 91-103.
- Wong, S., Shanks, R., & Hodzic, A. (2004). Interfacial improvements in poly (3-hydroxybutyrate)-flax fibre composites with hydrogen bonding additives. *Composites science and technology*, *64*(9), 1321-1330.

CHAPTER 4. BIODEGRADATION PROPERTIES OF COMPATIBILIZED BIOPOLYMER COMPOSITES

Abstract

Because of the environmental sustainability concerns regarding petroleum-based polymers, biodegradable polymers from renewable and biobased resources are gaining popularity for use in commercial applications. It is critical to design biobased biodegradable polymers to be cost effective, resistance to environmental factors during use, and quickly biodegradable under disposal conditions. Although degradation properties of biopolymers are quantified, biodegradation of their composites and the effect of compatibilization on biodegradation properties are not well understood. In this study, five biobased biodegradable polymers were compatibilized with 1-2 wt% maleic anhydride (MA), and their biodegradation was evaluated against composites without MA under different soil temperatures. The composite samples were prepared with 30 wt% wood fiber and one of the five biopolymers: poly(lactic acid) (PLA), polyhydroxybutyrate (PHB), poly(3-hydroxybutyrate-co-3-hydroxyvalerate) (PHBV), Bioflex (PLA blend), or Solanyl (starch based). The composites were subjected to soil burial analysis for 60 days under two different temperatures of 30°C and 60°C. The samples were characterized for morphological, physical and mechanical properties. Weight loss and increased water absorption were observed in all soil buried specimens. Surface deterioration was more visible in 60°C soil buried samples with drastic color change and roughened surfaces due to increased hydrolysis and hydrophilicity of biopolymers at higher temperatures. Mechanical properties were decreased with soil biodegradation. Even though the compatibilized composites showed lower biodegradation at 30°C, the 60°C biodegradation of compatibilized composites

were higher than the composites without MA. The results confirm that compatibilization not only improves mechanical properties but also biodegradation at elevated temperatures.

Introduction

Synthetic and petroleum based polymers cause substantial environmental problems at disposal. Annual global production of plastic is about 300 million tons. Even though recycling is an effective solution, only about 10% of plastics are being recycled each year. Around 7 million metric tons of plastic fragments end up in the sea every year, harming nearly 267 different animal species due to plastic entanglement and ingestion. About 60-95% of the land-based sources of marine pollution are plastics debris (Lytle, 2009; Wassener, 2011). Petroleum based polymers also cause air pollution during production. For each ounce of polyethylene production, about five ounces of carbon dioxide are emitted (*Glazner, 2015*).

Biodegradable polymers produced from renewable and biobased resources are considered highly sustainable. They reduce waste accumulation, CO₂ emission, and the dependency on petroleum-based fuels and products. Although biobased polymers have numerous benefits, they are restricted in many applications due to high cost and a few undesirable properties such as slow biodegradation rate, sensitivity to thermal degradation, and high brittleness. Compared to the rate of waste accumulation, the degradation rate of biobased polymers such as PLA is still too slow (Niaounakis, Kontou, & Xanthis, 2011). To improve these properties and reduce the cost, biobased polymers could be blended with biodegradable natural cellulose fibers. Natural lignocellulosic fibers are expected to increase the biodegradability of the fibers while imparting desirable material properties for certain applications. Wood fiber is an inexpensive and readily available byproduct from wood processing operations that is reused for manufacturing polymer composites. Nevertheless, due to poor interfacial adhesion between the hydrophobic polymer and

the hydrophilic fiber, incorporating fibers to polymer matrices causes decrease in some properties such as impact and tensile strength. By introducing reactive functional groups such as compatibilizers, mechanical properties of these biopolymer composites could be enhanced. The biodegradation behavior of biopolymer composites with natural fibers and compatibilizers at different conditions is not well known yet. Some studies showed that even though the addition of compatibilizers to biocomposites improved the mechanical properties, biodegradability of the composites reduced due to increased water resistance (C.-S. Wu, 2009; C. S. Wu, 2006, 2012).

In biodegradation, degraded products are completely assimilated as a food source by soil microorganisms. It ensures the safe and effective returning of carbon into the ecosystem. Biodegradability of polymers does not necessarily assure the degradation of the polymer in any environment under any conditions. Rate of biodegradability depends on factors such as temperature and humidity of the environment, processing conditions, and polymer characteristics such as molecular weight, crystallinity, and plasticizers or additives added to the polymer. When a compatibilizer such as maleic anhydride (MA) is grafted, improvement in adhesion between the polymer substrate and the fiber can be observed due to formation of both hydrogen and covalent bonds with fiber and polymer. Consequently, at lower temperatures, compatibilized composites have poor biodegradation due to hindered water absorption. However, increased water absorption of polymer matrices at elevated temperature (60°C) has been reported in the literature (Balakrishnan, Hassan, Imran, & Wahit, 2011; Gunning, Geever, Killion, Lyons, & Higginbotham, 2014; Itävaara, Karjomaa, & Selin, 2002). Higher water absorption increases polymer hydrophilicity, resulting in chemical hydrolysis as well as higher microbe attachments on the polymer surface (Itävaara et al., 2002).

The hypothesis of this research is that biodegradation of polymers could be higher at elevated temperatures due to increased water absorption. Biodegradation of compatibilized composites also could be higher than that of uncompatibilized composites if the increased attachment of WF could expand the surface area available for biodegradation when the bonds between the WF and the polymer hydrolyze at higher temperatures. The objectives of this study are to 1) evaluate and compare the biodegradability of biocomposites made with different types of biopolymers and a wood fiber filler, and 2) quantify the effect of compatibilization of the biopolymer-wood fiber composites on biodegradation properties at different temperatures.

Experimental

In this study, five types of MA-compatibilized biocomposites were prepared by compounding wood fiber (WF) with five different types of biopolymers: poly(lactic acid) (PLA), Bioflex (BF), Solanyl (SL), poly(3-hydroxybutyric acid) (PHB), and poly(3-hydroxybutyrate-co-3-hydroxyvalerate) (PHBV). The PLA is a biodegradable polyester produced by polymerization of lactic acid. Both PHB and PHBV are polyhydroxyalkanoates (PHA). The PHA is a linear polyester produced by bacterial fermentation of sugar or lipids. Bioflex is a PLA blend, and Solanyl is a potato starch based polymer. All the specimens were subjected to soil biodegradation at two different temperatures, 30°C and 60°C. Weight loss, water absorption, hardness and compressive tests were undertaken to predict the biodegradation performance. The surface morphology changes due to soil biodegradation were studied by optical microscopy and color changes.

Materials

The PLA used in this study was type 2003D from NatureWorks LLC (Minnetonka, MN). The PHB (ENMAT Y3000P) and PHBV (ENMAT Y1000P) were supplied by TianAN

Biopolymer (Ningbo City, Zhejiang Province, China). Bioflex (BF) biopolymer (Bio-Flex® F2110) was obtained from FKUR Plastics (Willich, Germany). Solanyl (SL) biopolymer (Solanyl® C2201) was from Rodenburg Biopolymers (Oosterhout, Netherlands). Maleic anhydride (63200), Luperox® P: tert-Butyl peroxybenzoate (TBPB), benzoyl peroxide (BP), and Luperox 101: 2,5-bis(tert-butylperoxy)-2,5-dimethylhexane (L101) were purchased from Sigma-Aldrich Chemical Co. (St. Louis, MO). Oak wood fiber was used in this study.

Polymer Composite Manufacturing

Preparation of Grafted Polymer

All the polymer pellets were dried according to guidelines provided by the supplier, which included drying for 2 hours (h) at 80°C for PHB and PHBV, 6 h at 80°C for PLA, 4 h at 45°C for SL, and 3 h at 60°C for BF. Each of the dried polymers were then hand-mixed with 2-3% of MA and 0.5-1 % selected initiator (Table 2.1). For extrusion of the mixtures, a micro 18 lab-scale twin screw extruder with a 40/1 length to diameter ratio (Leistritz Ltd., Somerville, NJ) was used (Table 2.2). To remove any moisture present, extruded pellets were dried in an oven for 12 h at 80°C.

Preparation of WF composites

All the composites consisted of 30 wt% of WF loading. According to the compositions indicated in Table 2.3, each of the neat polymer pellets were mixed with WF and/or grafted polymer pellets. The mixtures were then extruded (Table 2.2), and dried for 24 h at 80°C in an oven.

Compression Molding

Using different temperatures and time for each of the polymer types, extruded pellets were compression molded into 150 mm square and 5 mm thick sheets with a Carver hot press

(model 3856, Carver Inc., Wabash, IN) at 50 atm pressure (Table 2.4). The molded sheets were slowly cooled under ambient conditions to prevent cracking.

Soil Biodegradation

Soil burial degradation experiments were carried out according to ASTM G160 standard ("ASTM G160," 2012) under temperature and moisture controlled conditions in an environmental chamber. The surrounding atmosphere was maintained at 80% relative humidity (RH). The moisture content of soil was maintained at 30% by adding water periodically. Soil biodegradation test was conducted at two different temperature settings of 30°C and 60°C. Sample specimens of 31.75 mm × 31.75 mm size were buried in glass bottles containing a soil mixture at a depth of 127 mm. Soil mixture was included fertile topsoil, well-rotted and shredded horse manure and coarse sand. The prepared soil was sifted through 6.4 mm mesh screen. The soil pH was maintained between 6.5 to 7.5, and checked periodically. Samples were dug out of soil after 60 days, and washed thoroughly with distilled water and dried to constant weight at 50% RH. Biodegradability of the samples was assessed by measuring the weight loss of the samples using Eq. 4.1. All results are the average of three replicates.

$$\text{Weight loss (\%)} = \frac{W_0 - W_1}{W_0} \times 100 \quad (\text{Eq. 4.1})$$

Where, W_0 and W_1 are sample weights before and after the soil burial test, respectively, after conditioning samples at 25°C and 50% RH.

Characterization of Composites

Water Absorption

The water absorption of the samples was measured using Equation 4.2 as specified by ASTM D570 ("ASTM D570," 2010) standard. Weights were measured periodically for 5 weeks. Dimensions of the test specimens were 38.1 mm in length and width, and 5 mm in thickness.

$$\% \text{Increase in weight } (M_t) = \frac{\text{wet weight} - \text{conditioned weight}}{\text{conditioned weight}} \times 100 \quad (\text{Eq. 4.2})$$

Optical Microscopy

Surface conditions of the specimens before and after soil burial analysis were observed using OMAX AMSCOPE microscope (S7M7045/SZM7045TR, Omax, yeonggi-do, Korea). OMAX A3590U video camera (D/N: UCMOSO9000KPB, P/N: TP609000B) and ToupView 3.7 software was used for capturing images at 30X magnification, and to examine the images.

Color Measurement

The surface colors of the samples were measured using X-Rite Spectrophotometer (Model SP62, S/N 000737, X-Rite, Grandville, MI). CIELAB color system with L^* , a^* , b^* coordinates was used to evaluate the color changes. The parameter L^* represents the lightness coordinate, which ranges between 100 (white) and 0 (dark). The a^* represents the red ($+a^*$) to green ($-a^*$), and b^* represents the yellow ($+b^*$) to blue ($-b^*$) coordinates. The color difference (ΔE^*) was calculated using Eq. 4.3 in ASTM D2244 standard (D. ASTM, 2003):

$$\Delta E^* = \sqrt{(\Delta L^*)^2 + (\Delta a^*)^2 + (\Delta b^*)^2} \quad (\text{Eq. 4.3})$$

where, ΔL^* , Δa^* , and Δb^* represent the change in initial values of L^* , a^* , and b^* by the end of soil burial analysis, respectively.

Hardness

Hardness tests were carried out according to ASTM D2240 standard (D. ASTM, 2000) (manual operation method) using a type D durometer (Model 409, S/N 02015, Davis Instrumentation, Vernon Hills, IL). The resistance force of the penetrated durometer pin in the test specimen is calculated using Eq. 4.4 (ASTM D2240 standard):

$$\text{Force, N} = (0.4445)HD \quad (\text{Eq. 4.4})$$

where, HD is the hardness reading on type D durometer.

Compressive Strength

Compressive strength was determined according to ASTM D695 standard (ASTM, 2015) on Instron 5567 load frame (Instron, Norwood, MA) with a 30kN load cell. Cross head rate was 1.3 mm/min. Specimens were 12.7 by 12.7 mm square and 5 mm in thickness.

Data Analysis

Tukey's test of multiple comparisons ($P < 0.05$) was applied to determine the significant difference between the properties of each polymer formulation before soil burial, and after 30°C and 60°C soil burial. Data analysis was performed with Minitab software (version 18, Minitab Inc., PA).

Results and Discussion

Water Absorption

Water absorption is a key factor affecting material degradation. After 60 days of soil burial at 30°C, all the samples except for SL composites, showed similar M_m values as before soil burial (Figure 4.1). Solanyl (SL) and its composites exhibited the highest water absorption (M_m) compared to other specimens. After 30°C soil burial (SB), the M_m of SL, SL/WF and MA-

g-SL/WF were 36%, 50% and 44% respectively. This can be attributed to higher hydrophilicity of both SL and WF. Compatibilized PLA, BF and PHBV composites exhibited lower M_m values compared to their uncompatibilized composites.

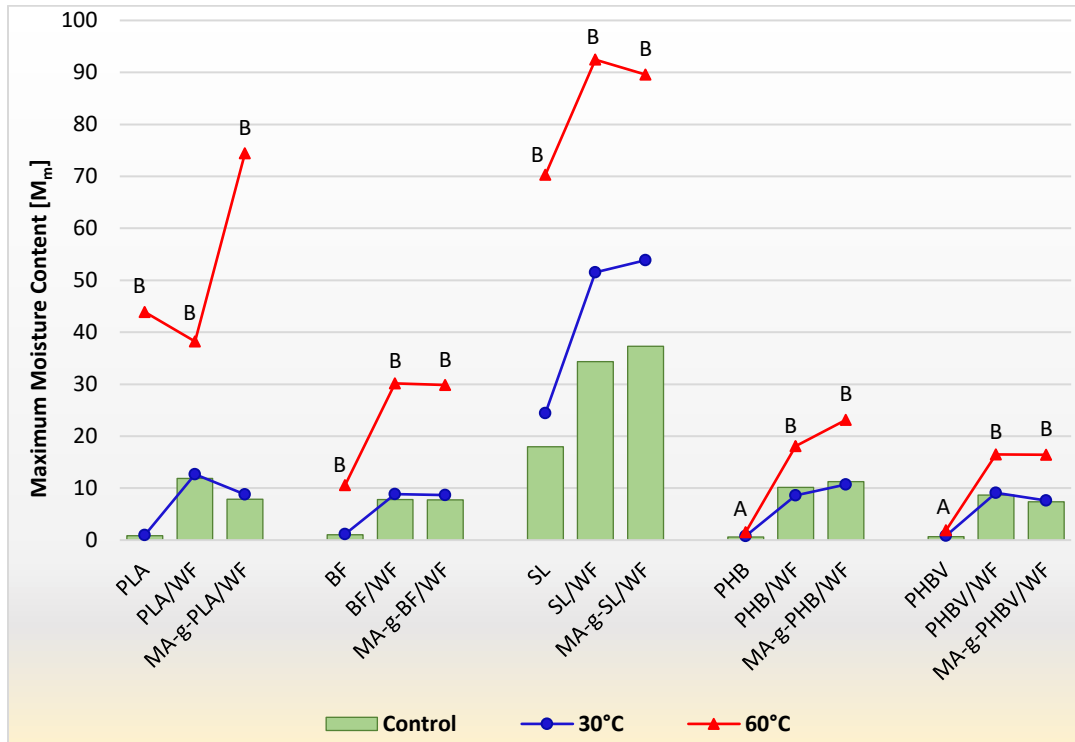


Figure 4.1. Maximum moisture content of all the neat polymers and composites before soil burial (SB), and after soil burial at 30°C and 60°C. Different letters indicate statistically significant difference of the specimens after SB at 60°C with respect to specimens after SB at 30°C. NOTE: All the specimens after soil burial at 30°C are in group 'A' ($P < 0.05$).

On the other hand, after 60°C SB, all the specimens exhibited substantial increase in water absorption. Water diffusion into the polymer sample causes swelling of cellulosic fibers, and enhanced biodegradation. Contrast to water absorption after 30°C SB, compatibilized PLA, BF and PHBV composites after 60°C SB exhibited higher or similar M_m values with respect to the composites without MA. The water absorption of MA-g-PHB/WF was still higher than PHB/WF after degradation at both temperatures. Neat PHB and PHBV showed the lowest water

absorption after degradation test at both temperatures. This can be attributed to higher degree of crystallinity. Crystalline regions are less susceptible to degradation (Balakrishnan et al., 2011).

Soil Biodegradation

Biodegradation of the buried specimens were determined by the weight loss of the material. Specimens degraded at 60°C showed a significant % weight loss compared to specimens degraded at 30°C (Figure 4.2). Most importantly, the compatibilized PLA, BF and PHBV exhibited lower weight loss than their uncompatibilized composites after 30°C SB, but a higher rate of biodegradation after 60°C SB. The degradation behavior of compatibilized PHB and SL were different than the other three biopolymer composites.

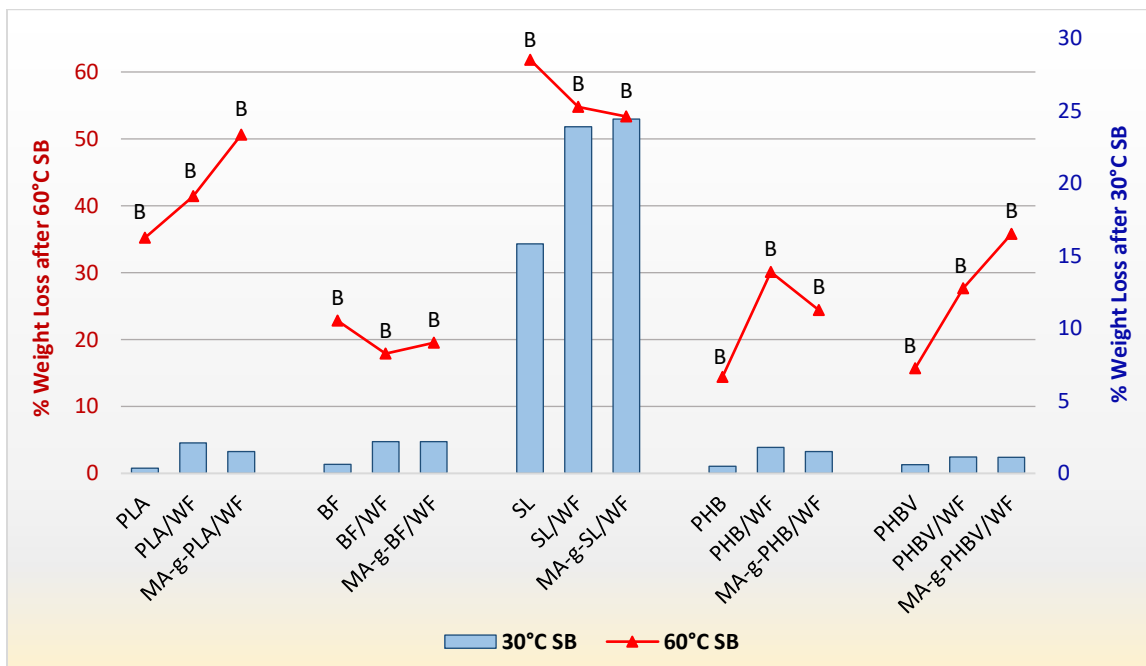


Figure 4.2. % Weight loss of all the neat polymers and composites after soil burial (SB) at 30°C and 60°C. Different letters indicate statistically significant difference of the specimens after SB at 60°C with respect to specimens after SB at 30°C.

NOTE: All the specimens after soil burial at 30°C are in group 'A' ($P < 0.05$).

Optical Microscopy

Micrographs of the samples before soil burial showed that all the neat polymers and their composites with smooth surfaces with polymer layers on top indicating proper fiber encapsulation (Krehula, Katančić, Siročić, & Hrnjak-Murgić, 2014). After soil burial, all the specimens showed roughened surfaces. The first stage of biodegradation involves microorganism attacking the surface of specimens. As the bacteria digest the polymer, surface roughness increases (Gunning, Geever, Killion, Lyons, & Higginbotham, 2013).

The surface cracking was visible on all the specimens after soil burial at both temperatures (Table 4.1-4.3). However, the formation of cracks and voids were more prominent for the specimens buried at 60°C. Specimens were more fragile after 60°C soil burial (SB) compared to the specimens buried at 30°C. For example, neat PLA and its composites only had a few voids on the surface after 30°C SB (Table 4.1). After 60°C SB, both neat PLA and its composites exhibited more surface cracks and voids, and an extremely fragile texture. The samples broke down into small pieces eventually. Compatibilized composites subjected to 60°C SB exhibited larger voids and more destruction of the material with respect to their uncompatibilized composites.

Table 4.1. Comparison of surface morphology of the specimens before, and after soil burial at 30°C and 60°C: PLA, PLA/WF, MA-g-PLA/WF, BF, BF/WF, MA-g-BF/WF.




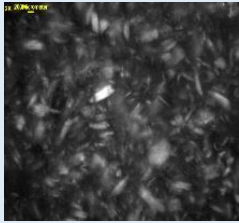


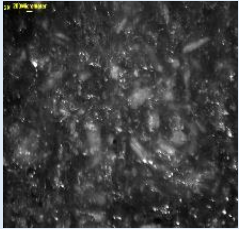





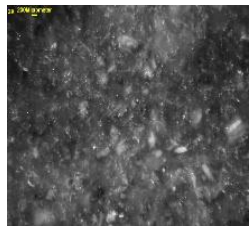

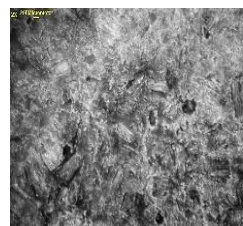
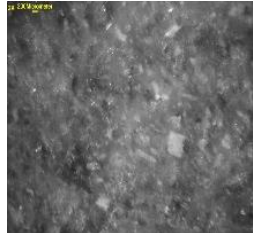
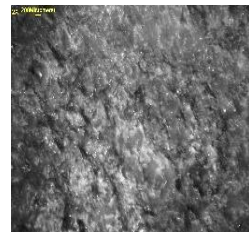
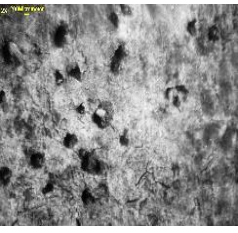
Composition	Control (before soil burial)	30°C soil burial	60°C soil burial
PLA			
PLA/WF			
MA-g-PLA/WF			
BF			
BF/WF			
MA-g-BF/WF			

Table 4.2. Comparison of surface morphology of the specimens before, and after soil burial at 30°C and 60°C: PHB, PHB/WF, MA-g-PHB/WF, PHBV, PHBV/WF, MA-g-PHBV/WF.






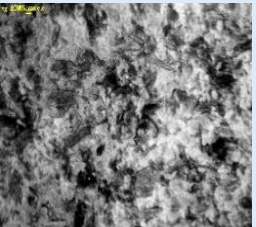





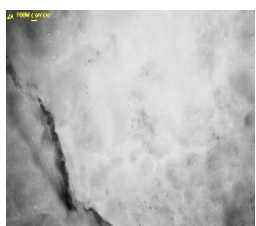
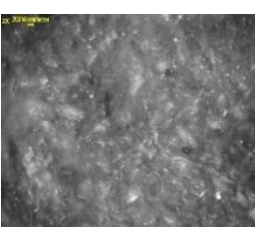

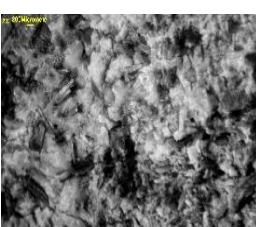
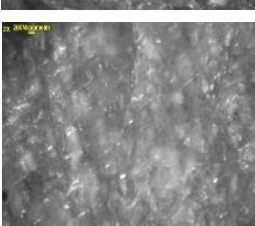
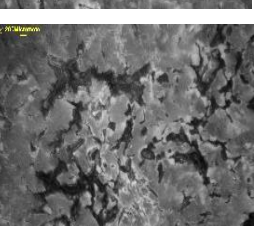



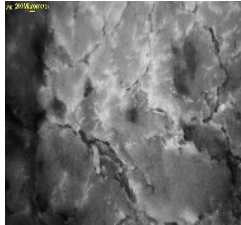
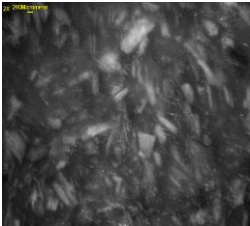
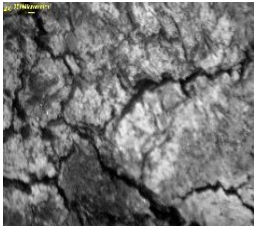
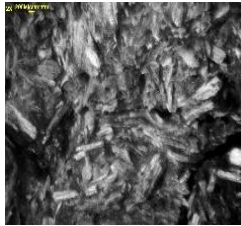
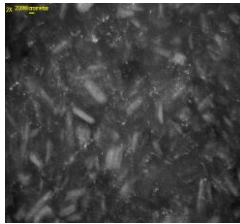
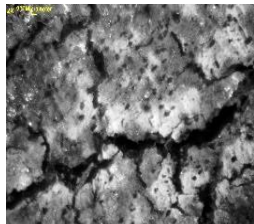

Composition	Control (before soil burial)	30°C soil burial	60°C soil burial
PHB			
PHB/WF			
MA-g-PHB/WF			
PHBV			
PHBV/WF			
MA-g-PHBV/WF			

Table 4.3. Comparison of surface morphology of the specimens before, and after soil burial at 30°C and 60°C: SL, SL/WF, MA-g-SL/WF.

Composition	Control (before soil burial)	30°C soil burial	60°C soil burial
SL			
SL/WF			
MA-g-SL/WF			

Surface Color

Lightness (ΔL^*) of the all specimens except PLA decreased after degradation at 30°C (Figure 4.3). Neat PLA and its composites exhibited white surface after 30°C SB (Table 4.4). The decrease in ΔL^* for non-PLA specimens can be attributed to development of small black spots on the surface. Neat SL specimens also developed green color spots. Specimens subjected to 60°C SB exhibited greater color change than that of the specimens after 30°C SB. It is noteworthy that the color change of PLA, PLA/WF, MA-g-PLA/WF and MA-g-SL/WF after 60°C SB could not be measured as these specimens broke down completely. After 60°C SB, white surfaces of neat BF and PHB turned yellowish. Neat SL completely turned into dark brown (Table 4.4). Color of neat PHBV and its composites including PHB composites faded. Similar to

composites buried at 30°C, all the other composites at 60°C SB exhibited black spots all over the surface along with some fading.

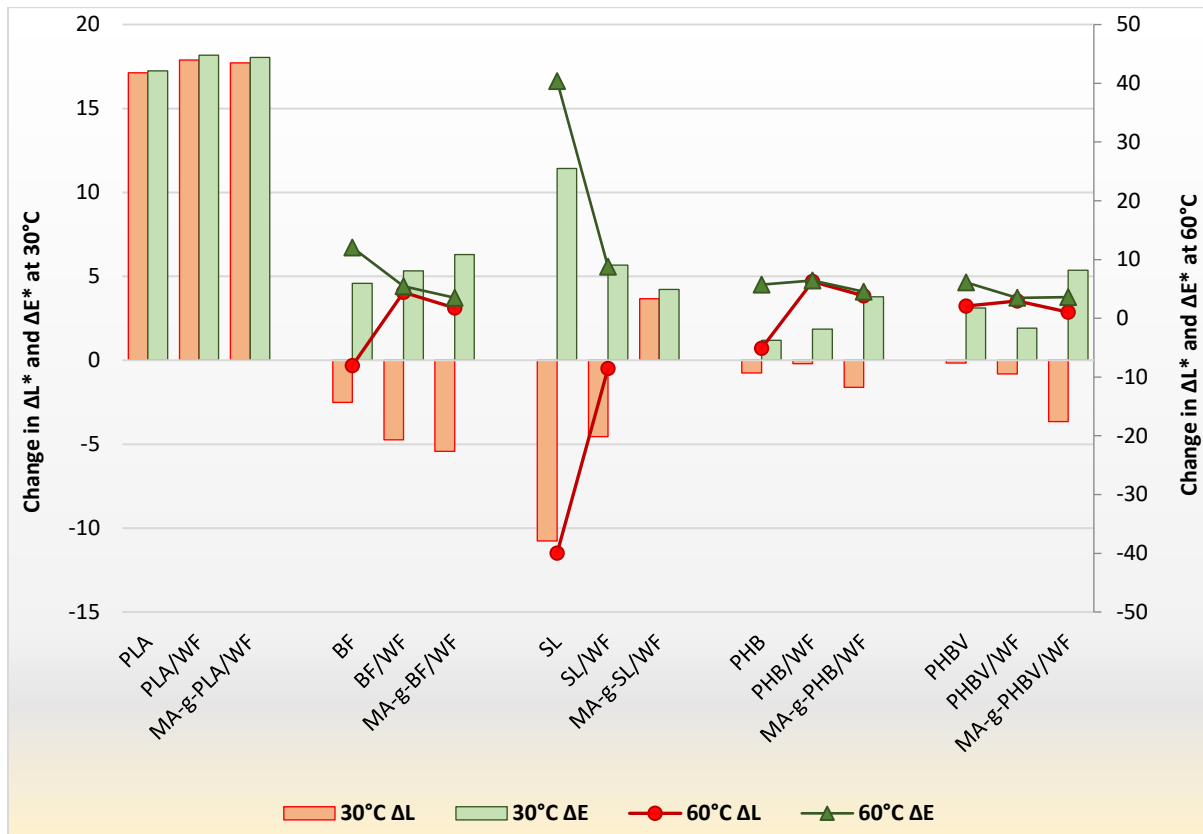

















Figure 4.3. The lightness (ΔL^*) and total color changes (ΔE^*) of the specimens after soil burial at 30°C and 60°C.

Table 4.4. Digital camera photos of the specimens before, and after soil burial at 30°C and 60°C: PLA, PLA/WE, BF/WF, SL, MA-g-PHBV/WF.

Composition	Control (before soil burial)	30°C soil burial	60°C soil burial
PLA			
PLA/WF			
BF/WF			
SL			
MA-g-PHBV/WF			

Whitening of the soil buried specimens can be attributed to increased surface roughness (Michel & Billington, 2012; Rahman et al., 2011). As the bacteria digest the polymer, surface roughness increases. When the specimen interacts with microbes, state of the specimen change significantly (Ochi, 2011). Starch is degraded by bacterial or fungal strains, whereas PLA is

degraded by fungal strains. PHB is degraded by numerous microorganisms in various ecosystems. During degradation, PHA polymer is considerably excessive in size to be conveyed directly through the bacterial cell wall, so it should be permuted into corresponding hydroxyl acid monomers (Gilmore, Fuller, & Lenz, 1990). The compost is a very suitable environment for the biodegradation of such materials. Clearly, specimens after 60°C SB showed higher color change and more destruction of the material (Figure 4.3, Table 4.4). Before the action of microorganisms, it is possible that the high temperature and relative humidity facilitated the hydrolytic degradation of the polymer material (Iovino, Zullo, Rao, Cassar, & Gianfreda, 2008). Exposing polymers to various degrading conditions such as weathering, ageing and soil burying results in different transformations of polymers due to light, thermal and chemical agents. These abiotic parameters are useful factors in initiating the biodegradation process, as they help to weaken the polymer structures (Jakubowicz, Yarahmadi, & Petersen, 2006; Lucas et al., 2008).

Mechanical Properties

For specimens buried at 30°C, hardness properties were affected to lesser degree (Figure 4.4). Similar to water absorption test, only neat SL and its composites showed a significant reduction with respect to their control samples. The highest reduction of 45% can be observed for MA-g-SL/WF. On the other hand, hardness of PHBV/WF and MA-g-PHBV/WF significantly increased compared to their composites before soil burial. Hardness of specimens buried at 60°C could not be measured as the specimens were too thin according to ASTM standard.

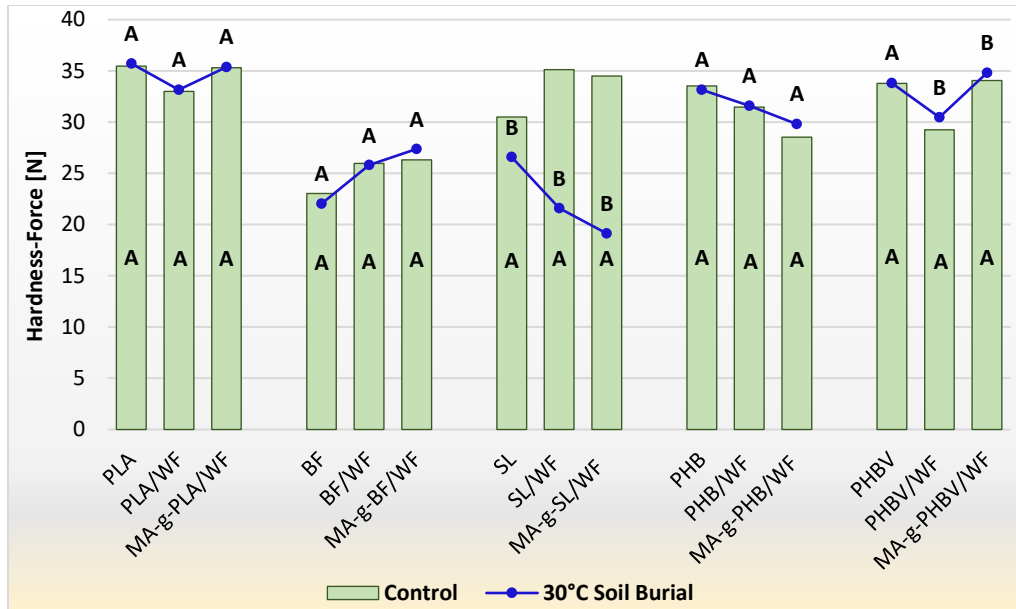


Figure 4.4. Surface hardness of all the neat biopolymers and composites before and after soil burial at 30°C. Different letters indicate statistically significant difference of the specimen on the property after soil burial at 30°C with respect to specimens before soil burial.

Unlike hardness property, compressive strength was significantly reduced after biodegradation at 30°C for PLA/WF, BF/WF and SL with respect to the specimens before soil burial (Figure 4.5). Neat SL and its composites exhibited substantial reductions, both of its composites having the highest drop of 90%. However, MA-g-PHB/WF and PHBV/WF showed considerable increase of the strength compared to their unburied samples. Except for BF and PHB, compressive properties could not be determined for specimens buried at 60°C as they were too thin (<3 mm). All the tested samples of 60°C SB exhibited significant drop of strength compared to unburied and 30°C SB specimens, where neat BF and its composites had the highest drop of 90%. Significant reduction in compressive modulus can be observed for 30°C soil buried compatibilized composites of PLA, SL, PHB, and uncompatibilized composites of BF, SL, PHB and PHBV with respect to their specimens before soil burial (Figure 4.6). For specimens buried at 60°C, except for neat PHB, all the tested specimens exhibited significant decrease in compressive modulus compared to unburied and 30°C SB specimens.

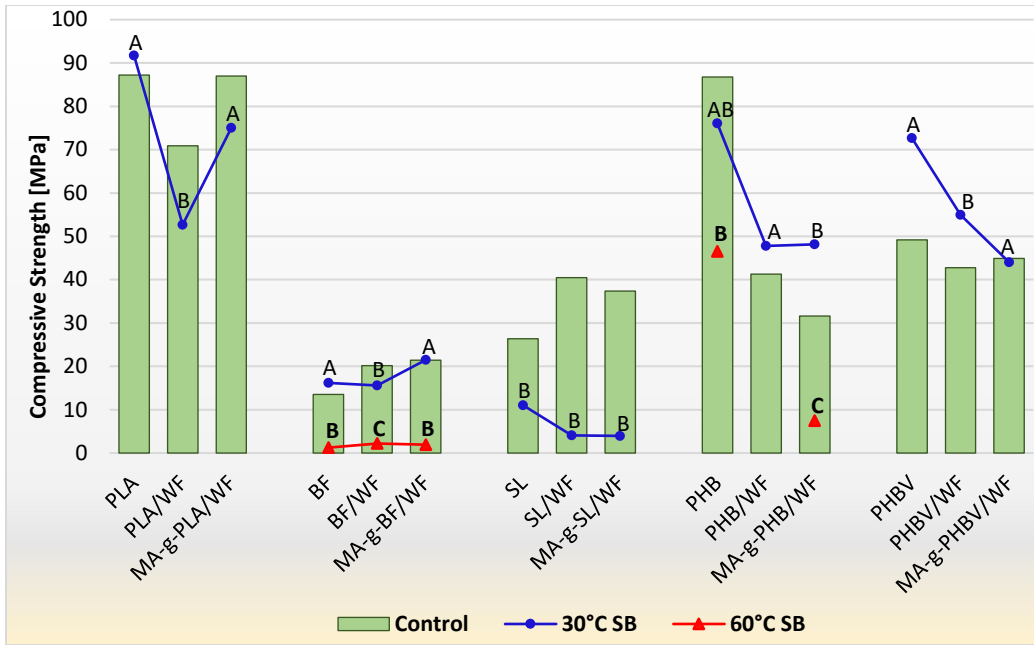


Figure 4.5. Compressive strength of the biopolymer compositions before and after soil burial (SB) at 30°C and at 60°C. Different letters indicate statistically significant difference of the specimen on the property after SB at 30°C and at 60°C with respect to specimens before SB. NOTE: All the specimens before soil burial are in group ‘A’ ($P < 0.05$).

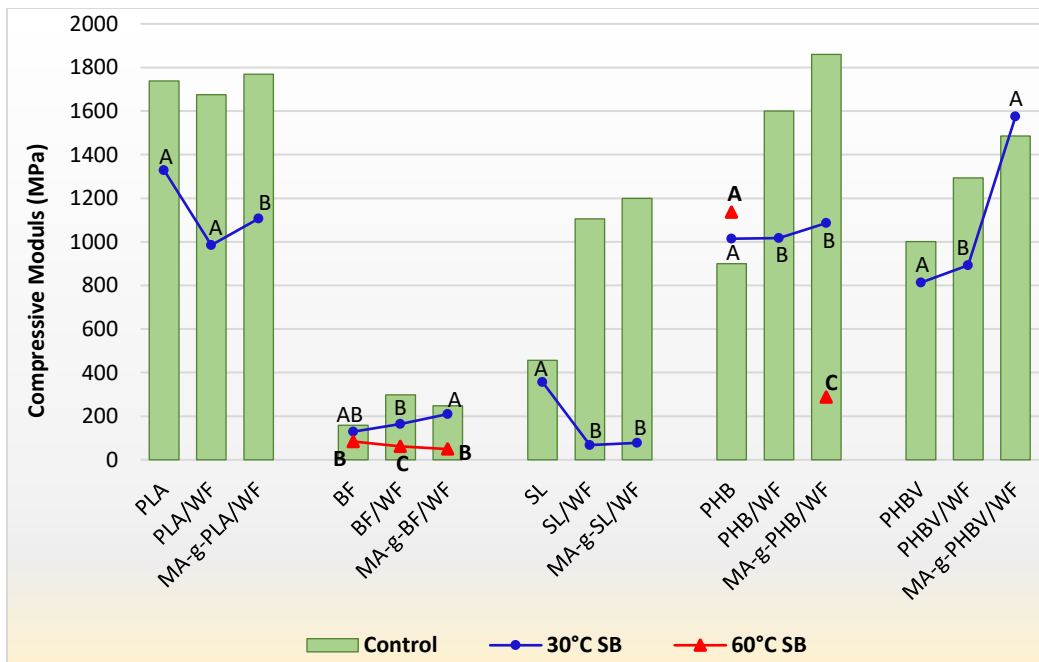


Figure 4.6. Compressive modulus of all the neat biopolymers and composites before and after soil burial (SB) at 30°C and at 60°C. Different letters indicate statistically significant difference of the specimens after SB at 30°C and 60°C with respect to specimens before SB. NOTE: All the specimens before soil burial are in group ‘A’ ($P < 0.05$).

When the specimens interacted with microbes in soil, strength properties changed substantially as the surface matrix layer cracked under the combined action of microorganisms and water (Ochi, 2011). For composites, fiber–matrix interaction was weakened, and cracks were formed due to swelling of hydrophilic WF. Consequently, the structure was loosened, and the force required to rupture the material was decreased resulting weaker mechanical properties.

Discussion

Weight loss%, material destruction, and reduction in strength properties were higher for 60°C SB samples. The higher the temperature of the degradation environment, the higher the rates of chemical hydrolysis and hydrophilicity of the polymers are (Itävaara et al., 2002). As evidenced, water absorption of the material substantially increased at 60°C, thus, increasing the microbe attachments. Consequently, all the polymer samples showed significant increase in % weight loss after 60°C SB than after 30°C SB. When polymers are exposed to high temperatures, microstructural changes and molecular rearrangements occur in the material (Iovino et al., 2008). At temperatures higher than the glass transition temperature (T_g) of the polymer, the flexibility of the polymer chain increases, enabling the higher diffusivity of water into the matrix (Balakrishnan et al., 2011). The T_g of PLA, BF and SL is between 55-65°C (Yatigala, Bajwa, & Bajwa, 2017). Accordingly, all these polymer samples exhibited higher water absorption, and therefore higher weight loss% after 60°C SB compared to 30°C SB. For neat PHB and PHBV, water absorption and biodegradation rate did not seem to correlate. For instance, the biodegradation of neat PHBV at 60°C was higher, even though the water absorption capacity of the specimens was not changed (Figure 4.1-4.2). During biodegradation, the microorganisms attack the surface of the polymer first (Gunning et al., 2013). As the bacteria digest through the polymer specimen, complete disappearance of composites/matrices can be

observed (Iovino et al., 2008). The remaining material (after SB) of some of the specimens such as PHB and PHBV showed a robust structure. This could be due to microorganisms not being able to reach all the way through the specimens as evidenced by lower water absorption capacity of these remaining material.

Biodegradation rate of polymers was different from each other. Weight loss% of neat BF was lower than those of neat PLA. Soil Biodegradation of PLA based polymers strongly depends on the copolyester and additives (Barragán, Pelacho, & Martin-Closas, 2010). Neat PHB and PHBV had the lowest biodegradation at both temperatures. Degradation is faster when the molecular weight of polymers are low (Prados & Maicas, 2016). Higher molecular weight lowers the solubility of the polymer, reducing the microbial attack (Shah et al., 2008). Insolubility of polymers reduces the availability of substrates to bacteria that can be assimilated through the cellular membrane. Molecular weight of PHB and PHBV range from 300,000 - 400,000 g/mol. For PLA it is around 72,000 g/mol, while it is around 75,000 g/mol for BF. Solanyl has a molecular weight of around 61,000 g/mol, the lowest of the five biopolymers considered in this study. In addition to water absorption, biodegradation appeared to be linked closely to the molecular weight of these polymers.

Most of the composites showed more degradation than neat polymers. This can be ascribed to higher moisture absorption of hydrophilic WF. All composites subjected to degradation showed cracks between the polymer matrix and WF. When water is absorbed, WF detach from the polymer matrix. As the surface matrix layer is cracked under the combined actions of microorganisms and water, both degradation agents penetrate deeper into the composite, resulting in more degradation (Batista, Silva, Coelho, Pezzin, & Pezzin, 2010).

Lower biodegradation of compatibilized composites compared to uncompatibilized composites after 30°C SB can be attributed to reduced water absorption of the MA grafted composites due to improved fiber-matrix adhesion. Most thermoplastics are hydrophobic matters that are incompatible with hydrophilic WF, resulting in poor fiber-matrix interaction. Compatibilized biopolymer/natural fiber composites are fabricated to increase the interfacial adhesion between the polymer matrix and the fibers (Gunning et al., 2014). The compatibilizer, MA, interacts with hydroxyl groups of cellulose and lignin of the fiber to form covalent or hydrogen bonds. Therefore, the fibers are well attached with matrix. In contrast to 30°C SB, after 60°C SB, compatibilized composites showed increased biodegradation with respect to the uncompatibilized composites. At higher temperatures, bonds such as covalent ester carbonyl bonds between the polymer and the fiber hydrolyzes, allowing the debonded fibers and matrix to absorb more water. If the fibers are well attached with the matrix due to compatibilization, debonding of fiber and matrix can result in even higher biodegradation due to higher surface area available for biodegradation [8]. This is visible in MA-g-PLA/WF samples after 60°C SB as they exhibited larger voids and more degradation of the material compared to PLA/WF at 60°C SB (Table 4.1).

Conclusion

Five different types of biodegradable biobased composites were prepared by blending wood fiber with biopolymers: PLA, Bioflex (PLA blend), Solanyl (starch based), PHB, or PHBV. Maleic anhydride (MA) was used to compatibilize the composites. Soil microbial degradation of the specimens was apparent with surface color change, roughened surface, and microcracks of the specimens, which led to higher water absorption. Solanyl and its composites showed the highest biodegradation. Destruction of the material, weight loss, and mechanical

strength loss were more prominent for the specimens after biodegradation at 60°C than after 30°C biodegradation. Elevated temperatures enhance the hydrolysis and hydrophilicity of biodegradable polymers, thus, resulting in higher rate of biodegradation. Some polymer materials buried at 30°C exhibited significant improvements in hardness and compressive properties. Composites showed more degradation than neat polymers due to hydrophilicity of the wood fiber filler. Even though the compatibilized composites showed lower biodegradation than their composites without MA at 30°C, biodegradation was higher in compatibilized composites at 60°C.

References

- ASTM. (2015). ASTM D695 Standard Test Method for Compressive Properties of Rigid Plastics- 2015. In.
- ASTM D570. (2010). In *Standard Test Method for Water Absorption of Plastics*: American Society for Testing and Materials.
- ASTM, D. (2000). 2240, Standard Test Method for Rubber Property-Durometer Hardness. *Figure 5. left column shows visual surface degradation of the urethane after (top to bottom), 18.*
- ASTM, D. (2003). 2244:“Standard Practice for Calculation of Color Tolerances and Color Differences from Instrumentally Measured Color Coordinates”. *American Society for Testing and Materials, West Conshohocken, PA.*
- ASTM G160. (2012). In *Standard Practice for Evaluating Microbial Susceptibility of Nonmetallic Materials By Laboratory Soil Burial.*

- Balakrishnan, H., Hassan, A., Imran, M., & Wahit, M. U. (2011). Aging of toughened polylactic acid nanocomposites: water absorption, hygrothermal degradation and soil burial analysis. *Journal of Polymers and the Environment*, *19*(4), 863-875.
- Barragán, D., Pelacho, A., & Martin-Closas, L. (2010). *A respirometric test for assessing the biodegradability of mulch films in the soil*. Paper presented at the XXVIII International Horticultural Congress on Science and Horticulture for People (IHC2010): International Symposium on 938.
- Batista, K., Silva, D., Coelho, L., Pezzin, S., & Pezzin, A. (2010). Soil biodegradation of PHBV/peach palm particles biocomposites. *Journal of Polymers and the Environment*, *18*(3), 346-354.
- Gilmore, D. F., Fuller, R. C., & Lenz, R. (1990). Biodegradation of poly (beta-hydroxyalkanoates). *Degradable materials: perspectives, issues and opportunities*. CRC, Boston, 481-514.
- Glazner, E. (2015). Plastic Pollution and Climate Change. Retrieved from <http://www.plasticpollutioncoalition.org/pft/2015/11/17/plastic-pollution-and-climate-change>
- Gunning, M. A., Geever, L. M., Killion, J. A., Lyons, J. G., & Higginbotham, C. L. (2013). Mechanical and biodegradation performance of short natural fibre polyhydroxybutyrate composites. *Polymer Testing*, *32*(8), 1603-1611.
- Gunning, M. A., Geever, L. M., Killion, J. A., Lyons, J. G., & Higginbotham, C. L. (2014). Effect of Compatibilizer Content on the Mechanical Properties of Bioplastic Composites via Hot Melt Extrusion. *Polymer-Plastics Technology and Engineering*, *53*(12), 1223-1235.

- Iovino, R., Zullo, R., Rao, M., Cassar, L., & Gianfreda, L. (2008). Biodegradation of poly (lactic acid)/starch/coir biocomposites under controlled composting conditions. *Polymer Degradation and Stability*, 93(1), 147-157.
- Itävaara, M., Karjomaa, S., & Selin, J.-F. (2002). Biodegradation of polylactide in aerobic and anaerobic thermophilic conditions. *Chemosphere*, 46(6), 879-885.
- Jakubowicz, I., Yarahmadi, N., & Petersen, H. (2006). Evaluation of the rate of abiotic degradation of biodegradable polyethylene in various environments. *Polymer degradation and stability*, 91(7), 1556-1562.
- Krehula, L. K., Katančić, Z., Siročić, A. P., & Hrnjak-Murgić, Z. (2014). Weathering of high-density polyethylene-wood plastic composites. *Journal of Wood Chemistry and Technology*, 34(1), 39-54.
- Lucas, N., Bienaime, C., Belloy, C., Queneudec, M., Silvestre, F., & Nava-Saucedo, J.-E. (2008). Polymer biodegradation: Mechanisms and estimation techniques—A review. *Chemosphere*, 73(4), 429-442.
- Lytle, C. L. G. (2009). WHEN THE MERMAIDS CRY: THE GREAT PLASTIC TIDE.
Retrieved from <http://plastic-pollution.org/>
- Michel, A., & Billington, S. (2012). Characterization of poly-hydroxybutyrate films and hemp fiber reinforced composites exposed to accelerated weathering. *Polymer Degradation and Stability*, 97(6), 870-878.
- Niaounakis, M., Kontou, E., & Xanthis, M. (2011). Effects of aging on the thermomechanical properties of poly (lactic acid). *Journal of Applied Polymer Science*, 119(1), 472-481.
- Ochi, S. (2011). Durability of starch based biodegradable plastics reinforced with Manila hemp fibers. *Materials*, 4(3), 457-468.

- Prados, E., & Maicas, S. (2016). Bacterial Production of Hydroxyalkanoates (PHA). *Universal Journal of Microbiology Research*, 4(1), 23-30.
- Rahman, W. A. W. A., Sin, L. T., Rahmat, A. R., Isa, N., Salleh, M., & Mokhtar, M. (2011). Comparison of rice husk-filled polyethylene composite and natural wood under weathering effects. *Journal of Composite Materials*, 45(13), 1403-1410.
- Shah, A. A., Hasan, F., Hameed, A., & Ahmed, S. (2008). Biological degradation of plastics: a comprehensive review. *Biotechnology advances*, 26(3), 246-265.
- Wassener, B. (2011). Raising Awareness pf Plastic Waste. *The New York Times*. Retrieved from <http://www.nytimes.com/2011/08/15/business/energy-environment/raising-awareness-of-plastic-waste.html>
- Wu, C.-S. (2009). Renewable resource-based composites of recycled natural fibers and maleated polylactide bioplastic: Characterization and biodegradability. *Polymer Degradation and Stability*, 94(7), 1076-1084.
- Wu, C. S. (2006). Assessing biodegradability and mechanical, thermal, and morphological properties of an acrylic acid-modified poly (3-hydroxybutyric acid)/wood flours biocomposite. *Journal of applied polymer science*, 102(4), 3565-3574.
- Wu, C. S. (2012). Preparation, characterization, and biodegradability of renewable resource-based composites from recycled polylactide bioplastic and sisal fibers. *Journal of Applied Polymer Science*, 123(1), 347-355.
- Yatigala, N., Bajwa, D., & Bajwa, S. (2017). *Compatibilization Improves Physico-Mechanical Properties of Biodegradable Biobased Polymer Composites*.

CHAPTER 5. GENERAL CONCLUSIONS

Polymer derived from renewable resources are gaining attention as non-toxic, low impact alternatives to undegradable petroleum based polymers.

Five different types of biodegradable biobased composites were prepared by blending wood fiber with biopolymers: PLA, Bioflex (BF, PLA blend), Solanyl (SL, starch based), PHB, or PHBV. Maleic Anhydride (MA) was used to compatibilize the composites. Compatibilization improved thermal properties such as glass transition temperature, melting temperature, degradation temperature and crystallinity in PLA, BF and PHBV composites. Resistance to water and mechanical properties such as flexural, impact and hardness improved due to increased fiber-matrix interaction in PLA, BF and PHBV composites. Failure to graft MA to PHB successfully, and the similarity of molecular weight of grafted and ungrafted SL explain the unresponsiveness of these composites to compatibilization.

It is important to study the behavior of the biocomposites in long-term outdoor conditions to understand their durability. Therefore, biocomposites were subjected to accelerated weathering for 2000 h under 4 h of condensation cycle and 8 h of UV exposure. With increased weathering exposure, increased surface degradation was evident through roughened surface, surface color change, and microcracks in the specimens. The degraded samples exhibited higher moisture absorption. Due to plasticization effect of absorbed water, glass transition temperature and melting temperature decreased, and crystallinity increased. Since the formed crystalline regions were mechanically weaker, impact, flexural and hardness properties decreased. Some polymer materials exhibited significant improvements in flexural modulus and hardness. Composites showed higher degradation compared to neat polymers due to reduced fiber-matrix interaction. Though the compatibilization improved thermal and physico-mechanical properties,

no considerable difference was shown between the composites with and without MA after weathering.

One of the downsides of compatibilization could be reduction in biodegradation of the biocomposites. To increase the soil microbial degradation, biocomposites were buried in soil at two different temperatures of 30°C and 60°C. Destruction of the material, weight loss, increased water absorption, and mechanical strength loss were significantly higher at 60°C than at 30°C. Higher temperature enhances the hydrolysis and hydrophilicity of biopolymers, increasing the rate of biodegradation. Some polymer materials exhibited significant improvements in hardness and compressive properties at 30°C. Most composites exhibited higher deterioration of the material compared to neat polymers. Even though the compatibilized composites showed reduced biodegradation compared to composites without MA at 30°C, biodegradation was higher in composites with MA at 60°C.

Potential applications of the compatibilized composites in this study are garden fences and golf tees (Tatara, DiOrio, & Ziemer, 2008). The composites without MA can be used in planting cups and take-away food trays (Schwarzkopf & Burnard, 2016). Properties such as flexural strength and modulus, impact strength, and water absorption of these applications are similar to the composites produced in this study (Z-Trust, 2004).

The study indicates a possibility of designing sustainable and inexpensive biodegradable biobased polymer composites with increased strength and soil biodegradation properties, without affecting their UV degradation characteristics.

References

- Schwarzkopf, M. J., & Burnard, M. D. (2016). Wood-Plastic Composites—Performance and Environmental Impacts. In *Environmental Impacts of Traditional and Innovative Forest-based Bioproducts* (pp. 19-43): Springer.
- Tatara, R. A., DiOrio, N. R., & Ziemer, N. L. (2008). Eco-Friendly Golf Tees Filled with Corn-Based DDGS. In Northern Illinois University: United States Environmental Protection Agency.
- Z-Trust, I. E. (2004). Technical Information- The Test Requirements of Ly/t1613. In W. Features (Ed.): Z-Trust Import & Export.

CHAPTER 6. RECOMMENDATIONS FOR FUTURE WORK

Creating biocomposites by incorporating wood fiber and compatibilizer into biopolymers provide solution in terms of cost, strength and biodegradation properties. However, widespread usage of PLA and PHA has been limited due to narrow melt processing window and slow crystallization rate than conventional plastics (Khosravi-Darani & Bucci, 2015).

Out of the five biopolymers used in the study, Bioflex (BF, PLA blend) was the only biopolymer that provided a smooth processing in extruding. It was difficult to receive continuous extruded strands of PLA/fiber. The PHB was extremely susceptible to thermal degradation during extrusion. The extruded SL strands expanded when it came out of the extruder, which made it difficult to cut into pallets. During compression molding, all the materials exhibited tackiness except for PLA. However, use of Teflon sheets aided in avoiding unnecessary tackiness. The addition of wood fiber or compatibilizer did not have a significant positive impact on processing of the biopolymers except for SL. When wood fiber was incorporated to SL, it was less tacky during compression molding, and did not expand much during extrusion.

Other processing methods such as in 3D printing, PLA creates bubbles or spurting at the nozzle. Since PLA can react with water at high temperatures and undergo de-polymerization, discoloration and a reduction of properties can be observed in 3D printed parts. Even though PLA can be dried, this could alter the crystallinity ratio of PLA and resulting in changed extrusion temperature and characteristics (Chilson, 2013). In film blowing process, the shape of the PLA bubble is unstable due to low melt strength of PLA. The resulting films tend to have large variation of dimension and thickness. (Hongdilokkul et al., 2015). Since PLA has low heat distortion temperature, developing crystallinity in PLA has additional steps in processing such as one-step process/in-mold annealing, and two-step process/post-annealing (Hongdilokkul et al.,

2015; Manjure & Annan, 2016). Using PHAs in some automotive applications is a failure due to difficult melt processing and limited availability of knowledge to identify the best operational parameters to avoid thermal degradation (Barletta, Trovalusci, Puopolo, Tagliaferri, & Vesco, 2016).

Accordingly, if these materials/composites are to replace petroleum-based products in majority of applications, biopolymers need more modifications. Otherwise, extensive use of these biopolymer and composites would not be practical. Even though the addition of fibers to neat biopolymer reduces the cost, production cost would still be high due to time consuming and difficult processing. For future work, it would be invaluable if the neat biopolymers were engineered to be easy to process. Perhaps, addition of chain extenders, enzymes, plasticizers and chemicals/additives could help reduce processing difficulties (Khosravi-Darani & Bucci, 2015). More research studies should be done evaluating how the addition of different kind of chemicals/additives impact on processing techniques such as extrusion, 3D printing, film blowing, compression molding and injection molding.

References

- Barletta, M., Trovalusci, F., Puopolo, M., Tagliaferri, V., & Vesco, S. (2016). Engineering and Processing of Poly (HydroxyButyrate)(PHB) Modified by Nano-sized Graphene Nanoplatelets (GNP) and Amino-Functionalized Silica (A-fnSiO₂). *Journal of Polymers and the Environment*, 24(1), 1-11.
- Chilson, L. (2013). The Difference Between ABS and PLA for 3D Printing. Retrieved from <https://www.protoparadigm.com/news-updates/the-difference-between-abs-and-pla-for-3d-printing/>

- Hongdilokkul, P., Keeratipinit, K., Chawthai, S., Hararak, B., Seadan, M., & Suttiruengwong, S. (2015). *A study on properties of PLA/PBAT from blown film process*. Paper presented at the IOP Conference Series: Materials Science and Engineering.
- Khosravi-Darani, K., & Bucci, D. (2015). Application of poly (hydroxyalkanoate) in food packaging: Improvements by nanotechnology. *Chemical and Biochemical Engineering Quarterly*, 29(2), 275-285.
- Manjure, S., & Annan, M. (2016). Injection molding of PLA cutlery. *bioplastics MAGAZINE*, 11.

APPENDIX A. ADDITIONAL INFORMATION OF BIOFLEX BIOPOLYMER

Bioflex (Bio-Flex® F 2110) used in this study is a polymer-blend based on PLA, contains copolyester, mineral fillers and recyclable additives (Kucharczyk et al., 2012). Bioflex (BF) is certified as compostable material according to European standard EN 13432, and is a USDA certified biobased product. The main component of BF is PLA. When tested for MW, BF had a MW of 75000 g/mol, while it was 72000 g/mol for PLA. Researches prefer to use BF instead of PLA due to easy processing (Kucharczyk et al., 2012). In order to determine the chemical difference between the PLA and BF, FTIR analysis was performed (Figure A1).

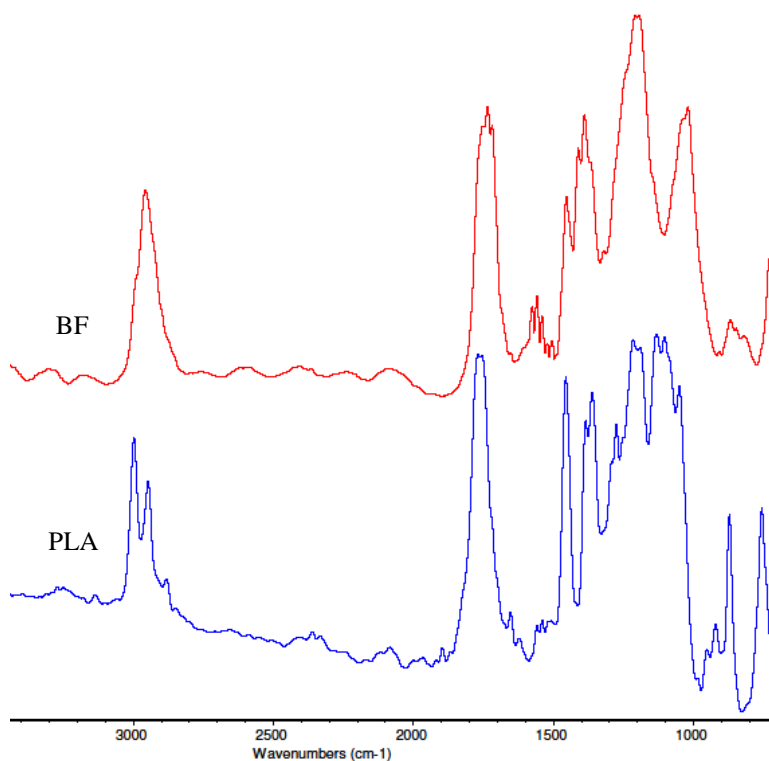


Figure A1. FTIR spectra of PLA and Bioflex (BF).

The PLA spectrum showed CH₃ stretching at 3000–2930 cm⁻¹. The strong IR bands at 2997.8 and 2947 cm⁻¹ can be assigned to the CH stretching region (Spiridon, Paduraru, Zaltariov, & Darie, 2013). Conversely, BF only had one peak at 2957.6 cm⁻¹. The C=O stretching between

1730-1760 cm^{-1} was shown for both PLA and BF. The peaks presented between 1550-1580 cm^{-1} for BF could be due to N-H bending (Cui et al., 2001; Yang, 2011). These peaks were not in PLA spectra. Peaks between 1350-1450 cm^{-1} can be attributed to CH_2 & CH_3 deformation. The O=C=O stretching at 1200–1050 cm^{-1} are characteristics of ester bonds (Orozco, Brostow, Chonkaew, & Lopez, 2009). Only 2 peaks were presented for BF in this range in contrast to 3 peaks of PLA. The peaks around 870 cm^{-1} were for amorphous phase of the polymer. Peak at 756 cm^{-1} represents the crystalline phases of PLA, and this peak was not in BF spectra.

References

- Cui, X., Lee, V. A., Raphael, Y., Wiler, J. A., Hetke, J. F., Anderson, D. J., & Martin, D. C. (2001). Surface modification of neural recording electrodes with conducting polymer/biomolecule blends. *Journal of Biomedical Materials Research Part A*, 56(2), 261-272.
- Kucharczyk, P., Otgonzu, O., Kitano, T., Gregorova, A., Kreuh, D., Cvelbar, U., . . . Saha, P. (2012). Correlation of morphology and viscoelastic properties of partially biodegradable polymer blends based on polyamide 6 and polylactide copolyester. *Polymer-Plastics Technology and Engineering*, 51(14), 1432-1442.
- Orozco, V. H., Brostow, W., Chonkaew, W., & Lopez, B. L. (2009). *Preparation and characterization of poly (Lactic acid)-g-maleic anhydride+ starch blends*. Paper presented at the Macromolecular symposia.
- Spiridon, I., Paduraru, O. M., Zaltariov, M. F., & Darie, R. N. (2013). Influence of keratin on polylactic acid/chitosan composite properties. Behavior upon accelerated weathering. *Industrial & Engineering Chemistry Research*, 52(29), 9822-9833.
- Yang, C. (2011). *Chemical Analysis of Polymeric Materials Using Infrared Spectroscopy*.